TÉCNICO LISBOA

Design of a Test Bench for Micro Combustion Engines

Hugo Cristiano Pereira da Silva Brogueira

Thesis to obtain the Master of Science Degree in

Mechanical Engineering

Supervisors: Prof. André Calado Marta
Prof. Virgínia Isabel Monteiro Nabais Infante

Examination Committee

Chairperson: Prof. João Orlando Marques Gameiro Folgado
Supervisor: Prof. André Calado Marta
Member of the Committee: Prof. Luís Alberto Gonçalves de Sousa

June 2016

Resumo

Este estudo consiste no projecto, construção e instrumentação de um banco de ensaios para testar micro motores de combustão utilizados em veículos de radio-modelismo. Foram utilizados vários sensores e actuadores para obter as especificações de desempenho do motor. Não existe nenhum banco de ensaios *standard* para micro motores, pelo que este equipamento pretende fornecer aos pilotos informação viável, algo que muitas vezes não se verifica. Foram considerados vários requerimentos técnicos para que o banco de ensaios seja seguro, eficaz e prático de utilizar. Parte dos componentes foram produzidos, outros adquiridos e, numa fase final da construção, o banco de ensaios foi montado juntamente com todas as peças de modelismo necessárias. Um dos objectivos é caracterizar um micro motor de 3.5 cc. Para isso, o banco de ensaios foi projectado para obter os diagramas de potência e torque e a curva do consumo de combustível. Estes resultados são mostrados num computador através de uma placa de aquisição de dados capaz de efectuar todas as leituras e processamento necessários à caracterização.

Numa primeira fase, foi feito um projecto conceptual para definir a base do projecto. Depois de uma cuidadosa pesquisa sobre bancos de ensaio e micro motores, o conceito abriu caminho ao projecto real de um dinamómetro de inércia. Foi desenvolvido um programa em *LabView* para o sistema de aquisição de dados, incluindo o próprio controlo dos actuadores. Foram produzidos componentes no Instituto Superior Técnico e, finalmente, o banco de ensaios foi montado com o devido volante de inércia e todos os componentes electrónicos necessários. Foram feitos testes para o motor eléctrico de um giroscópio para validar a instrumentação e depois foi então testado o motor *glow plug* de 3.5 cc, cujos resultados das curvas de potência validaram todo o projecto do banco de ensaios.

O dinamómetro de inércia é viável e flexível, uma vez que consegue testar micro motores de 2.0 a 20.0 cc. O programa que gere os testes de aceleração é totalmente automático, permitindo ao banco de ensaios ter uma boa repetibilidade que é essencial à aquisição de dados realísticos.

Palavras-chave: Curvas de potência, dinamómetro de inércia, micro motores, desempenho, aquisição de dados.

Abstract

This study is about the design, construction and instrumentation of a test bench for testing micro combustion engines used in model vehicles. Several sensors and actuators were used to obtain its performance specifications. There is no standard test bench for micro engines, so this equipment intends to present drivers with viable information, something that is missing. Several technical requirements were considered for the test bench to be safe, effective and practical to use. Some of the components were manufactured while others were off-the-shelf and, at a final stage of the construction, the test bench was assembled with all the required model parts. One of the objectives is to characterise a 3.5 cc micro engine. For that, the test bench was designed to obtain the power and torque diagrams and the fuel consumption rate. These results are displayed on a PC through a data acquisition board able to conduct all the necessary readings and processing for characterisation.

First a conceptual design was made to assess the idea behind the project. After a thorough research on test benches and micro engines, the concept gave way to the actual design of an inertia dynamometer. A program in *LabView* was developed for the data acquisition system including the actual control of the actuators. Components were produced in Instituto Superior Técnico and, finally, the test bench was assembled with the required flywheel and all the necessary electronic components. Tests were made for an electric motor driving a gyroscope to validate the instrumentation and then the 3.5 cc glow plug engine was tested, whose results of the power curves validated the whole design of the test bench.

The inertia dynamometer is viable and flexible, able to test any kind of micro engine from 2.0 to 20.0 cc. The program running the acceleration tests is fully automatic, allowing the test bench to have good repeatability which is essential to get realistic data.

Keywords: Power curves, inertia dynamometer, micro engines, performance, data acquisition.

Contents

List of Tables

List of Figures

Nomenclature

Greek symbols

α	Angular acceleration.
Δ	Interval.
μ	Friction coefficient.
ω	Angular velocity.
ρ	Density.
σ	Normal stress.
τ	Shear stress.
θ	Angle.

Roman symbols

d	Diameter.
e	Thickness.
F	Force.
I	Moment of inertia.
M	Bending moment.
m	Mass.
N	Rotation in RPM.
n	Factor of safety.
P	Power.
p	Pressure.
R	Outer radius.
r	Inner radius.

T Torque.

V Shear force.

W Weight.

Subscripts

0 Initial.

f Final.

max Maximum.

min Minimum.

x, y, z Cartesian components.

Glossary

BDC	Bottom Dead Center
CD	Cold Drawn
CI	Compression Ignition
ICE	Internal Combustion Engine
RPM	Rotations Per Minute
SI	Spark Ignition
TDC	Top Dead Center

Chapter 1

Introduction

This study is about micro Internal Combustion Engines (ICE) and the need to characterise them. These engines are largely used in model cars, boats and aircraft, and their technology has grown a lot in the past few decades to a high level of mechanical engineering. The challenge is to accurately determine their performance capabilities, something their manufacturers fail to provide realisticly.

To characterise them, a test bench for micro engines was designed, constructed and instrumented. It is able to test engines from different manufacturers and to obtain the performance specifications of interest with a data acquisition system. After the assembly of all the sensors and actuators, it generates the diagrams of torque and power with engine rotation speed, as well as the fuel consumption rate.

This chapter will make reference to the motivation for the master thesis and its objectives. An introduction to micro engines, their history and applications are also going to be addressed.

1.1 Motivation

There is a large number of micro engines manufacturers worldwide but most of them does not share performance data of their own product. They often use marketing maneuvers to magnify engine specifications, in order to sell a supposed better engine than the one of a different brand. Some of the manufacturers have tried to make their own test bench and it is possible that some of them have developed a way of testing the engines. The problem is that there is no standard test bench for micro engines, there is no way for the different brands to test their engines in order to give reliable information to the customers. If one needs to compare a given type of engine from different manufacturers, he will just have to blindly trust the marketing catalogue information.

Full-size engines have been tested for decades to give accurate data about their performance specifications. A sample dynamometer test of a full-size road car can be seen in Figure 1.1.

Developing a test bench for micro ICE will definitely revolutionize the world of model vehicles for both customers and manufacturers.

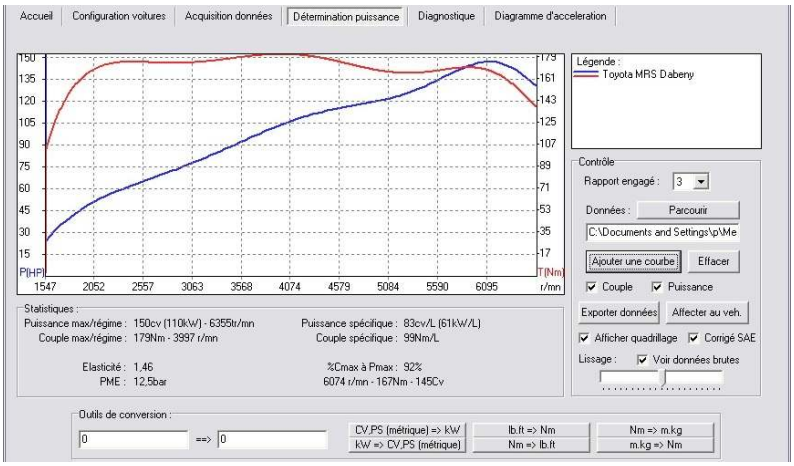

Figure 1.1: Power and torque curves for a Toyota MR-S (DynOBD software).

1.2 Micro Engines and their Applications

Micro engines, also known as model engines, are part of a much larger range of ICE. If classified in terms of dimensions, there are three major families, summarized in Table 1.1.

Type	Application	mass	Power range
Micro engine	Racing cars [1], model boats and aircraft	$\leq 1\,Kg$	$\leq 3\,kW$
Full-size engine	motorcycles, cars, fishing boats, trucks	*1 - 1 500 Kg*	*3 - 1000 kW*
	airplanes, locomotives, dams, large pumps	*1 500 - 100 000 Kg*	*1000 - 10 000 kW*
Marine engine	large cruise ships, oil tankers, freighters	*100 000 - 2 000 000 Kg*	*10 000 - 80 000 kW* [2]

Table 1.1: Engines classification regarding their dimensions.

Micro engines have been invented since the late XIX century. Thomas Ray Arden [3], born in New York in 1890, was passionate about them. He designed between 300 and 400 gasoline model engines sold through the 1920s. In 1939, he introduced his first reciprocating valve-in-piston engine, the revolutionary Mighty Atom .097. After that, he kept designing and improving his Atom engines (Figure 1.2) but only after World War II, his greatest discovery would take place.

Figure 1.2: Ray Arden holding one of his Atom engines for airpanes [3].

The war puts an halt on most model business and developments until its end in 1945. All of a sudden, thousands of troops return from war creating a demand for recreational items, specifically model airplanes, engines and anything that flew. At this point, methanol became available as an alternative model fuel mix and Ray starts developing methanol based fuel blends. At the time he is developing more powerful, lighter and extremely compact model airplane engines, now called Arden .099 and .199, a couple of his friends were running a spark ignition model engine on a methanol based mixture and, when they turned it off, the engine kept running. They found out that the ground strap of the spark plug had broken off and the center electrode was still glowing red hot. Ray and his friend Ben Shereshaw immediately start developing experimental glow plugs capable of sustaining the power cycle without burning out. So in 1947, Arden invented the modern day Glow Plug micro engine [3], which would revolutionize the industry of model engines.

A micro engine is part of a larger range of model engines, used in radio-controlled modelling to power model cars, boats and aircraft, as illustrated in Figure 1.3. Micro and model engines are often seen as synonymous but in this dissertation, a more conservative definition is being considered. Micro engines comprise only the single-cylinder that go up to 20 cc of displacement, produce up to 4.0 hp (3.0 kW) of power and reach up to 45 000 rpm.

(a) Model racing car with assembled micro engine.

(b) Starting the Glow Plug engine of a model airplane.

Figure 1.3: Applications of micro engines.

1.3 Objectives

The objective of the dissertation is to design, construct and instrument a test bench to test micro ICE. It must be designed to characterise micro engines up to 20 cc. They may differ in power and dimensions so it is imperative for the test bench to be robust and have adjustable supports. Finally, an engine is being tested to validate the design. The test bench must be able to provide:

- **Torque vs RPM diagram**
- **Power vs RPM diagram**
- **Fuel Consumption rate vs RPM diagram**

The test bench must be practical and easy to use. By implementing several sensors and actuators, it should reach an adequate level of automation for the operator to have no concerns about safety or accuracy.

The objectives of the dissertation are schematically given in Figure 1.4.

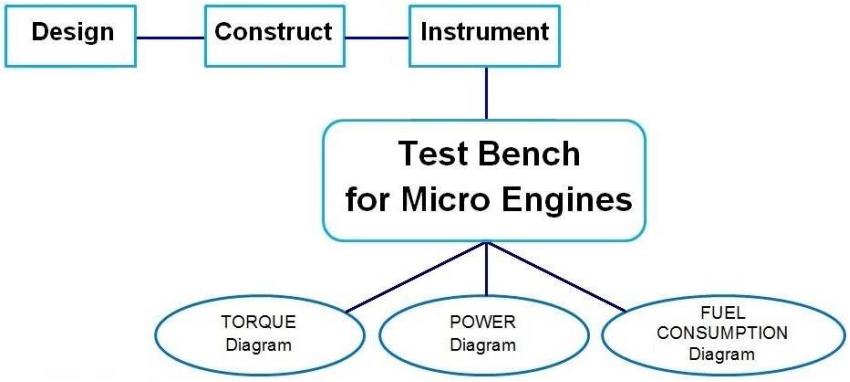

Figure 1.4: Objectives of the dissertation.

A 3.5cc micro engine of a model car will be tested to demonstrate and validate the design.

1.4 Thesis Outline

This chapter makes reference to the motivation for the dissertation, its objectives, and gives a general definition of micro engines and their applications.

The Micro Engines Overview chapter (2) shows a general definition of ICE and a thorough definition of the micro engines working principle, as well as some performance specifications.

In the Engine Test Benches chapter (3), a complete review of all types of test benches is given. The main ones are compared to each other to decide which to implement for designing the test bench.

In the Conceptual Design chapter (4), a list of the main technical requirements is given and then a review of possible solutions to attend the design at hand. By comparison, the most viable solution is chosen.

The Data Acquisition System chapter (5) shows all the sensors and actuators chosen for instrumenting the test bench.

In the Detailed Design chapter (6), the mechanical design for the test bench is addressed. Detailed sizings and a structural analysis are made.

The Assembly and Wiring Layout chapter (7) gives all details for production, assembly and wiring of the test bench. A program to read the collected data is also created with an interface for the operator.

Some sample test runs are given in the Demonstration Test Runs chapter (8) to validate the whole design.

Finally, the Conclusion chapter (9) summarizes the main achievements of this thesis and points future possible developments.

Chapter 2

Micro Engines Overview

The most common micro engine is the glow plug engine, known this way because of the method of fuel ignition, a glow plug. An example is shown in Figure 2.1. Even though it deserves a bit more of attention, micro engines yet comprise spark ignition and diesel engines.

Figure 2.1: Glow plug engine of a model car [1].

2.1 Internal Combustion Engines

An engine is an equipment able to transform any type of energy into mechanical energy. This section is about ICE, thermal engines which produce mechanical power by means of combustion of a fuel inside the combustion chamber. There are two major types of ICE, which will be further discussed: the Spark Ignition engine (SI) and the Compression Ignition engine (CI), also known as Diesel engine [4]. These are reciprocating engines, meaning the combustion is intermittent and obeys a given cycle. The piston is connected to a crankshaft and, as it reciprocates up and down, it causes the crankshaft to rotate giving the output shaft a rotational torque [4]. There is another important group of ICE, where the combustion is continuous and occurs in a different component (different from the one where the work is made), the gas turbines, which will not be discussed.

Spark Ignition engines (SI) are characterized by an ignition accomplished by a spark in the combustion chamber, which ignites the mixture (air + fuel). SI and CI engines differ in their thermodynamic cycle. The working cycle of SI engines, Otto Cycle [2], comprises four thermodynamic evolutions within the Compression and Power strokes: **1) Isentropic compression** (1-2), **2) Constant volume heat addition** (2-3), **3) Isentropic expansion** (3-4), **4) Constant volume heat rejection** (4-1).

Compression Ignition (CI) or Diesel engines are characterized by a self ignition process. Instead of a mixture, there is only air in the combustion chamber prior to combustion and what happens is a fuel injection, which reacts with the present molecules of oxygen at high temperature and pressure causing the mixture to self ignite. The working cycle of CI engines, Diesel Cycle [2], comprises: **1) Isentropic compression** (1-2), **2) Constant pressure heat addition** (2-3), **3) Isentropic expansion** (3-4), **4) Constant volume heat rejection** (4-1).

More details can be found in [4].

So far, the four-stroke engine has been the main subject but, as it was referred earlier, there are the two-stroke engines, which will be the real case study being the most common ones in micro engines. The two-stroke engine has the same principles of power as a four-stroke. It is also a reciprocating ICE that experiences all the four main stages (Intake, Compression, Power and Exhaust) by means of combustion. However, it makes them in a single ”loop” completing the cycle in just two strokes, due to the fact that the intake and exhaust are simultaneous and take place between the two single strokes within the working cycle: Compression (ascendant movement) and Power (descendent movement). At each rotation of the crankshaft, the engine completes a cycle. The combustion process is similar in a two- and four-stroke engine, taking place when the piston is in the TDC by a spark (SI) or fuel injection (CI).

2.2 Glow Plug Engine

The main subject of the dissertation is the glow plug micro engine. This is a two-stroke ICE which resembles more to a SI engine, since the mixture (methanol + nitromethane + air) is introduced in the combustion chamber prior to combustion and it requires as well an ignition source for explosion, although there is no need for a spark.

Like the name suggests, the ignition is accomplished by a glow plug (Figure 2.2), a durable helical wire filament, recessed into the plug tip, made of platinum which has a catalytic effect in the combustion [5]. To start the engine, an electric current runs through the plug, the platinum filament glows hot and the mixture ignites due to high heat. After combustion and while the piston runs the power and compression strokes, the wire remains hot due to thermal inertia and, mainly, due to the catalytic combustion reaction of methanol remaining on the platinum filament. This way, the glow plug remains hot, allowing it to ignite the next charge, thus sustaining the working cycle. At this time, the electrical connection is no longer needed.

Figure 2.2: Typical glow plug of a glow plug engine.

2.2.1 Two-Stroke Glow Plug

Despite the fact there are two- and four-stroke glow plug engines, the drivers choice has been the two-stroke for its high power to weight ratio.

As it can be seen in Figure 2.3, the working cycle is similar to a full-size two-stroke engine but there is an important difference in the port system, namely, the route of the mixture and the cylinder design. There is no inlet port on the engine block, the mixture enters the crankcase directly from the inside of the crankshaft and then enters the combustion chamber through the intake port [5].

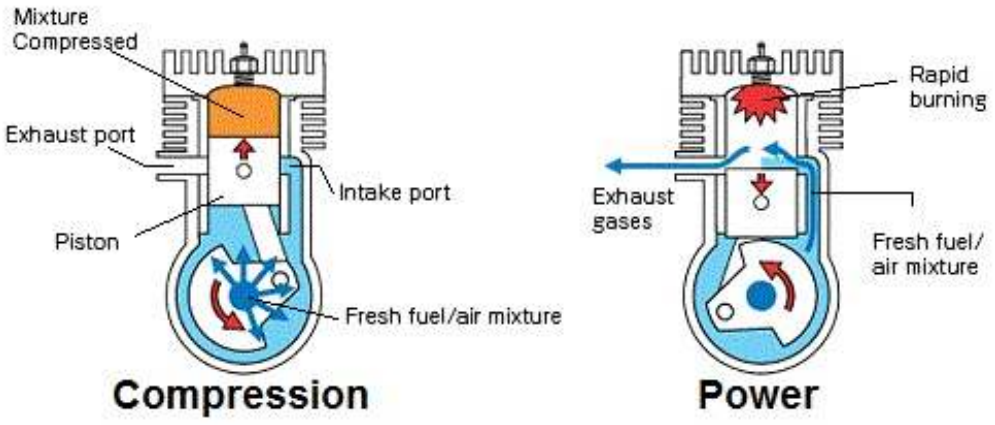

Figure 2.3: Working cycle of a two-stroke micro engine.

The main components of this engine are listed in Figure 2.4 and Table 2.1.

Intake and Exhaust System

It is very important to have a well-defined flow pattern within the combustion chamber because of the enormous rotational speeds experienced by these engines. The intake and exhaust transfers are simultaneous and it is imperative to have an effective scavenging to promote a more complete replacing

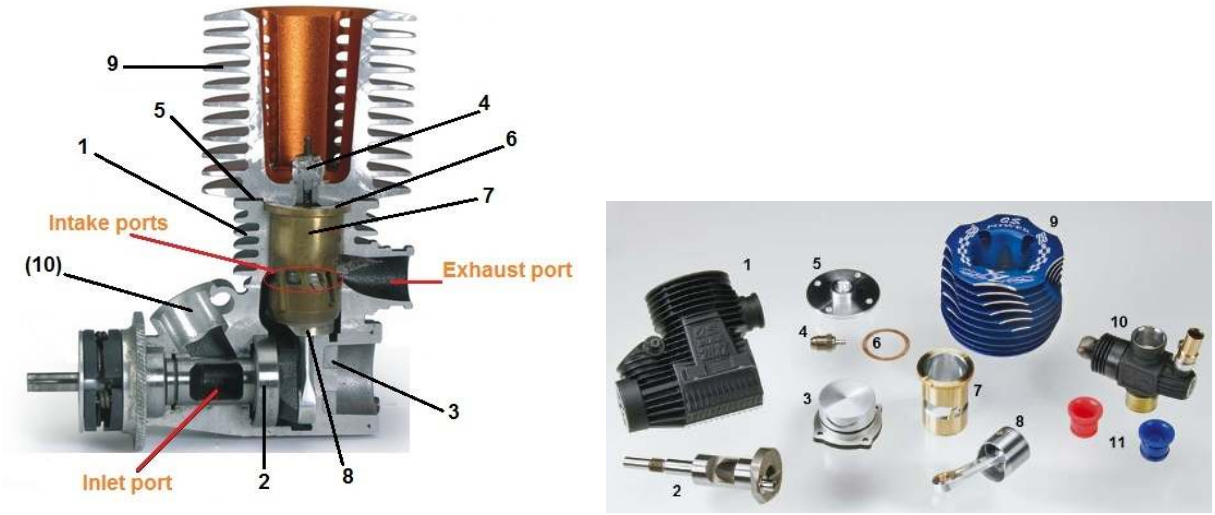

(a) Mid-section of a Glow Plug engine.

(b) Glow Plug components.

Figure 2.4: Listed parts of a glow plug micro engine.

Component	Definition	Function
1	Engine block	Harbors the cylinder and all moving parts
2	Crankshaft	Provides the output rotation. Delivers air/fuel mixture
3	Cover plate	Allows access for disassembly and maintenance
4	Glow plug	Heating element to ignite the mixture
5	Inner head	Attached on top of the engine block, locates the glow plug
6	Head Gasket	Accommodates the top of the cylinder and secures the desired clearance volume
7	Cylinder	Piston liner. Prevents wear on the engine block
8	Piston	Reciprocates up and down causing the crankshaft to rotate
9	Outer head	Cools the engine
10	Carburetor	Mixes air and fuel and directs the mixture
11	Carburetor reducer	Adjusts the air stream to enter the carburetor

Table 2.1: Definition and function of the glow plug components.

of the burned charge with a fresh charge. The intake and exhaust ports are cutted in the cylinder wall but, in the case of micro engines, the shape and location of the ports are slightly different, promoting the desired more efficient transfer of intake and exhaust gases. The system is called ”Schnuerle Porting” which suggests a loop (or backflow) scavenging. This port system is named after its inventor Adolf Schnurle [6] and it is implemented in two-stroke micro engines since the 1970s.

The ports are now located along an entire section of the cylinder wall. There is one exhaust port and, right next to it, at least two smaller intake ports on either side of it and more in the opposite side (Figure 2.5). This way, the gases are encouraged to move in several horizontal loops, flowing across the piston crown, while the fresh charges are entering the combustion chamber. The burnt gases are pushed out through the exhaust port and, because this is slightly higher, there is a simultaneous venturi effect which tends to suck in the mixture while they are exiting (better scavenging than the obsolete crossflow) [6].

(a) Cylinder with 3 intake ports, components of the 21XZ-B VII O.S. Engine [1].

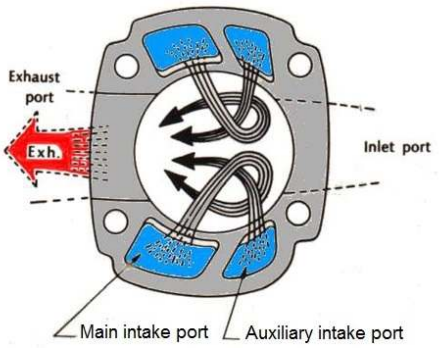

(b) Schematic of the gas flow.

Figure 2.5: Intake and exhaust ports in a micro engine cylinder. Loop scavenging.

2.2.2 Admission Process

The mixture between air and fuel before admission is accomplished by a carburetor. It is used a Variable-Venturi carburetor (Figure 2.6). It has a throttle valve and a needle valve secured to a slide, which moves inside the carburetor according to the throttle position [7]. The slide is connected to a mechanical arm (throttle linkage). By varying the venturi cross section, it controls both air and fuel quantities in a direct relation. The needle valve allows a precise regulation of the fuel flow, since it uses a tapered pin to gradually open a space at the end-section of the needle seat, from which glow fuel is entering the carburetor.

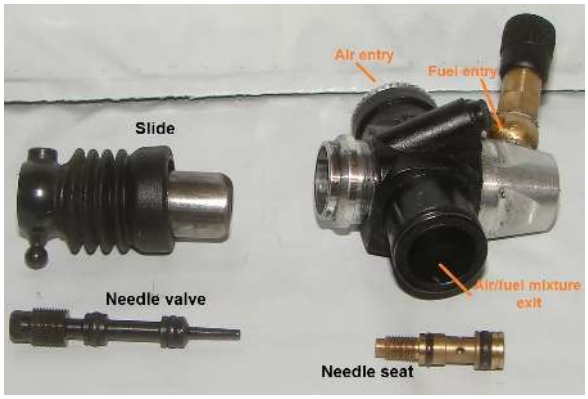

(a) Disassembled carburetor

(b) Tuning parts of the carburetor.

Figure 2.6: Carburetor of a glow plug micro engine.

The main components and their function are listed in Table 2.2.

Components	**Function**
Throttle linkage	Mechanical arm to actuate the carburetor slide
LSN (Low Speed Needle)	Controls air and fuel mixture for idle and zero to partial throttle
HSN (High Speed Needle)	Controls air and fuel mixture for partial to full throttle
Idle speed screw	Regulates the venturi opening gap to allow more or less air to mix with fuel during idle speed

Table 2.2: Function of the carburetor tuning parts.

2.2.3 Starting System

The starting of these engines is accomplished by heating the glow plug with a ”glow starter” (a small and portable rechargeable battery that connects directly on the glow plug), which can be seen in Figure 2.7 a). It applies a direct current of 3 amperes and 1.5 volts on the glow plug, initially heating the filament (now glowing red hot). The engine is then spun from the outside using a manual crank or a purpose-built electric motor (Figure 2.7 b)), introducing fuel in the combustion chamber [5]. Once the fuel has ignited and the engine is running, the electrical connection is removed.

(a) Glow starter (b) Electric motor

Figure 2.7: Typical electrical tools to start a glow plug engine.

2.3 Fuels and Lubricants

The fuel used in micro engines is not entirely pure as in full-size engines (generally). Since there is no room for external cooling systems and independent oiling, the fuel contains a percentage of oil to lubricate all moving parts in the engine, from the carburetor to the exhaust port, and also to dissipate heat, cooling down the engine and its surroundings. In addition, there are some ingredients added to improve engine performance.

The fuel used in glow plug engines is a mixture of methanol, nitromethane and oil, called ”glow fuel”. The main constituent is methanol (CH_3OH) [8], that is why it is consider an alcohol fuel.

Methanol is an alcohol, whose burn is capable of achieving large amounts of power. In fact, it offers an increased thermal efficiency and increased power output (compared to gasoline) due to its higher octane number, which allows the fuel to withstand more compression before detonating, and higher heat of vaporization. At the same time it provides the bulk of the fuel, it also works as a solvent for the other constituents. Its vapors are responsible for keeping the glow plug glowing red hot by a catalytic reaction with the platinum wire.

Nitromethane (CH_3NO_2) is used as a power increaser. Although the same given amount of nitromethane contains less energy than methanol, it increases the amount of available oxygen in the combustion chamber, allowing the engine to draw in less air and more fuel [5]. This increased amount

of fuel results in an higher power output and also helps to cool the engine. Despite its improvement in engine performance, nitromethane is expensive and, in some countries, often difficult to obtain, so some glow fuels have no nitromethane at all.

The most commonly used lubricants are castor oil or synthetic oils, sometimes a mixture of both. The typical glow fuel contents are given in Table 2.3.

Ingredients	Content
Methanol	60-90%
Nitromethane	0-30%
Oil	10-20%

Table 2.3: Typical glow fuel contents.

2.4 Emissions and Noise

In terms of emissions, micro engines such as the glow plug that run on methanol (mainly) tend to be more environmental friendly. They also produce the same harmful emissions like NOx, CO2, CO and particles, but in smaller amounts because they run on alcohol. Tests have been made using E85 fuel (85% ethanol) in SI engines to assess the results on burn emissions [9]. It showed that ethanol has the potential to reduce NOx emissions by 25-32% and CO by 12-24%. CO2 also decrease due to the lower carbon-to-hydrogen ratio of the alcohol. Toxic emissions of benzene and 1.3 Butadiene also decrease.

Glow plug engines tend to make a lot of noise. That is because, in some cases, combustion may still be occurring when the exhaust port is uncovered, causing a significant amount of noise. It is related to the rich mixtures that cause the combustion of the increased amount of fuel to take a bit more time, until a point where the piston has already reached the exhaust port line within the power stroke.

2.5 Performance Specifications

The performance specifications of micro engines are naturally considered before acquiring one, being the maximum power the most important for drivers. It is possible to see in Table 2.4 why the glow plug engine is, usually, the racing drivers choice. It is the type of micro engine that generates the largest amount of power for a given displacement.

The combustion accomplished by the glow plug is much faster than in a SI engine. Also, it allows to throttle over a wider range of powers than the diesel engines, despite their better fuel efficiency and superior torque.

Fuel consumption is an important aspect, mainly for aircraft because it is unacceptable to run out of fuel during flight. Methanol has a low energy content (22 MJ/Kg) [8] and stoichiometric air/fuel ratio (6.42:1), so the fuel consumption in a glow plug engine is higher than with hydrocarbon fuels like gasoline (45 MJ/Kg) or diesel (48 MJ/Kg) for SI and diesel engines [4], respectively.

Vehicle	Engine type	Displacement [cc]	Rotation [RPM]	Max Power [HP]
Car	2-stroke Glow Plug	2.0	5000 - 45000	0.70 - 1.72
		3.0	3000 - 40000	1.33 - 2.40
		3.5	3000 - 45000	1.77 - 2.71
		4.5	4000 - 38000	3.26
Boat	2-stroke Glow Plug	3.0	3000 - 32000	1.33
		3.5	3000 - 45000	1.28 - 2.71
Helicopter	2-stroke Glow Plug	8.0	2000 - 20000	1.87
		9.0	2000 - 20000	2.07 - 2.10
		15.0	2000 - 16500	3.55
		17.0	2000 - 16500	3.75
	2-stroke SI	15.0	2000 - 16000	2.76
Airplane	2-stroke Glow Plug	5.5	2500 - 19000	1.28
		10.5	2500 - 16000	1.73
		15.5	2000 - 16000	2.86
		20.0	1800 - 9500	3.1 - 3.3
	4-stroke Glow Plug	10.0	2400 - 11000	1.08
		13.0	2200 - 10000	1.28
		15.5	2100 - 11000	1.68
		20.0	2000 - 12000	2.07
	2-stroke SI	15.0	2000 - 15000	2.37
		20.0	1800 - 9000	2.60

Table 2.4: Performance specifications of micro engines [1].

O.S. Engine	Displacement (cc)	Fuel consumption (ml/min)
12 XZ	2.10	37
15 CV	2.49	40
18 CV	3.00	43
21 XZ	3.49	45

Table 2.5: Fuel consumption of micro engines [1].

The fuel consumption rates depend on many other factors like nitromethane content, air mixture, RPM, condition of the engine and atmospheric conditions. The values in Table 2.5 are for an average run floating between idle and full throttle regimes.

Despite the inferior power output of the 4-stroke micro engine (Table 2.4), they have a much better fuel efficiency and that is why they are largely used in model airplanes. Not in model cars where speed and bottom-end quick response are essential.

Chapter 3

Engine Test Benches

3.1 Overview of Test Bench Types

There are two main types of test benches for power assessment, commonly known as ”dynos” (from dynamometer): the engine and the chassis dynamometer. The engine dynamometers are either coupled directly to the engine or via gears/chain/belt and are used to measure power and torque output of an engine (Figure 3.1 a)). The chassis dynamometers are used to measure power output at the wheels, making the vehicle to drive on a set of rollers (Figure 3.1 b)).

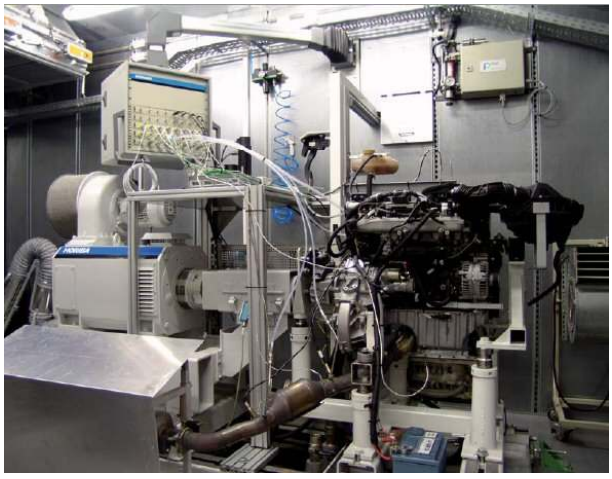

(a) Engine dyno [10].

(b) Chassis dyno [11].

Figure 3.1: Types of test benches.

According to the way of getting the data, these dynamometers are divided in two major groups: inertia dynamometer (also known as acceleration dynamometer) and steady-state dynamometer. The inertia dynamometer works by having the engine accelerate an inertial mass (often called flywheel) during a certain amount of time until the torque evolution is fully collected, meaning the engine has run its full power from idling to maximum rotational speed [12]. Steady state dynamometers use a brake (also named absorber or retarder) to apply a load to the engine and hold it at a constant speed against the open throttle, where an electronic "load cell" reads the torque transmitted to the brakes [13]. These two groups of dynamometers are briefly described in the following sections.

3.2 Engine Inertia Dynamometer

It is important to understand the physics of a dynamometer. The main goal is to obtain the power (P) diagram, which comes associated with torque (T) and rotational speed (ω) of the drive shaft. By measuring both, power is calculated as

$$P[W] = T[N.m] \times \omega[rad/s]\,, \tag{3.1}$$

where the conversion of angular velocity from the usual rotations per minute (RPM) to the SI units is given by

$$\omega = 2 \times \pi \times \frac{N[RPM]}{60}\,.$$

Torque is associated with the inertial mass that the engine is rotating and the rotational acceleration (α) of the drive shaft (from idle speed to full power). It gives an idea of the ability of an engine to rapidly accelerate the vehicle (or any other mass associated) to the desired power regime. In case of a flywheel, the instant torque is given by

$$T[N.m] = I[Kg.m^2] \times \alpha[rad/s^2]\,, \tag{3.2}$$

where *I* is the moment of inertia of the flywheel and shaft all together (although the inertia of the shaft itself might be negligible) and α is its angular acceleration.

With reference to Figure 3.2, the main components of an inertia dynamometer are:

1. **Engine**: Engine to be tested. Secured in the designated supports.
2. **Drive shaft**: Driven by the engine. Comprises the flywheel and the decoupler, required components for the test runs.
3. **Gear train**: Allows the drive shaft to rotate in a lower speed than the crankshaft.
4. **Decoupler**: Overrunning clutch responsible for the detachment of the flywheel from the engine. Allows it to slow down freely after closing the throttle.

Figure 3.2: Components of an inertia dynamometer.

5. **Flywheel**: Simulates the inertia experienced by the engine. It suffers the Torque applied by it.
6. **Bearing(s)**: Secures the drive shaft. In general, two bearings are used to support and allow free rotation with minimal friction.
7. **Fuel lines**: Allow fuel admission from a designated fuel tank.
8. **Throttle control**: Device to actuate the throttle, usually by a cable or mechanical arm.
9. **Brake**: In general, a braking system is installed to stop the flywheel. In alternative, it can rotate freely after a run and eventually stops due to friction.

3.2.1 Flywheel Specifications

The flywheel is the inertial mass that the engine has to accelerate. Depending on its shape, the moment of inertia relative to the rotation axis passing by its center can be evaluated as in Table 3.1 [14].

$I = 1/2 \times m \times R^2$	**solid cylinder or disc**
$I = 1/2 \times m \times ({R_1}^2 + {R_2}^2)$	**hollow cylinder or disc**
$I = m \times R^2$	**thin-wall hollow cylinder or ring**

Table 3.1: Moment of inertia for different shapes.

Inertia is proportional to the mass multiplied by the radius squared of the inertial mass. So to have a high inertia with less weight, it is better to enlarge the flywheel radius rather than increase its mass. For example, doubling the radius increases the previous inertia four times with the same mass. A larger and thinner flywheel is perfectly acceptable as long as the technical requirements at hand in terms of dimensions are respected.

The amount of inertia to implement is critical to get good results. In this type of test bench, the engine is tested by accelerating it from idle speed to maximum speed at full power. The acceleration time (Δt) should be around 10 seconds and there is a reason why the test should not be too fast nor to slow. If it is too fast, the engine own inertia plays a significant part in the reading and the run will not be very representative of the real operating conditions. If the acceleration is too slow, the engine temperatures will rise and detonation can occur [14].

If testing engines with large power ratings, the flywheel inertia can be a large compromise. So for this purpose, it is common to use not one but a set of flywheels. This way it is possible to change the flywheels used in the dynamometer to maintain a reasonable acceleration time when running smaller or larger engines.

The inertia necessary for the flywheel is related to the rotational speed of the drive shaft. The higher the rotational speed, the lower inertia must be. Although it is much safer to have a higher inertia in the flywheel operating at lower rotations per minute. To ensure that, it is common to use a reduction gear to connect the crankshaft to the drive shaft allowing a lower output speed.

The output speed is related to the inertia by the angular acceleration. According to the technical requirements of the test bench, a study is made to assess the ideal rotational speed of the drive shaft. From kinematics, the angular velocity and acceleration are related by

$$\alpha = \frac{\mathrm{d}\omega}{\mathrm{d}t}\,. \tag{3.3}$$

Knowing that and then again considering a constant angular acceleration, the mean angular acceleration can be estimated by

$$\alpha = \int_0^f \frac{\mathrm{d}\omega}{\mathrm{d}t}\,\mathrm{d}t = \frac{\omega_f - \omega_0}{\Delta t}\,, \tag{3.4}$$

where ω_0 and ω_f are the initial and final angular velocities, respectively, and Δt the acceleration time.

The ideal rotational speed of the drive shaft depends on factors like bearing and gearing speed limits. Once it is determined, and knowing the expected maximum rotational speed of the engine, an intermediate gearing (direct or with a chain/belt) is used with the desired gear ratio given by

$$i = \frac{\omega_1}{\omega_2}\,, \tag{3.5}$$

where ω_1 is the maximum crankshaft speed and ω_2 the maximum drive shaft speed.

Controllable Inertia Flywheel

A flywheel can be designed with an apparatus that permits its rotational inertia to be controlled during rotation, as exemplified in Figure 3.3.

The flywheel attached to the drive shaft has two control masses attached such that they can move radially, approximately orthogonal to the rotational axis, in slots in the flywheel structure. The control masses are mechanically attached to a shaft collar which rotates with and axially translates on the

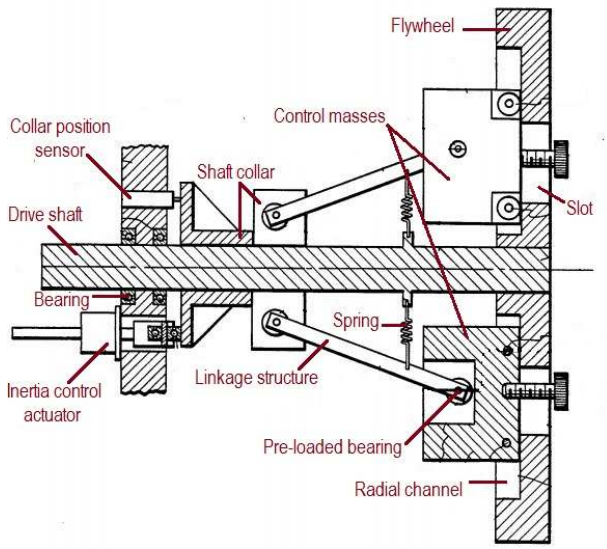

Figure 3.3: Schematic of the controllable inertia flywheel [15].

surface of the splined drive shaft. An electrical actuator controls the axial position of the shaft collar on the drive shaft and the resultant radial position of the control masses on the flywheel [15].

3.2.2 Flywheel Balancing

A flywheel is never entirely balanced and, because of that, radial forces are generated causing vibration and fatigue problems. This is why it is imperative to conduct a balancing analysis for the flywheel to reduce those vibrations and ensure a stable rotation, especially in high speed cases. The balancing consists in a distribution of small masses to reduce the radial forces. The goal is to reach an equilibrium where those masses compensate the geometric flaws in the flywheel due to errors in fabrication or variable density.

There are two kinds of balancing: static and dynamic. Like the name suggests, the static balancing is made by observing the behaviour of the flywheel in a static position. It is supported on two low friction points and forced to rotate slowly. When it stops, it will oscillate at an equilibrium position where the unbalanced point is in the lower side. To solve the unbalance, masses are added or removed in strategic points to ensure radial balancing. They should be located away from the rotation axis to cause higher effect. Otherwise, bigger masses are required. The dynamic balancing consists in conducting an equilibrium of moments to prevent vibration and undesired solicitations on the supports. For that, the masses must be evenly distributed radially and across the flywheel. They are strategically located in given balance planes for a null polar moment of inertia. These are illustrated in Figure 3.4.

Physics

The flywheel rotates at a given angular speed, ω, in reference to a fix axis of rotation, z. The polar moment, M_O, in order to a fix pole O (Figure 3.5) is given by the derivative of the angular moment, H_O,

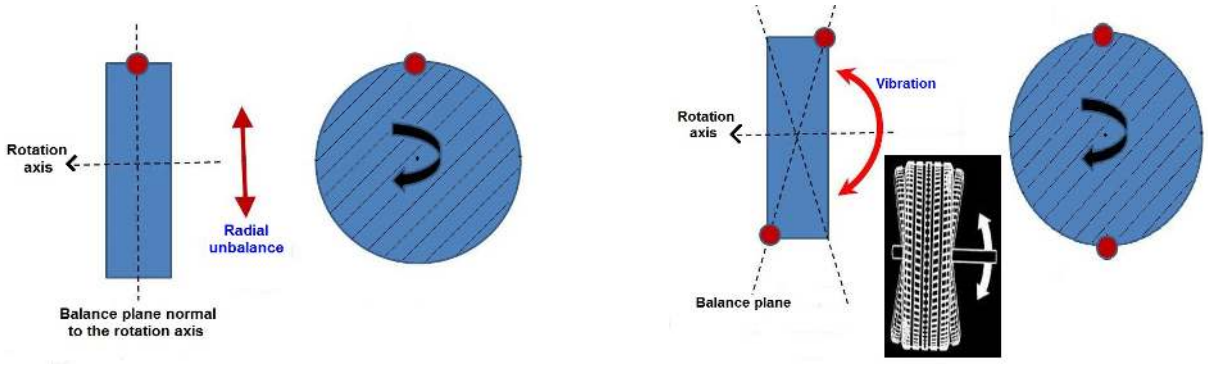

(a) Static balance.

(b) Dynamic balance.

Figure 3.4: Types of balancing [16].

$$\vec{M_O} = \frac{d}{dt}\vec{H_O} = \frac{d}{dt}([I_O]\,\vec{\omega}) \tag{3.6}$$

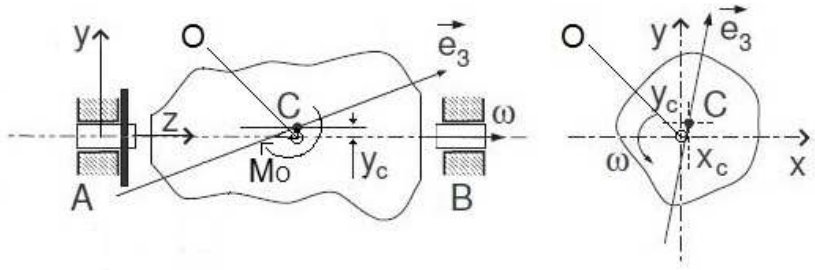

Figure 3.5: Physics involving an unbalance flywheel [16].

The equation of the angular moment in the axis system of the flywheel (*O, x, y, z*) is given by [16]

$$\vec{H_O} = -\,J_{xy}\omega\vec{e_x} \;-\; J_{yz}\omega\vec{e_y} \;+\; J_{zz}\omega\vec{e_z} \tag{3.7}$$

where $J_{xy} = \int_M x.y\,dm\;;\; J_{xz} = \int_M x.z\,dm\;;\; J_{zz} = \int_M (x^2+y^2)\,dm$

Differentiating in order to time for a constant angular speed, the polar moment of inertia is given by

$$\vec{M_O} = -\,J_{xz}\omega^2\vec{e_y} \;+\; J_{yz}\omega^2\vec{e_x}\,. \tag{3.8}$$

According to the centroid theorem [16], the radial force is given by

$$F = M\frac{d^2}{dt^2}\,(x_c e_x) \;+\; M\frac{d^2}{dt^2}\,(y_c e_y) = -\,Mx_c\omega^2\vec{e_x} \;-\; My_c\omega^2\vec{e_y} \tag{3.9}$$

When M_O and F are equal to zero, the radial forces are null meaning the axis of rotation is actually a central inertia axis. At this point the flywheel is balanced.

Standards

The balancing of rotation masses must obey to given standards according to its application and rotation speed. Vibrations and dynamic solicitations will always exist but they must be corrected to acceptable limits. The standard ISO 1940 refers to the balancing quality of rigid rotors [16]. On the basis of world-wide experience and similarity considerations, balance quality grades (G) have been established which permit a classification of the balance quality requirements for typical machinery. These grades go from the minimum G 4000 to the highest precision G 0.4 as it can be seen in Table 3.2.

Grade	Equipment
G 4000	crankshaft of marine engines
G 250	crankshaft of 4-cylinder diesel engines
G 40	automobile wheels; drive shafts
G 6.3	flywheels; pump rotors
G 2.5	gas turbines; CNC actuation
G 0.4	high precision spindles; gyroscopes

Table 3.2: Different degrees of the balancing standard.

The "G" number is the product of the permissible unbalance (center of gravity displacement, e_{per}) and the angular velocity (ω) of the rotor at maximum operating speed. It is constant for rotors of the same type,

$$G = e_{per}[mm] \times \omega[rad/s]\,. \tag{3.10}$$

This is based on the fact that geometrically similar rotors running at the same speed will have similar stresses in the rotor and its bearings.

The permissible residual unbalance (U_{per}) can be derived on the basis of a selected balance quality grade, *G*, by the following equation

$$U_{per}[g.mm] = 1000\,\frac{G \times m[Kg]}{\omega[rad/s]} \tag{3.11}$$

where *m* is the rotor mass.

Balancing methods and equipments

The most common way to conduct a static balancing is using the gravitational method. The flywheel rotates freely until it stops in a given equilibrium position. The goal is to add masses on top or to remove mass on the lower side in an iterative process until the flywheel ceases to present repeated equilibrium points. For dynamic balancing it is common to use two types of machines: fixed supports or flexible supports. The results determine where to add or remove mass.

Fixed supports The flywheel rotates in reference to a fixed geometric axis and the solicitations in the supports are measured through piezoelectric sensors or extensometers. The rotation speed must

be considerably less than the critical rotation speed to prevent deflections.

Flexible supports The flywheel behaves as if free in space. The supports move due to the experienced solicitations and its displacements and speed are measured. The rotation speed must be considerably higher than the critical rotation speed to get accurate results. Note that the supports are highly flexible to prevent damage (Figure 3.6).

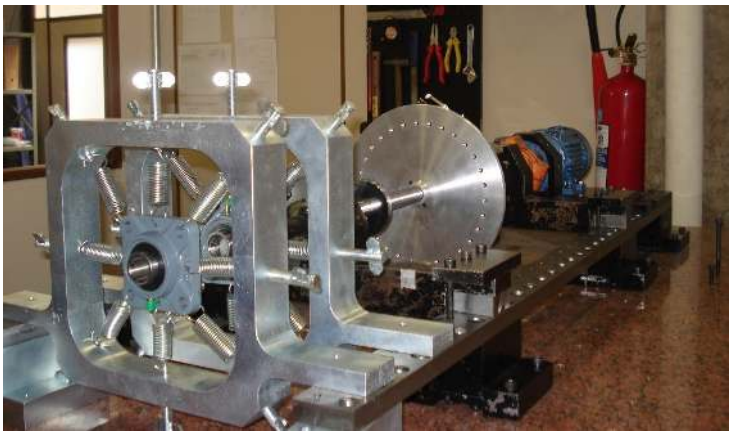

Figure 3.6: Balance equipment of flexible supports [17].

3.2.3 Safety Mechanisms

Braking System

A dynamometer must always have a braking system for safety. In an emergency situation, the operator must be able to stop the drive shaft to prevent any kind of damage or serious injury. Besides, if one is able to brake the flywheel, the drive shaft will stop much faster between runs, saving a lot of time in testing. Waiting for the flywheel to gradually stop by itself can take a long time because only frictional losses are occurring.

The braking of a flywheel is often accomplished through a disc brake. There are two main regimes regarding this type of braking: uniform wear and uniform pressure. The first represents the behaviour of used brakes, where the initial wear has taken place and the disks have worn down to a point where uniform wear is established. The second refers to operating conditions where uniform pressure can be assumed over the area of the disk. This last one is the regime that best represents the braking of a flywheel comprising low torques, because it is safe to assume that this will not worn down, at least significantly, so pressure is uniform $p = p_a$.

Considering the annular pad (Figure 3.7), the applied force is given by

$$F = \int p \, \mathrm{d}A = p \times A_c = p_a \times (\theta_2 - \theta_1) \int_r^R r \, \mathrm{d}r = p_a \times \frac{1}{2}(\theta_2 - \theta_1)(R^2 - r^2)\,, \tag{3.12}$$

where p_a is the constant applied pressure, A_c the contact area, r and R define the inner and outer pad radius, and θ_1 and θ_2 define the initial and final circumferential pad angles.

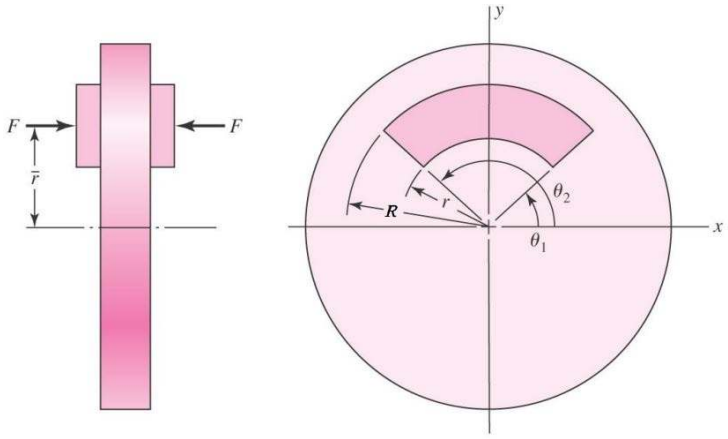

Figure 3.7: Disc brake with two annular pads.

The braking torque produced is given by

$$T = \int r\, F_a \,\mathrm{d}r = \int r\, \mu\, F \,\mathrm{d}r = (\theta_2 - \theta_1)\, \mu\, p_a \int_r^R r^2 \,\mathrm{d}r = \frac{1}{3}(\theta_2 - \theta_1)\, \mu\, p_a (R^3 - r^3)\,, \tag{3.13}$$

where F_a is the friction force and μ the friction coefficient.

The braking torque can be related to the required force by combining equations (3.12) and (3.13), yielding

$$T = \frac{2}{3} F \mu \frac{R^3 - r^3}{R^2 - r^2}\,. \tag{3.14}$$

The torque is for a single pair of mating surfaces. This value must therefore be multiplied by two, the number of pairs of surfaces in contact in the case of Figure 3.7. Finally, equation (3.14) is solved in order to F to find the required force.

The brakes are to be used continuously to gradually slow down the drive shaft and attached flywheel. If the brakes are applied too hard, it causes an high torsion load along the shaft and, if they suddenly stop the flywheel, the test bench frame can flip over or damage the supports. Although it dissipates a lot of energy, the braking system has time to cool down between runs.

For use in a micro engine dynamometer, the brakes are only mechanical because the inertial mass is not that high when compared to the large flywheels used in dynamometers for full-size engines, so the required force F is low. The disc brake is to be mounted on the flywheel or near it. Once again, mounting requirements are to be considered, like load points or limits. The most common methods of actuation are by lever, cable or pedal. For testing micro engines, it is very important for the brakes to be perfectly aligned to maintain the needed gap for a free motion. If the brake pads are ”dragging” on the disc, power losses may occur leading to inaccurate results.

Overrunning clutch

If the engine does not have a clutch to actuate and disconnect its output power from the drive shaft, a one-way (overrunning) clutch must be implemented to allow the engine to stop or quickly return to idle

speed after a run, while the flywheel is still rotating. Due to its overrunning ability, only the engine can power the drive shaft and never the other way around [18].

If there was no clutch, the engine would be forced to act as a brake, which could damage it. Excessive engine braking can be hard on an engine due to internal stresses and lack of lubrication in case of two-stroke engines. At the end of the run, the engine turns to closed throttle conditions and, in a two-stroke, the lubrication applied within the air/fuel mixture ceases to exist or remains minimal.

The one-way clutch usually consists on an inner-ring and an outer-ring divided by a device. In Figure 3.8, this device are trapped rollers that only allow the inner-ring to drive the outer-ring in the shown direction. When the inner stops, the outer will overrun it because of the decoupling of the rollers.

Figure 3.8: Outer ring of a trapped roller clutch (overrunnig).

A centrifugal clutch can also work as a safety mechanism if the drive shaft, for some reason, exceeds the expected rotational speed or a determined value of torque. If so, the clutch is configured to be actuated and slip preventing any kind of damage.

To start the engine through the flywheel, the clutch must be locked, which is not possible with a normal one-way clutch. So if one is to be used in the drive shaft of a micro engine inertia dynamometer, room has to be left available to start the engine directly on the crankshaft.

3.2.4 Data Collection

For data collection, sensors are implemented to assess engine rotational speed by accelerating the inertial mass from idle to maximum speed. Knowing the exact amount of inertia being driven, the data is then displayed on a PC, through an acquisition board, to obtain accurate power and torque diagrams. To avoid connecting the sensors directly to the engine, which can be near to impossible especially in micro engines, the software used to present the data may consider the gear ratio between the crankshaft and drive shaft, allowing to store the correct values of torque and rotation even with the sensors mounted on the drive shaft. Possible slipping within the clutch, when present, has to be taken into account. In these cases, the best solution is to set the sensors directly on the crankshaft.

RC nitro [19] has published an article about the 18 TZ-X O.S. micro engine, used in model cars. It shows a dynamometer test carried out for power and torque evolutions, whose results are shown in Figure 3.9. As it can be seen, it gave a maximum power of 2.28 BHP (Break Horse Power). Accordingly to the O.S. Engine catalogue [1], it should be around 1.77 HP. This disparity clearly illustrates the need to define a standard testing procedure for micro engines.

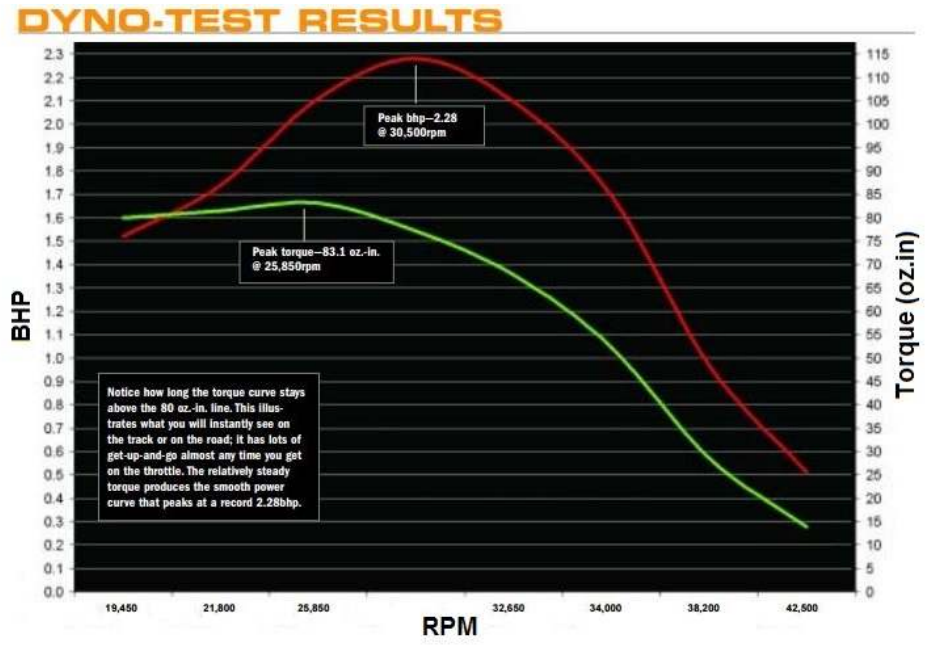

Figure 3.9: Dyno test results for a glow plug micro engine [19].

Inertia dynamometers measure engine performance during a fixed rate of acceleration (usually full throttle). This acceleration testing duplicates better the real world, where engines are seldom operated at steady RPM or load. They also allow an operator to conduct more tests and data collecting per unit day.

Current weather conditions like temperature, humidity and absolute barometric pressure should also be input to the software, for the data to be corrected to standard day conditions. This will allow consistency in the results as the environmental test conditions change.

Not just accuracy but also repeatability are very important. If a company needs to test a wide range of engines, the results must be consistent at each run. Sometimes it does not matter if the diagram has a perfect curve, what matters is maintaining the same conditions at each run so that we can get viable results. Inertia dynamometers tend to offer higher repeatability than steady state dynamometers because, in contrast to the steady state dynamometers, they have nothing that alters the conditions of data collection like a given load or speed. These conditions can be hard to maintain along several tests.

3.3 Steady State Dynamometer

Steady-state dynamometers use power absorbers to apply a given load to the engine and read the torque transmitted by maintaining it at constant RPM.

There are several types of steady-state dynamometers accordingly to the power absorber used, namely: fan dynamometer, eddy current dynamometer and electric motor dynamometers. Some of them are more historical while others are largely used nowadays. A summary of their characteristics, to understand their differences, capabilities and limitations, follows [14]:

- **Fan dynamometer**: A fan is used to blow air to provide engine load. The absorbed torque by the fan brake may be adjusted by changing the gearing or by restricting the airflow through the fan.
- **Eddy Current dynamometer**: This is an electromagnetic brake that allows very precise load and speed control (+/- 1 to 2 RPM). It is currently the most common absorber used in modern chassis dynamometers. It requires an electrically conductive core, shaft, or disc moving across a magnetic field to produce resistance to movement. The electromagnet voltage is usually controlled by a computer, using changes in the magnetic field to match the power output being applied.
- **Electric Motor dynamometers**: In these dynamometers, the absorber is an AC or DC electric motor. They can operate as a generator that is driven by the engine or as a motor that drives the engine. The rotational inertia of the absorber is transmitted by a "load cell" transducer that provides an electrical signal proportional to torque. The control unit for an AC motor is a variable-frequency drive, while for a DC motor is a DC drive.

In Figure 3.10 it is possible to see two examples of steady-state dynamometers.

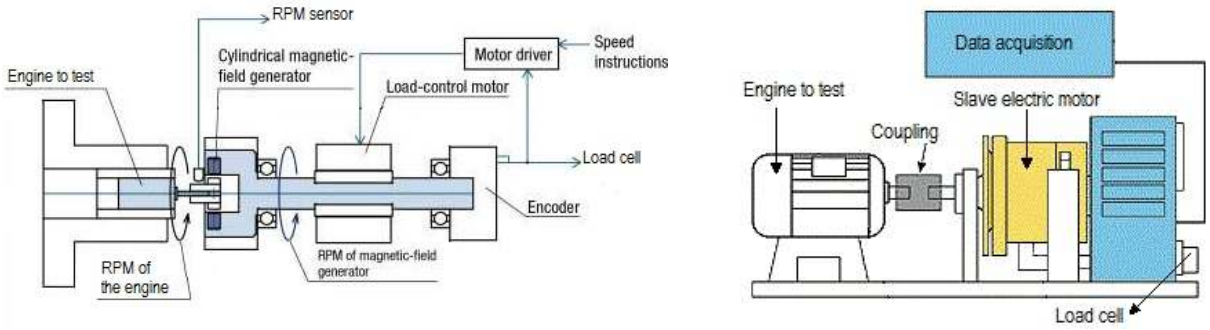

(a) Eddy current dyno. (b) Electric motor dyno.

Figure 3.10: Common Types of steady-state dynamometers.

3.3.1 Test Types

Steady-state tests are taken at constant speed or at constant load on the engine, depending on its objective. Generally, they produce the most reliable data in terms of accuracy, even though they require more complex systems [14].

A constant-speed test is one of the most convenient ways to establish a performance map or establish the best mixture and spark requirements for SI engines. In this test, the throttle increases or decreases torque while the absorber varies load to maintain the engine at constant RPM. At each of the various throttle positions, the parameters for engine control will vary as well.

At constant load, the test is conducted maintaining the engine at constant torque. In this case, throttle position variations will change the value of RPM. The more powerful the engine, the more quickly it can raise RPMs under a given load. These tests are common for testing an engine for a particular application with an expected load. It will determine how various engine setups handle a typical load encountered in the job in question.

Both constant speed and constant load testing require load cells to read or control torque values, respectively, and speed sensors. So steady-state dynamometers require a more complex data acquisition system than inertia dynamometers. The more precise the absorber is in maintaining test conditions, the more accurate the results will be.

The added complexity of these dynamometers reflects in their higher acquisition and operating costs.

3.4 Comparison Between Dyno Types

Figure 3.11 presents a chart of RPM vs time for a steady-state test at constant speed and for an acceleration test. The inertia dyno shows a uniform slope of RPM from idle to maximum speed while the steady-state dyno gives a constant value of RPM for a given speed or several values if step testing. It is difficult to compare the results of these tests unless the tests were the same type (such as acceleration or steady state) and, only then, when at the same conditions or rates of change.

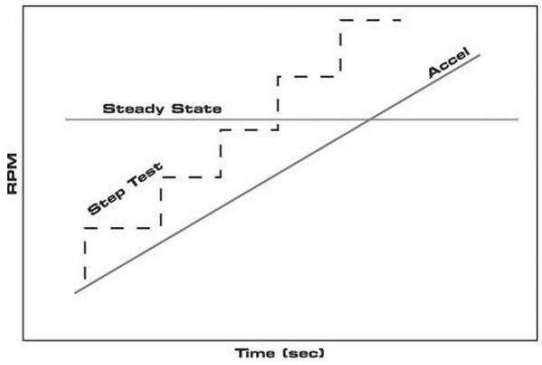

Figure 3.11: Comparison of RPM vs time charts between steady-state and inertia dynos [14].

It is unavoidable to compare the inertia to the steady-state dyno. To decide what the best solution is for the designer, their advantages and disadvantages need to be considered. This is summarized in Table 3.3. To comply with the objectives of this dissertation, the inertia dynamometer is the most viable choice. It represents better the real world conditions, while being simpler and cheaper [14].

Dyno type	Advantages	Disadvantages
Inertia	Cheaper and simpler. Good consistency and repeatability. Can be made portable, no need for large braking systems. Quick tests preventing wear and excessive temperatures on the engine. Simulates actual conditions just as if on the road because it is dynamic.	Drive shaft can reach excessive speed if not correctly designed. Requires gearing for adequate speeds. Requires a safety clutch to prevent engine damaging by having it brake the flywheel at closed throttle.
Steady State	Good accuracy. Safer because the testing is at constant speed or load. Ensures stable operating conditions while varying acceleration for mapping programmable engine management units.	More expensive and complex due to the load cell and precision required. Requires an heavy braking system to ensure constant speed for high torques. Requires a cooling system for the brake due to high heat generation. May cause the engine to overheat due to high running time against the brake under load. Repeatability can suffer if control electronics ”closed loop” system is not ideal.

Table 3.3: Advantages and disadvantages of inertia and steady-state dynamometers.

Chapter 4

Conceptual Design

4.1 Technical Requirements

The main goal of this study is to build an efficient test bench to accurately characterise micro engines. Considering the advantages and general characteristics of the inertia dynamometer as detailed in section 3.4, this is the solution that best represents our goal and it is the one being built. It is cheaper and simpler to design and implement; it does not require complex electronics to collect the data; the run is dynamic so it simulates the actual conditions of the real world; since the tests are quick, it prevents wear and excessive temperatures on the engine, which is very important for micro engines. The test bench is intended to be portable, supporting the choice of the inertia dynamometer type because it does not require large braking systems.

In this type of dynamometer, a drive shaft is to be designed and then connected to the engine. On this shaft, a flywheel is attached to simulate the inertia experienced by the real drive shaft while propelling the model vehicle in operating conditions, meaning transmission rotating mass and car/aircraft mass.

In this section, the most important technical requirements for the design at hand will be acknowledged.

4.1.1 Engine Specifications

Performance

It is important to acknowledge the performance specifications to correctly size the drive shaft and define the operating conditions to ensure accurate results.

The type of micro engine to be tested is the glow plug of a car. Table 2.4 from Chapter 2 is consulted to assess the maximum performance specifications of the most powerful micro engine typically used on cars. According to the O.S. Engine manufacturer [1], the 4.5cc for truggies is one of the most powerful and yet largely used, having a maximum crankshaft power output of 3.26 HP (2.43 kW) at 32 000 RPM.

According to the previous values, the estimation of maximum torque is found by Equation (3.1), yielding

$$T = \frac{P \times 60}{2 \times \pi \times N} = 0.725 N.m$$

Applying a conservative correction factor, the relevant performance specifications for the test bench to withstand are summarized in Table 4.1.

Power	2.5 kW
Torque	0.750 Nm
Max speed	40 000 rpm
Idle speed	10 000 rpm

Table 4.1: Micro engines performance specifications

Despite the fact that the dynamometer is more specific to car engines, a safety factor of 1.5 will be used to ensure that the test bench withstands the test of any kind of micro engine from 2.0 to 20.0 cc. If testing more powerful engines (between 2.5 and 3.0 of maximum power), the run will be faster. If testing less powerful engines (under 2.5 kW), the run shall take a bit more than the expected 10s discussed in Section 3.2.

This way, a fair equilibrium is achieved.

Dimensions

The general dimensions of a typical micro engine for model cars can be seen in Figure 4.1.

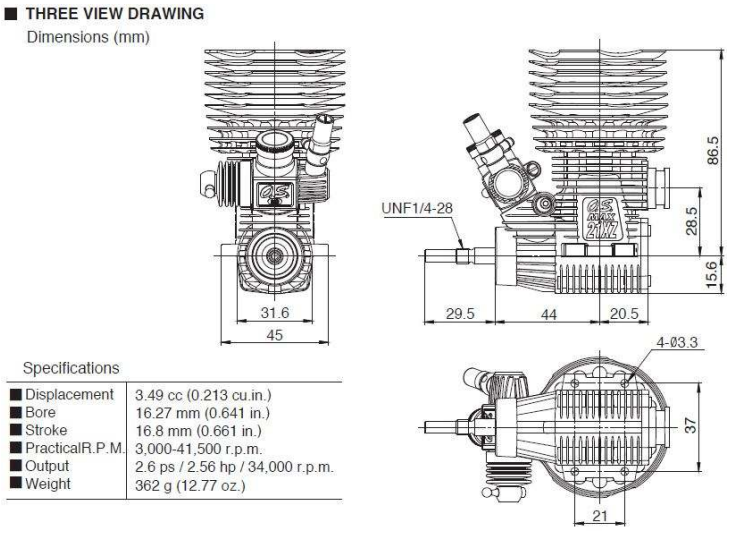

Figure 4.1: Dimensions of the 3.5 cc O.S. engine (21 XZ-B VII) [1].

The engine is fixed by four M3 bolts. They always form a rectangle but, depending on the constructor and the size of the engine, the distance between screw holes can vary. On the backside it goes from 31 to 38mm and on the sides from 11 to 21mm. The height from the support screws to the engine bottom goes up to 20mm for the larger engines.

Since the distance between screw holes for engine locking can vary, the engine support must ensure some freedom of positioning.

4.1.2 Drive Shaft

The drive shaft must have a given amount of inertia for the engine to complete a run in, approximately, 10 seconds (recommended value for inertia dynamometers).

Flywheel

For practical reasons, the flywheel should not exceed 300mm of diameter and 10Kg of mass. It must be perfectly balanced to ensure maximum stability at the highest RPMs.

Gear Train

For safety and balancing reasons, the rotation speed of the drive shaft must not exceed 10 000 rpm. A reduction gear needs to be implemented, given the engine maximum RPM greatly exceeds this value (Table 4.1).

Detachment System

When the engine stops after a run, it must decouple of the drive shaft to prevent engine overheating. So a detachment system has to be implemented somewhere between the engine crankshaft and the drive shaft.

4.1.3 Auxiliary Systems

Flywheel Braking

A braking system has to be set on the test bench to stop the flywheel after a run. It must be actuated in case the flywheel exceeds the maximum rotation speed of N = 10 000 rpm. It should also stop it fast enough to save time between runs, allowing the dynamometer to be more efficient.

Engine Cooling

The temperature at the engine cylinder head should not exceed 130°C, according to some drivers reports. As such, a cooling system is required for the test bench.

The micro engines are cooled by air. When installed in aircraft or car models, the air flow results from the motion of the vehicles. Consequently, in the test bench, a fan cooler needs to be considered. An electric powering is required for the fan.

Engine Fuel Supply and Exhaust

Engines have their muffler coming out on its left (considering the exhaust port to be at the rear). For practical reasons, the fuel tank must be placed on the opposite side of the muffler.

There are two kinds of mufflers. The ones that come out from the engine at a 90° angle used mostly in onroad cars, and the ones that come out at a 180° angle for offroad cars. In either layout, they always come out on the left of the engine (see figure 4.2). The drive shaft must then be placed on the right side of the engine. This way it will not interfere with the muffler.

A device to actuate the throttle must also be implemented, to control the engine load.

(a) 90º muffler (b) 180º muffler

Figure 4.2: Types of muffler for combustion micro engines.

Engine Starting System

As seen in Chapter 2, micro engines are started by a 12V electric motor (Figure 2.7 b)) connected to its crankshaft allowing it to rotate and start burning fuel. A device must be set to make the coupling and allow the electric motor to kick back at the moment the engine starts.

At the same time, the glow plug must be heated by a 1.5V glow starter (Figure 2.7 a)). This requires electric power for both the electric motor and the glow starter.

4.1.4 Summary

The technical requirements covered in this chapter are summarized in Table 4.2.

Description	Parameter	Value
Engine displacement vol.	D	2.0 - 20.0 cc
Maximum power	P_{max}	2.5 kW
Maximum torque	T_{max}	0.750 Nm
Safety factor	n	1.5
Engine max rot. speed	N_{max}	40 000 RPM
Engine idle rot. speed	N_{idle}	10 000 RPM
Engine max temperature	Tp_{max}	130 ºC
Run acceleration time	Δt	10 s
Flywheel diameter	$d_{flywheel}$	$\leq$ 300 mm
Flywheel mass	$m_{flywheel}$	$\leq$ 10 Kg
Drive shaft rot. speed	$N_{driveshaft}$	$\leq$ 10 000 rpm
Engine support dimensions	w	31 - 38 mm
	l	11 - 21 mm
	h	15 - 20 mm

Table 4.2: Technical requirements for the engine dynamometer.

4.2 Concept

Considering all the technical requirements detailed in the previous Section for the inertia dynamometer design, it is now possible to have an idea of how it can be built and the parts it must comprise. The objectives for the test bench are known. There are several solutions that may present an answer for the design at hand. In this Section, those possible solutions are being considered and the ones that best fulfil the requirements will be the guidelines for the inertia dynamometer design, including both the powertrain and auxiliary systems.

4.2.1 Powertrain

Drive Shaft

The rotating shaft can be solid or hollow. Since it must withstand the loads of the flywheel and the torque of the transmitting gear, the best solution is to use a solid shaft, which suffers less deflection [20] preventing the need to use larger diameters.

The layout of the components is very important for the shaft to work properly. In general, it is best to support load-carrying components between bearings, rather than cantilevered outboard of the bearings.

The drive shaft should be kept short to minimize bending moments and deflections. Two bearings should be enough to support it, since there are only two components causing bending (being the flywheel the main one). To minimize deflection, these must be placed near the bearings.

Since the design is for a low torque transmission, the bearings are being press-fitted to the shaft. There is no need for a shaft shoulder because there will be no thrust load [20].

Besides the press-fitting, the flywheel and gear may need a key to ensure torque transmission. It would fit in a groove in the shaft and correspondent component. Another solution to attach the components is to use an hub. A screw is used to lock it on the shaft in a section where a groove is set to receive the screw, preventing it to slide. The component is then coupled to the hub. This way, there is no need for a change in diameter along the shaft. Once again, retainer rings are non required because there will be no thrust loads from the components (except if considering an helical gear).

Flywheel Specifications

The flywheel is a round disc to be attached on the drive shaft to simulate the required inertia. At first sight, there are two ways of designing it; it can have the shape of a perfect disc (Figure 4.3 a)) or the shape of a disc with a thicker outer-ring (Figure 4.3 b)) concentrating its mass on the perimeter.

From the expression for the moment of inertia of rotating bodies, shown in Table 3.1, for a given inertia, the larger the radius, the smaller the mass. However, it is known form the technical requirements stated in Table 4.2 that the flywheel should only reach up to 300 mm of diameter.

Choosing a flywheel with a thicker outer-ring would reduce the mass of the flywheel for the same radius to give the required inertia. Despite its higher cost, due to the machining required in the center to leave the desired thin disc, it is the most viable solution. In this case, the moment of inertia is the sum of a thin inner-disc with a thicker outer-ring [21], yielding

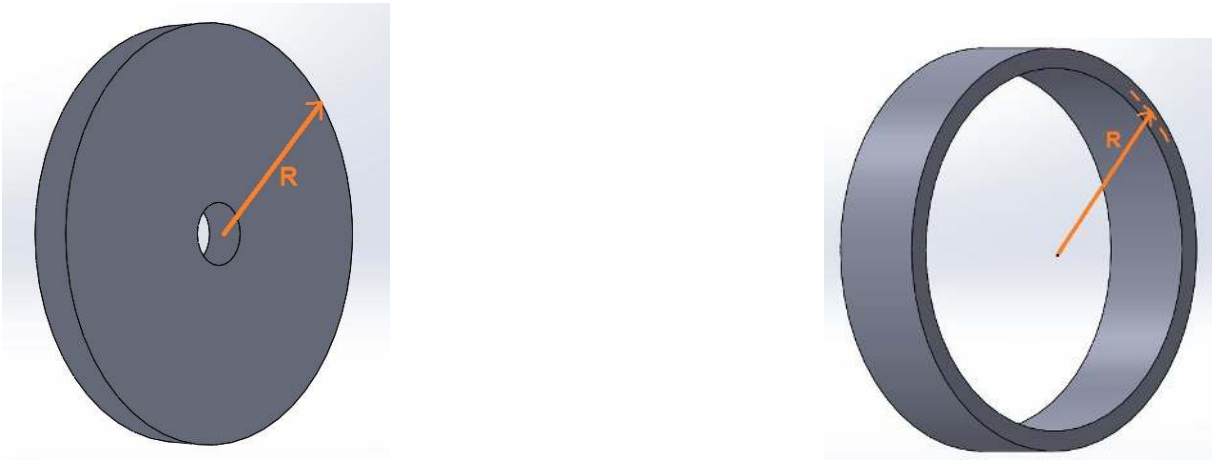

(a) Disc. $I = \frac{1}{2}\, m\, R^2$

(b) Ring. $I = m\, R^2$

Figure 4.3: Flywheel shapes and moment of inertia.

$$I = \frac{1}{2}\, m_{disc}\, {R_1}^2 + \frac{1}{2}\, m_{ring}\, ({R_1}^2 + {R_2}^2)\,, \tag{4.1}$$

where R_1 is the radius of the inner disc, and R_2 the outer radius of the flywheel.

For simplicity and cost effectiveness, the flywheel will be solid and consequently of constant inertia.

Gear Train

It is known that micro engines can reach up to 45 000 RPM. So a reduction gear must be used to ensure that the drive shaft speed does not exceed the specified maximum rotation speed of 10 000 RPM (see Table 4.2). This value is taken into account to calculate the required gear ratio. Note that the bearings must withstand this maximum speed as well.

The gear is accomplished by two cogwheels, one larger than the other. Its goal is to reduce the speed of the drive shaft according to a gear ratio given by

$$i = \frac{\omega_1}{\omega_2} = \frac{\phi_2}{\phi_1}\,, \tag{4.2}$$

where ω_1 and ϕ_1 are the engine crankshaft rotation speed and diameter, and ω_2 and ϕ_2 are the drive shaft rotation speed and diameter.

Being a reduction gear, the drive shaft rotation speed is expected to be i times lower than the rotation speed of the crankshaft.

There are two main ways of accomplishing the gear, directly or indirectly. Directly as in Figure 4.4 a), the cogwheels are simply coupled next to each other; while indirectly as in Figure 4.4 b), a belt or chain is used to accomplish the connection to a distant shaft.

In some gear trains, that require flexibility in the relative locations of the shafts, an indirect gear is used. Also, a belt gear does not suffer from frequent torque reversal as in some direct gears with ”kick back” against the drive from the crank, leading to excessive noise and wear. However, the belt gear would increase complexity for the test bench.

(a) Spur gear (b) Belt gear

Figure 4.4: Direct and indirect gears [20].

Since there is no need for the shafts to be distant from each other, it will be used a direct gear, which allows the inertia dynamometer to be more compact. The goal is to transmit motion from one shaft to another, parallel, shaft. So the type of cogwheel to be used is a spur gear (figure 4.4 a)). It has teeth parallel to the axis of rotation, as required, and is the simplest. An helical gear could also be used to transmit parallel motion, they are not as noisy because of the more gradual engaging of the teeth during meshing, but are more expensive and would cause thrust loads which are not desired.

Detachment System

The powertrain of the inertia dyno comprises the crankshaft, which transmits the engine power output, and the drive shaft, where the flywheel is set to simulate the inertia. To prevent engine overheating, a freewheel system must be assembled to allow the crankshaft to rotate free from the drive shaft after the engine throttle is closed (while the flywheel is still rotating).

There are two mechanisms capable of overrunning and largely used in applications like this:

- **One-way clutch**: consists in a set of two rings separated by a device that enables the movement of the outer ring just when the inner ring is powering it (or vice-versa). The inner ring is fitted to the ”power side” of the drive shaft while the outer ring is fitted to the ”driven side” making the coupling. The ”driven side” is free to overrun the other. An example is shown in Figure 4.5 a).

- **One-way bearing**: also known as ”cam clutch”, is simply a bearing with overrunning ability. It is mounted on the drive shaft housed by the component that is powering it. Also divided in two rings (inner- and outer-ring), it allows the rotation of the drive shaft to overrun the rotation of the component. Figure 4.5 b) shows an example of such mechanism.

Since the inertia is relatively low, it will be used a one-way bearing (cam clutch) fitted to the cogwheel. It endures the maximum speed of N = 10 000 rpm in the drive shaft and it is the cheapest. It will allow the drive shaft to detach from the gear train after a run, preventing the engine to suffer a torque load due to the yet rotating flywheel.

It is not expected the drive shaft to start rotating while the engine is starting on idle. A centrifugal clutch is to be installed in the engine crankshaft and it only couples when it reaches higher than idle

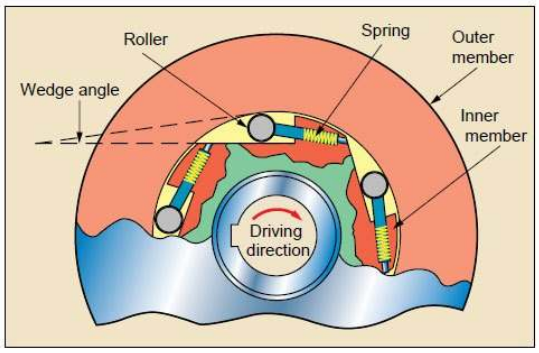

(a) Trapped roller clutch

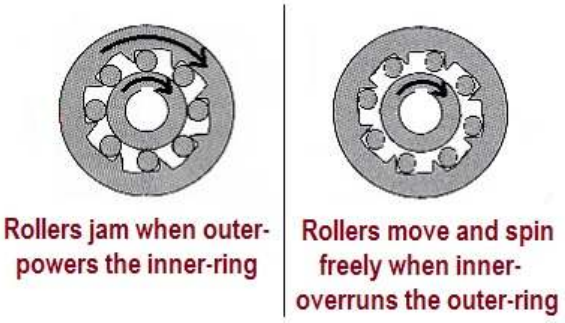

(b) One-way bearing

Figure 4.5: Overrunning mechanisms.

speed. This way it allows the engine to be started much easier, since the pinion attached to the engine clutch will not rotate at engine starting.

4.2.2 Auxiliary Systems

Braking System

The braking will be accomplished by a disc brake (Figure 4.6 a)). It is a compact and simple solution to implement. To reduce the required force to stop the drive shaft, the disc brake allows the actuation of two pads on each side of the disc.

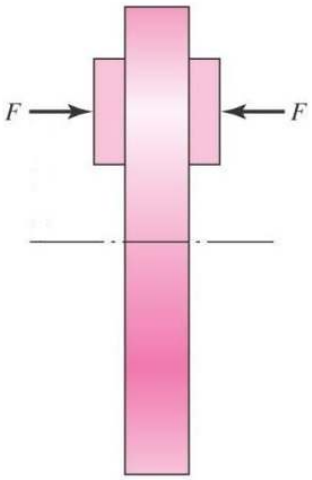

(a) Disc brake.

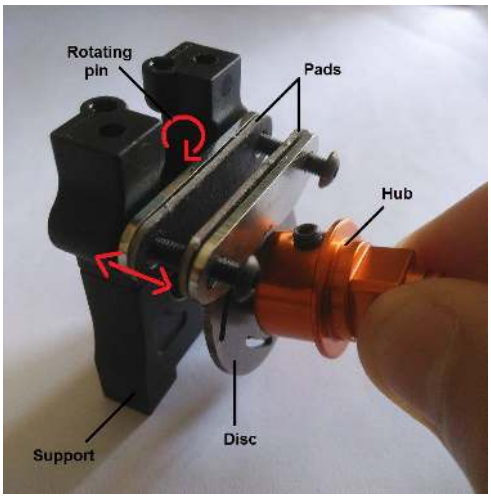

(b) Brake system.

Figure 4.6: Disc brake being implemented.

The system shall be similar to the one used in model cars. A small disc is attached to the drive shaft with two pads right next to it. One pad is static, the other one is actuated by a rotating pin, which will cause the pad to press the disc and, eventually, stop it within the two parallel pads. In Figure 4.6 b) is possible to see such system.

The breaking pads can be actuated by the same electric servo used for throttle control in model cars.

The actuating arm of the servo rotates in both clockwise and counter-clockwise directions. One way is for throttle control and the other is to actuate the rotating pin responsible for pushing the mobile braking pad.

Engine Cooling

Since the engine is air-cooled, a fan directed to it presents a viable solution for engine cooling. Knowing the temperature at the cylinder head should not exceed 130^{o}C, a temperature sensor will be set to measure it. Once it reaches 110^{o}C, the fan next to the engine shall be actuated to cool it down.

Engine Support

To give the required degrees of freedom for positioning the engine in the dyno, it has to comprise adjustable supports. One way of doing it is to build supports to move within rails or slots in the test bench. The rails allow a more precise movement of the parts but are more complex (Figure 4.7 a)).

Since the interest is just for a steady locking of the supports for the engine, the system of slots and squared head screws is more suitable and simpler. It only needs two pairs of slots to be cut, one on the frame (orange line in figure 4.7 b)) and another on the supports (yellow line), perpendicular to each other.

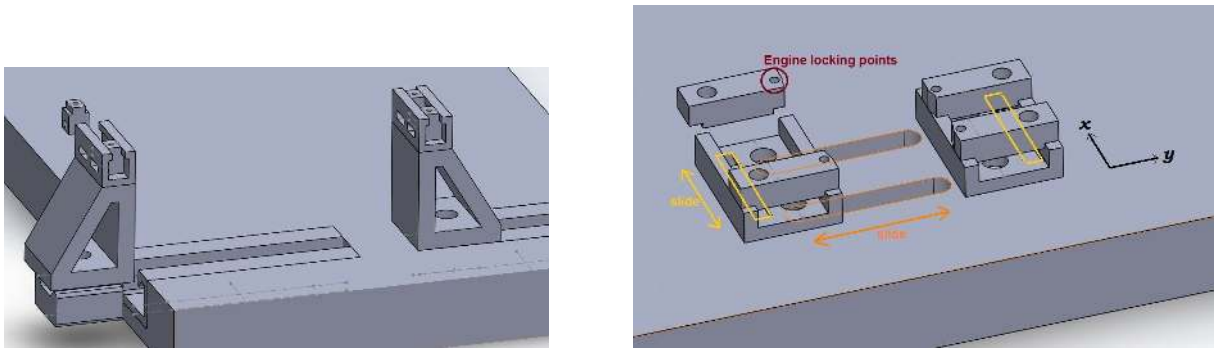

(a) Rail system

(b) Slot system

Figure 4.7: Possible solutions for adjustable supports.

The slots are designed in order to allow the screws to slide through them, giving these the freedom to lock its receiving supports on the desired position. The system is implemented in both x and y directions.

The top of the supports must have, in total, four screwed holes to lock the engine. Remembering that the distance between screw holes varies from the smallest to the largest engines, it will be given a freedom of 10 mm for the screws to slide in each direction.

Since the test bench is designed to test the micro engine of a car, an even simpler solution, yet limited, can be used in a first approach. The engines have standard dimensions for the supports, regarding the distance between screw holes on the side. Namely 11 mm for the smallest 2.1 cc, and 21 mm for the largest engines around 3.5 cc.

It is possible to build a frame similar to the chassis of a car and apply the standard support blocks to lock the engine. In Figure 4.8, it is possible to see the frame and the support blocks able to secure any engine from 2.1 cc to 4.5 cc.

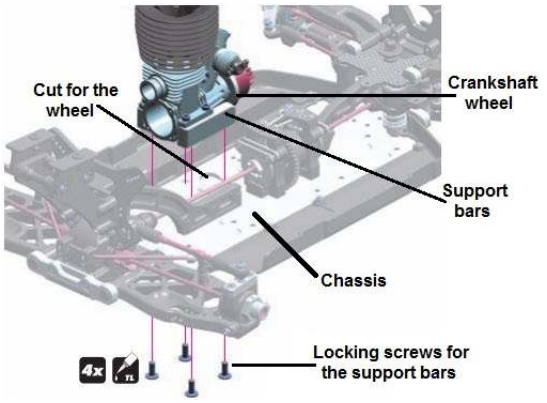

(a) Engine assembly on the chassis of XRay XB8 (part no. 351108).

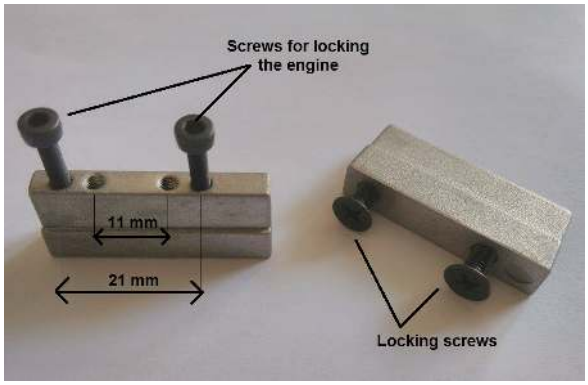

(b) Standard support bars.

Figure 4.8: Solution for standard support bars to lock the engine.

Slots will be needed for gear mesh adjustment in case different gear ratios are used. The support blocks will be allowed to move within the slots to lock the engine in the required axis line for the pinion.

Starting System

The device for engine starting is an electric motor typically used to start these engines (Figure 2.7 b).

To prevent vibrations and ensure maximum stability, both the crankshaft and drive shaft are placed as low as possible, so the best solution is to place them side by side. Accordingly to the layout of the shafts, the starter is being placed under the test stand. This way, it will not interfere with other components.

A rubber ring is attached to the electric motor. This is temporarily forced to make contact with the engine crankshaft wheel and impel it to rotate. This way, the engine will eventually start at the same time the glow plug is heated by a glow starter (Figure 2.7 a)).

The starter is set parallel to the engine to ensure both the rubber adapter and the crankshaft wheel are pressed parallel to each other. It must exert the required pressure to reach static friction. The device is attached to a hinge under the test bench and the gravity will ensure fast kick back when the engine starts. The required pressure is exercised by the dynamometer operator, which simply needs to let go after the engine is running. Such system can be seen in Figure 4.9.

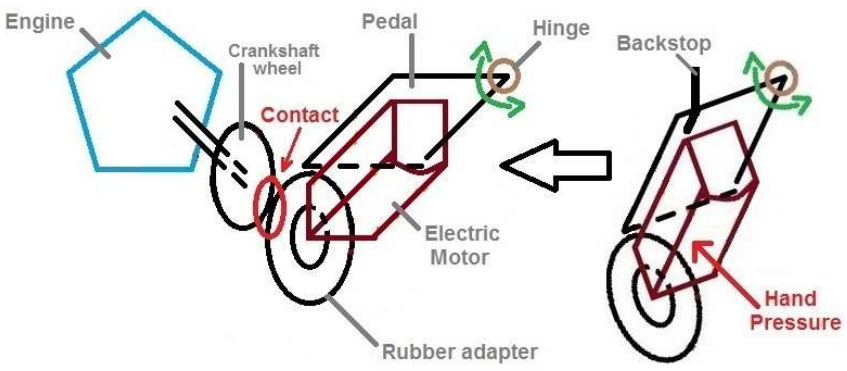

Figure 4.9: System for engine starting.

Throttle Control

To accelerate the engine, the throttle on the carburetor must be actuated. It is known from Chapter 2 that the carburetor is actuated by a mechanical arm attached to its side.

The goal is to actuate that mechanical arm through a device capable of pulling it for open throttle and return fast to its initial position for idle speed.

An effective solution is to apply the electric servo used in the model cars, which directly controls the position of the throttle by actuating the mechanical arm connected to the carburetor. Figure 4.10 shows the main components of this system.

Figure 4.10: Throttle servo.

The servo arm rotates causing a mechanical arm to pull the fuel nipple connected to the throttle. This rotation causes the opening of the throttle by sliding the needle valve for fuel admission. There is an extension return spring within the carburetor arm that allows the throttle to return to its idle position.

The electric servo can be used for both throttle and brake control as stated in section **??**. It is known that each rotation direction of the servo arm has the function of actuating the throttle and the brake, respectively. To allow the servo arm to quickly return to the initial position after braking, another return spring is used in the system (Figure 4.11), this time for compression. When the arm rotates to pull the braking pin, the opposite side will actuate that spring mounted on the throttle arm.

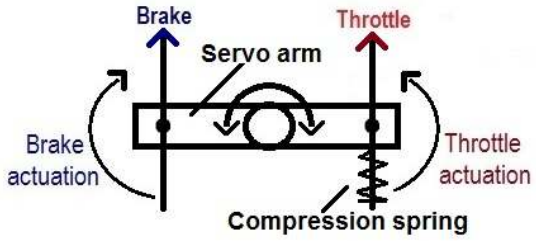

Figure 4.11: Servo for throttle and brake control.

Ventilation System

To use the test bench indoors, a ventilation system for the exhaust gases must be available. These engines, like any other combustion engine, produce harmful emissions that must be dissipated away from the operator. In case of testing a glow plug engine, the nitromethane included in the glow fuel is characterised by an intense smell.

4.3 Test Bench Layout

At this point, a more detailed idea of the frame outline and its components takes place. Considering that the test bench is going to be assembled on a table, cuts are made into it to ensure room for the flywheel, gear and crankshaft wheel to rotate freely. Figure 4.12 presents a layout of the inertia dynamometer to be built.

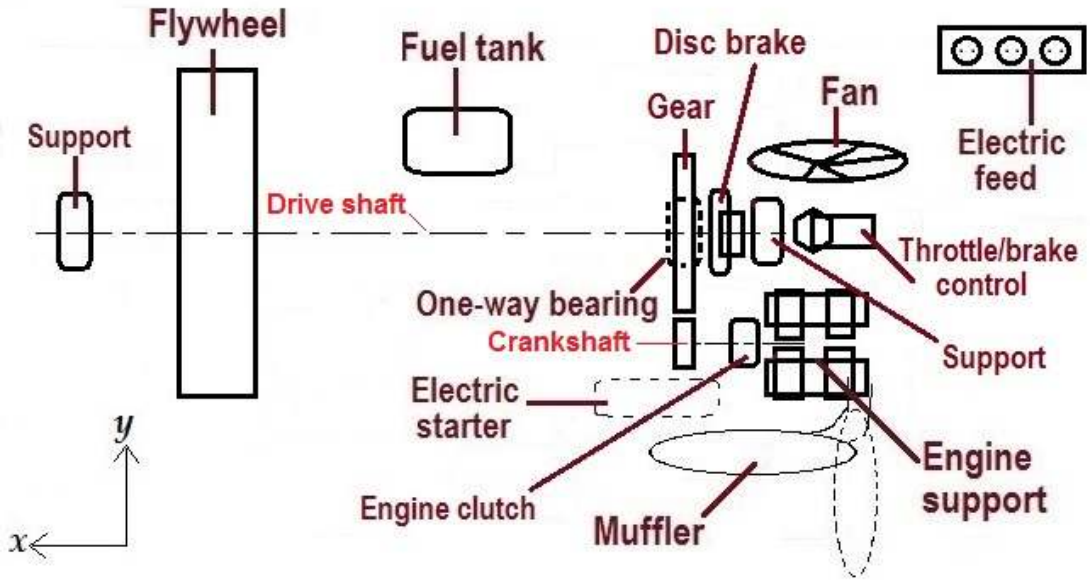

Figure 4.12: Layout of the test bench.

The drive shaft is supported in both ends. A flywheel is set to simulate the inertia experienced by the engine. The engine is locked side by side with the drive shaft in order for the crankshaft pinion to be aligned with the cogwheel completing the gear train. The auxiliary systems are set all around: fuel tank on the opposite side of the muffler, braking system between the gear and the support, an electric servo for throttle and brake control, a fan for engine cooling as close as possible from the engine and the electric starter is set under the frame.

Chapter 5

Data Acquisition System

An important part of the structural design is to ensure room for the necessary sensors and actuators. So, apart from creating stable conditions for engine testing, one has to decide where and how to instrument the test bench. In this chapter, the sensors and actuators to implement are chosen to obtain the desired power diagrams, torque diagrams and fuel consumption rates of the tested micro engines.

5.1 Technical Requirements

The required sensored quantities and their measuring ranges are summarized in Table 5.1.

Physical quantity	**Range**
Rotation Speed	3 000 - 45 000 rpm
Volumetric Flow	20 - 80 mL/min
Engine Temperature	0 - 150 ºC
Room Temperature	10 - 40 ºC
Atmospheric Pressure	800 - 1100 mbar

Table 5.1: Sensored quantities and their measuring ranges.

Knowing the function of the sensors and the range of input data they must be able to collect, it is possible to make a grounded choice.

5.2 Data Acquisition Board

To read all the sensors outputs and record them, a data acquisition (DAQ) system will be used. This system will be comprised of a data acquisition board connected to a computer. The DAQ board, previously acquired, is the National Instrument NI PCIe-6321 [22] (Figure 5.1), which has 16 analog +/-10 V inputs and outputs, connected to a computer running LabView, to read, process and record the data acquired from the sensors, and to control the cooling fan and throttle servo. It costs around 1000 euros. Its datasheet is present in Appendix A.

(a) Board NI PCIe-6321.

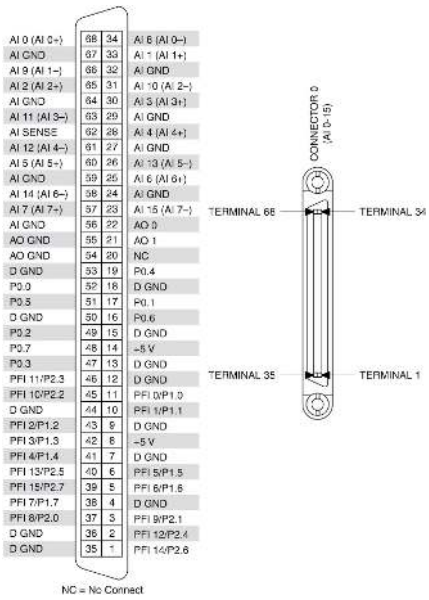

(b) Pinout schematic for the NI PCIe-6321.

Figure 5.1: Data acquisition board for the test bench (PCIe-6321).

In Figure 5.1 b) it is possible to see the pinout schematic of the DAQ board. AI refers to the Analog Inputs and AO to the Analog Outputs. The +5V terminal feeds the sensors. The PFI lines refer to the Programmable Function Interface (Digital), which serve as connections to virtually all internal timing signals. They can import a trigger or output various signals.

5.3 Sensors

5.3.1 Rotation Speed Sensor

After market search for a solution for RPM measurement, three possible sensors from *Vishay* were found capable of satisfying the given technical requirements:

- **CNY70**: is a reflective sensor that includes an infrared emitter and phototransistor in a leaded package which blocks visible light. It has an operating range between 0 and 5 mm. The typical output current under test is 1 mA and output voltage from 7V to 32V. It is used for optoelectronic scanning and index sensing. It costs 1.50 euros.
- **TCND5000**: is a reflective sensor that includes an infrared emitter and pin photodiode in a surface mount package which blocks visible light. It has an operating range between 2 and 25 mm. The typical output current under test is 0.11 μA and output voltage of 60V. It is used for proximity or motion sensing. It costs 5 euros.
- **TCRT5000**: is a reflective sensor that includes an infrared emitter and phototransistor in a leaded package which blocks visible light. It has an operating range between 0.2 and 15 mm. The typical output current under test is 1 mA and output voltage from 5V to 70V. It is used for position sensing for shaft encoder and optoelectronic scanning. It costs 3.50 euros.

It was chosen a reflective optical sensor with phototransistor output, which has an output current suitable to the range of input currents for the data acquisition board. According to the operating range, the most viable solution is the *CNY70* from *Vishay* [23]. It has a more compact operating range which allows more precise readings.

This sensor uses a phototransistor that will measure the number of rotations per minute (RPM) of the engine crankshaft. To accomplish it, a tape with a white and black part is introduced around all the perimeter of the crankshaft wheel, half white and half black. When passing on the black part of the tape, the sensor generates a signal (and voltage) with a different frequency. That change in frequency when multiplied by 60 (seconds in a minute) will give the exact number of RPM of the flywheel.

Another identical sensor is being set on the flywheel. The values obtained can be multiplied by the gear ratio to give the effective RPM of the engine. Comparing both values, it is possible to estimate the slipping losses in the clutch, due to lack of friction. In Figure 5.2 it is possible to see the sensor. Its datasheet is present in Appendix B.

Figure 5.2: Rotation speed sensor (phototransistor).

5.3.2 Volumetric Flow Sensor

The ideal volumetric flow sensor for fuel consumption rate assessment was the liquid flow meter **SLQ-QT500** from *Sensirion*. It is specially designed for hydrocarbons and water based liquids and can measure flow rates from 0 to 120 mL/min, with an accuracy of 5%. Another viable solution was the **SLI SLQ-HC60** also from *Sensirion*. It can measure flow rates from 0 to 80 mL/min, with an accuracy of 1%. However, these flow sensors stated above were too expensive (around 1 000 euros).

After market research, a much cheaper solution was found from *Omega*. The flow sensor to implement will be the **FTB311-EU** [24], capable of measuring flow rates from 30 to 300 mL/min, with an accuracy of 6%. According to the manufacturer, it is possible to consider flow rates from 20 mL also but with a worse accuracy of 10-15% approximately, which is acceptable. It costs 185 euros.

The FTB311 is an economical choice for low flow rate measurement. It uses an infra-red light beam that measures the flow according to the rotation of paddle wheels within the sensor. Each time the wheel rotates a DC square wave is output with a certain frequency. By multiplying it by a k-factor, it gives the volumetric flow in the required unit. The sensor has a 5 Vdc current sinking pulse output, which is suitable for the data acquisition board. An illustration of the sensor can be seen in Figure 5.3. Its datasheet is included in Appendix B.

Figure 5.3: Volumetric flow sensor FTB311.

5.3.3 Temperature Sensor

One temperature sensor is necessary to measure the temperature of the engine outer head and another one to measure room temperature. After market research, one viable solution was found for both of them.

To measure the temperature on the engine head, the sensor must have a measuring range form 0ºC to 150ºC. One possible solution is the sensor **LM35DZ**, a thermocouple able to measure temperatures from -40ºC to 150ºC from *Texas Instruments* [25]. Its output sensitivity is 10 $mV/ºC$ and it has an absolute error of, approximately, 0.5ºC. It has a supply voltage range of 4V to 30V. This sensor costs 2 euros.

To measure room temperature, these two sensors can be considered:

- **TMP37**: a thermocouple able to measure temperatures from 5ºC to 100ºC from *Analog Devices*. Its output sensitivity is 20 $mV/ºC$ and it has an absolute error of, approximately, 2ºC. It costs 0.70 euros.

- **LM335A**: a thermocouple able to measure temperatures from -40ºC to 100ºC from *Texas Instruments*. Its output sensitivity is 10 $mV/ºK$ and it has an absolute error of, approximately, 1ºC. It costs 1.60 euros.

These sensors for room temperature have a low voltage operation of around 5V and both comply to the technical requirements. Although they are cheaper, their absolute error is higher than it is for *LM35DZ*.

Since just two sensors are needed, the overall cost difference will not be significant, so the thermocouple chosen was the *LM35DZ* for both engine and room temperature measurement. It allows a suitable supply voltage of 5V and it has the lowest error. In Figure 5.4 it is possible to see an illustration of the sensor. Its datasheet is also present in Appendix B.

Figure 5.4: Temperature sensor LM35DZ.

5.3.4 Room Pressure Sensor

To measure room pressure, an analog absolute pressure sensor is required to connect to an analog input of the DAQ board. There are two possible solutions from *Infineon* that comply to the technical requirements:

- **KP236N6165**: a pressure sensor able to measure absolute pressures from 60KPa (600mbar) to 165KPa (1650mbar). It has an output sensitivity of 43.8 mV/kPa and a supply voltage from 4.5V to 5.5V. It costs 6.55 euros.
- **KP235**: a pressure sensor able to measure absolute pressures from 40KPa (400mbar) to 115KPa (1150mbar). It has an output sensitivity of 53.3 mV/kPa and a supply voltage from 4.5V to 5.5V. It has a MSL-1 (Moisture Sensitivity Level-1) and costs 7.90 euros

The pressure sensor chosen was the *KP236N6165* [26]. It has a lower error and it is cheaper. In Figure 5.5 it is possible to see an illustration of the sensor. Its datasheet is included in Appendix B.

Figure 5.5: Pressure sensor KP236N6165.

5.4 Actuators

There are two electrical actuators required for the test bench to work: the electric servo for throttle and brake control and a relay to switch the fan on and off.

5.4.1 Throttle/Brake Control

The servo for throttle and brake control will be similar to those used in model cars. There are two viable solutions to be implemented in the test bench:

- **Futaba BLS451**: a brushless electric servo with a torque of 10.6 Kg.cm and a speed of 0.10s/60º. Its dimensions are 39.9 x 20.1 x 37.1mm and it weights 58g. It costs 85 euros.
- **Futaba S9302**: a brushless electric servo with a torque of 13.6 Kg.cm and a speed of 0.11s/60º. Its dimensions are 40 x 20 x 37mm and it weights 61g. It costs 105 euros.

For the test bench it was chosen the servo *S9302* from *Futaba* [27]. It is robuster and not much more expensive. In Figure 5.6 it is possible to see an illustration of the servo.

Figure 5.6: Electric servo for throttle and brake control S9302.

5.4.2 Fan Control

It is known from the datasheet of the data acquisition board that the PCIe 6321 is capable of an output drive current of 5 mA up to 15 mA of overdrive current. The relay to switch the fan on and off must be able to be actuated with a current of 5mA at least. For this purpose, there are two possible solutions:

- **EC-500**: a DC 5V relay module manufactured by *Ledsandchips*. It is high level TTL (5V) and needs a trigger current of not less than 5 mA, which complies with the drive current of the data acquisition board. It costs 6 euros.
- **S203ZA**: a DC 5V relay manufactured by *Solid Technologies*. Also needs a trigger current of not less than 5 mA. It costs 4 euros.

The chosen relay to actuate the fan was the *EC-500*. It is more compact and easier to obtain. In Figure 5.7 a) it is possible to see a set of two of these relays.

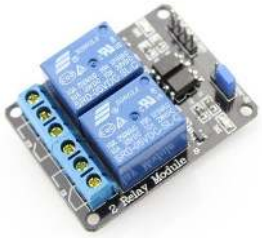

(a) 2-channel 5V relay.

(b) Fan for engine cooling.

Figure 5.7: Components for automatic engine cooling.

The fan used for engine cooling will be a *Corsair AF120* [28] with a dimension of 120 x 120 x 25mm (Figure 5.7 b)). It needs 7V - 12V of power supply and 0.4 A of current. It reaches 1500 rpm and its blades are designed for a high volume of air with less noise and turbulence. It costs 13 euros.

Chapter 6

Detailed Design

Before the actual mechanical design for construction, a previous 3D model is displayed to help defining the design at hand. Figure 6.1 shows a structural model of the test bench considering the solutions discussed on Chapter 4.

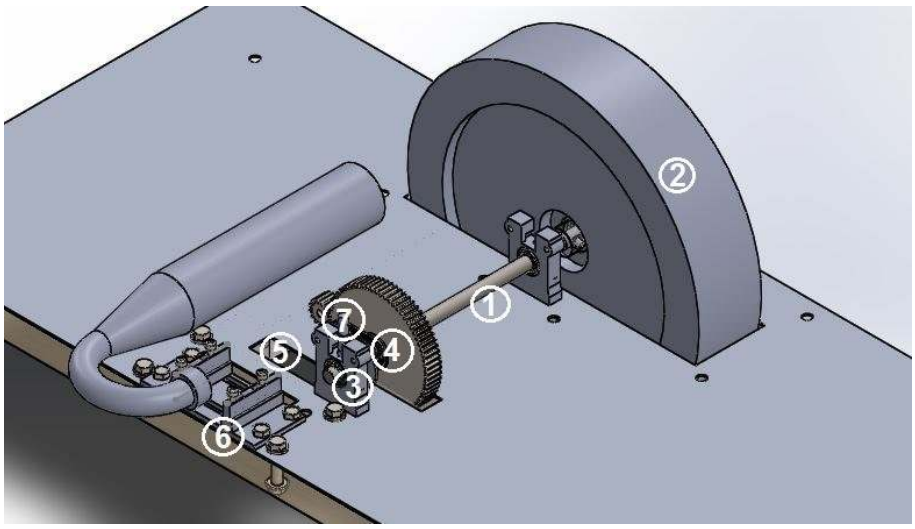

Figure 6.1: Structural model of the test bench.

Where the main components are:

1. Drive shaft;
2. Flywheel;
3. Ball-bearing support;
4. Gear train with one-way bearing;
5. Electric starter under the frame;
6. Flexible engine support;
7. Disc brake.

6.1 Materials

Typically, for solid shafts with a small diameter (under 10 mm), Cold Drawn (CD) steels are used. Thermal treatments change the mechanical properties of the material and influence its deflection under load. This is why cold drawn steels are better for small diameters, the shaft is hardened increasing its stiffness [20]. This way, they are able to withstand given loads with no significant deflection.

From AISI 1020 to 1050, there is the possibility of getting a cold drawn shaft able to withstand considerable mechanical solicitations. For a conservative analysis, AISI 1020 is chosen. It has a sufficient Yield Strength for an application like this and is the cheapest. In table 6.1 is possible to see the strength properties of these largely used CD steels.

AISI No.	Tensile Strength [MPa]	Yield Strength [MPa]
1020	470	390
1030	520	440
1035	550	460
1040	590	490
1045	630	530
1050	690	580

Table 6.1: Strength properties of common CD steels [20].

The flywheel will be made of steel. Other materials with lower densities would cause it to be much bigger to reach the required inertia.

The frame to support the ground components of the test bench will be a stainless steel sheet to prevent oxidation. It is later assembled on a wooden table where several rubber rings are used to prevent vibrations.

The supports for the drive shaft and the gear itself are made of a hard and light composite.

6.2 Mechanical Design

6.2.1 Drive Shaft

To size the drive shaft, it is important to know the maximum torque applied to it. It is known from the technical requirements summarized in Table 4.2 that this torque is 0.750 Nm (T_{engine}).

Remembering the maximum of N = 10 000 rpm for the drive shaft, and that the maximum rotational speed of micro engines is N = 45 000 rpm, the minimum gear ratio (*i*) given by Equation 3.5 is

$$i_{min} = \frac{45000}{10000} = 4.50\,.$$

To prevent the drive shaft to reach its maximum speed, it is being used a more conservative gear ratio of **i = 5**. Therefore, the applied torque on the drive shaft is given by

$$T_{transmitted} = T_{engine} \times i = 3.75Nm\,. \tag{6.1}$$

From Table 6.1, the steel to be used (AISI 1020 CD) has a yield strength of $\sigma_y = 390MPa$. Considering the safety factor $n = 1.5$, the maximum stress σ_{max} is given by

$$\sigma_{max} = \frac{\sigma_y}{n} = 260MPa \tag{6.2}$$

If the shaft was only subjected to torque (which is not), the maximum shear stress would be

$$\tau_{max} = \frac{T\,r}{J}\,, \tag{6.3}$$

where r is the shaft radius (to be calculated), and J the polar moment of inertia, $J = \frac{\pi}{2}\,r^4$.

From Von Mises criteria [20], the maximum shear stress is given by $\tau_{max} = \frac{\sigma_{max}}{\sqrt{3}} = 150MPa$.

Rewriting equation 6.3 as

$$\frac{T_{transmitted}}{\tau_{max}} = \frac{\pi}{2}\,r^3$$

and solving in order to r, yields

$r = \sqrt[3]{\frac{2\,T}{\pi\,\tau_{max}}} \Leftrightarrow r = 2.515\,mm$

So, as a first approach, the minimum diameter for the shaft if only subjected to torque is $d_{min} = 5.03 \approx 5.0mm$.

Due to the flywheel, the drive shaft will suffer a bending moment caused by its weight. To minimize it, the flywheel must be attached at a close distance from the shaft supports, meaning there will be used three supports (two next to the flywheel and one in the other end) instead of the original two previously thought in Chapter 4.

The shaft will have an effective length of **L = 220mm** (Figure 6.2). It needs to be this long to ensure the flywheel does not interfere with other components, namely a 180º muffler or the starter below the main frame.

A more thorough analysis is taking place considering all loads. Conducting an equilibrium analysis, it is possible to draw the load diagrams and assess the maximum torque and moment suffered by the shaft.

Static Analysis

From Section 6.2.2 in this chapter, it is known that the flywheel will have a mass of 9.81 Kg, which corresponds to a Weight of **W = 96.1 N**, considering $g = 9.8\,m/s^2$. The shaft is supported by simple ball

bearings (points A, C and D) restraining it only in the *y* direction. The flywheel is set at just 40mm from supports C and D (Figure 6.2). This way it causes a low bending moment.

The weight of the gear that makes contact with the engine crankshaft is being neglected because this is made of a light composite. Besides that, the bending moment is minimal because the cogwheel is set right next to support D. The free-body diagram can be seen in Figure 6.2.

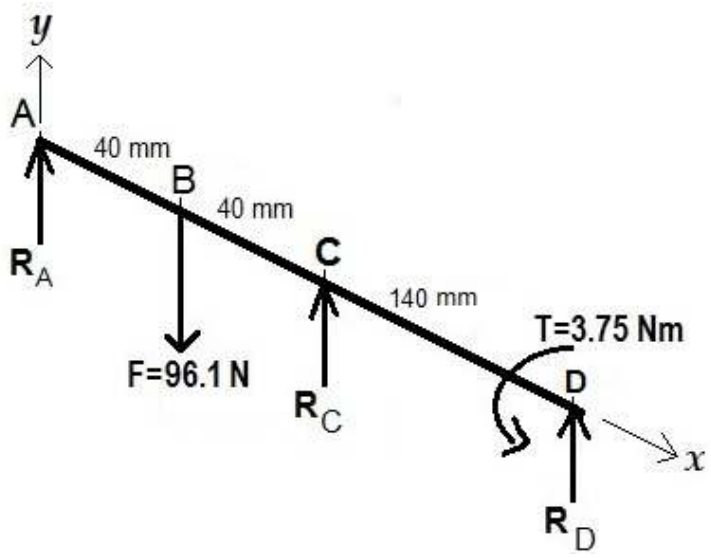

Figure 6.2: Free-body diagram.

Using the equilibrium equations for the applied loads to acknowledge R_A and R_C, it is possible to calculate the shear forces (V), torque (T) and bending moment (M) to draw its load diagrams:

$$\sum F = 0; \sum M = 0 \tag{6.4}$$

Resulting

$$\sum M_C = 0 \Leftrightarrow 0.08\, R_A - 0.04 \times 96.1N = 0 \Leftrightarrow R_A = \frac{0.04}{0.08} \times 96.1 \Leftrightarrow R_A = 48.05N$$

$$\sum F_y = 0 \Leftrightarrow R_C = 96.1N - R_A \Leftrightarrow R_C = 48.05N$$

The load diagrams for the drive shaft can be seen in Figure 6.3.

It is possible to see that Torque is constant between the gear and the flywheel and equal to 3.75 Nm. The maximum bending moment is given by $M = R_A \times 0.04 \Leftrightarrow M_{max} = 1.9Nm$.

There is no thrust load and since the shaft complies to the long shaft criteria ($\frac{L}{d} > 10$) [20], shear forces (V) are negligible.

Considering both T and M in the most solicited section of the shaft (B), the minimum diameter for static analysis, according to Von Mises theory [20], is given by

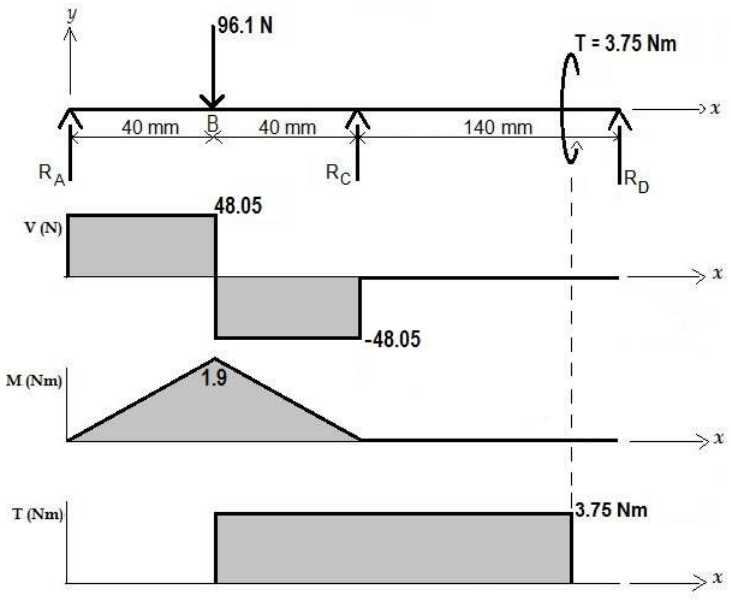

Figure 6.3: Shear, bending and torsional moments.

$$d_{min} = (\frac{32\,n}{\pi}\,\sigma_y\sqrt{M^2 + \frac{3}{4}T^2})^{\frac{1}{3}} = 5.3mm \tag{6.5}$$

where d_{min} is the minimum diameter, σ_y is the yield strength, M is the maximum Moment, T is the maximum Torque.

As such, a shaft with 6mm of diameter satisfies the criterion.

If press-fitting the components, it has to be considered a D/d = 1.1 (D the larger and d the shorter diameter) for assembly of the components in the shaft without friction. With it, is possible to estimate the minimum diameter of the rough rod to be turned.

Rod diameter	Shaft minimum diameter
6	4.96
7	5.79

Table 6.2: Possible rod diameters to comply with the minimum diameter of 5.3 mm. D/d = 1.1.

According to Table 6.2, if it is necessary for the shaft to have changes in diameter, the rod must have a 7 mm diameter to ensure the minimum diameter of 5.3 mm at the most solicited section.

Selection of components

After a thorough research regarding these model vehicles, a solution for the drive shaft and the attachment of its components is found. The drive shaft must have 8mm of diameter accordingly to the components found in Chapter 4 for the braking system. The support of the brake pads comprise 8mm ball bearings and it is only practical to consider them for supporting the shaft as well.

So a shaft with 8mm of diameter was chosen provided by *Poly Lanema*. It has an ISO h9 tolerance, which means its diameter error is inferior than 0.05 mm [29].

To lock the flywheel, a conical shaft clamp acquired in *Rolisa* [30] is being used. It has an inner diameter of 8mm and an outer diameter of 15mm with a flange of 27mm. This component has the ability of self-centering when applied by tightening the bolts securing the conical rings. It can be seen in Figure 6.4.

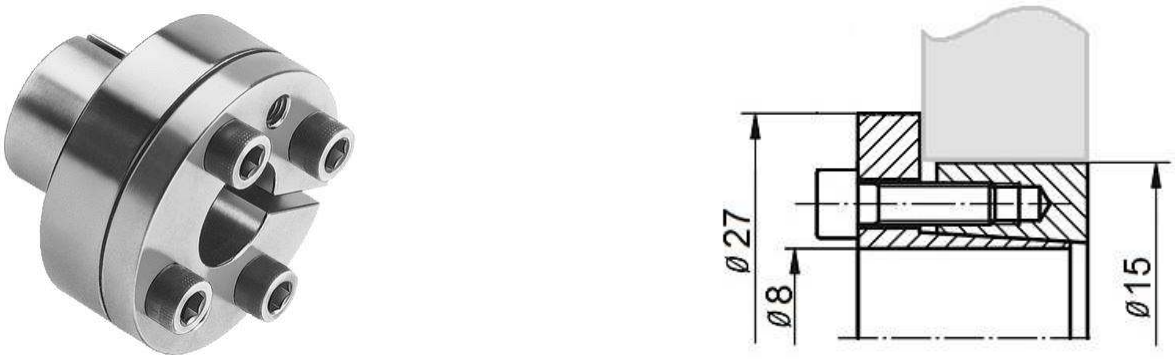

(a) Conical shaft clamp.

(b) Clamp dimensions.

Figure 6.4: Conical shaft clamp for locking the flywheel.

The shaft diameter exceeds the previously suggested 6mm. The safety factor should be much higher than the original value of 1.5. It is interesting to acknowledge that new *n*, given by

$$n = d^3 \times \frac{\pi\,\sigma_y}{32\sqrt{M^2 + \frac{3}{4}\,T^2}} = 5.2 \tag{6.6}$$

These reinforces the idea for the test bench to be able to test any kind of micro engine from 2.0 to 20.0 cc.

The supports for the drive shaft comprise high-speed rubber sealed ball-bearings (part no. 940817) and respective housings (part no. 354010), all components from XRay XB8 [7]. The ball bearings have a dimension of ϕ8 x 16 x 5 mm. The housings will be locked on the table frame by two bolts each.

6.2.2 Flywheel

Considering the flywheel to have the shape of a disc, the moment of inertia is given by $I = \frac{1}{2}\,m\,R^2$.

It is known from Chapter 3 that the required inertia for the flywheel to comprehend is given by equation (3.2),

$$T[N.m] = I[Kg.m^2] \times \alpha[rad/s^2]\,.$$

To calculate it, the angular acceleration (α) must be estimated from ω_0 to ω_f. From the technical requirements, it is known that the common micro engine goes up to 40 000 rpm and that the idle speed is, usually, 10 000 rpm.

Considering the gear ratio, i=5, $\omega_0 = \frac{10000}{5} = 2000\,rpm = 209.44\,rad/s$

and $\omega_f = \frac{40000}{5} = 8000\,rpm = 837.76\,rad/s$.

From equation (3.3),

$$\omega_f = \omega_0 + \alpha \times \Delta t$$

and considering $\Delta t = 10\,s$ from the technical requirements, results an average angular acceleration of $\alpha = 62.83\,rad/s^2$.

Consequently, Equation 3.2 yields the desired moment of inertia of the flywheel,

$$I = \frac{T}{\alpha} = 0.0597\,Kg.m^2$$

From Chapter **??**, it is known that the flywheel can have up to 300 mm of diameter and its mass must not exceed 10 Kg. It will be sized down until a fair equilibrium of mass and radius is found. Table 6.3 presents the relation between radius and mass for the given inertia, considering a disc shape.

Radius [mm]	**Mass [Kg]**
50	47.75
75	21.22
100	11.94
125	7.64
150	5.31

Table 6.3: Relation between radius and mass for the flywheel in a disc shape.

A radius of 125 mm comprehends a mass of 7.64 Kg, which seems acceptable. The disc would have a thickness of 20 mm. However, if considering a smaller disc with an outer ring, the flywheel could be sized down to a radius of, approximately, 100 mm with a mass much smaller than 11.94 Kg.

The inertia for a disc and outer ring is given by Equation (4.1)

$$I = \frac{1}{2}\,m_{disc}\,{R_1}^2 + \frac{1}{2}\,m_{ring}\,({R_1}^2 + {R_2}^2)$$

An iterative process is made to assess the required dimensions of the outer ring to ensure the maximum of 10 Kg for the flywheel. The results are shown in Table 6.4. The density of the steel is $7850Kg/m^3$, accordingly to the supplier *Ramada Aços* [31].

Thickness e_o	45 mm
R_1	80 mm
R_2	105 mm

Table 6.4: Dimensions for the outer ring of the flywheel.

The mass of the outer ring is given by

$$m_{ring} = \rho\,e_o\,\pi\,({R_2}^2 - {R_1}^2) = 5.12\,Kg \tag{6.7}$$

From equation 6.2.2, $m_{disc} = 4.71\,Kg$. So the total mass of the flywheel with a radius of 105 mm is

given by

$$m = m_{disc} + m_{ring} = 9.83\,Kg \tag{6.8}$$

which is 2 Kg lighter than a regular disc with a radius of 100 mm.

To finish the sizing, the thickness of the inner disc is given by $e_i = \frac{m_{disc}}{\rho\,\pi\,R_1^2} = 30\,mm$.

The dimensions of the flywheel are shown in Figure 6.5 considering both the sizing and the shaft clamp to fix it.

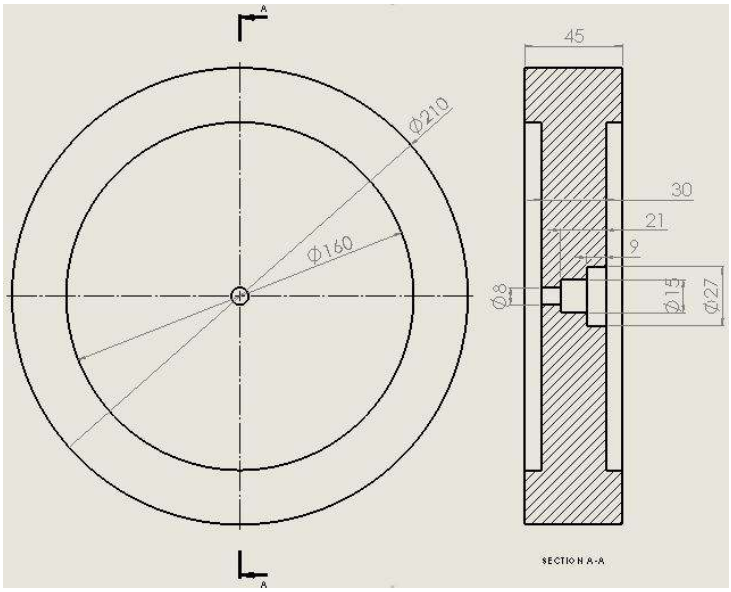

Figure 6.5: Dimensions of the flywheel.

6.2.3 Disc Brake

It will be used a disc brake similar to the system used in model vehicles. The disc is from XRay (part no. 334110). It is locked to the drive shaft by a hub also from XRay (part no. 344141).

The braking pads to actuate the disc are from XRay XB8 (part no. 354130) made of ferodo. Knowing they actuate at uniform pressure $p = p_a$, and simplifying the contact area to $A_c = \frac{\pi}{4} \times (R^2 - r^2)$ for an equivalent annular pad of 90º, the braking force given by Equation (3.12) is

$$F = p \times A_c = p_a \times \frac{\pi}{4} \times (R^2 - r^2) \tag{6.9}$$

where p_a is the applied pressure by the pads, R the outer radius = 15mm, and r the inner radius = 7mm.

In Figure 6.6 is possible to see the pads used for the braking system and its dimensions for an equivalent annular pad actuating the disc.

The contact area for each pad is $A_c = \frac{\pi}{4}\,(R^2 - r^2) = 138.23\,mm^2$. The larger it is, the lower is the pressure for the required force. Integrating the product of the friction force and the radius, the Torque is

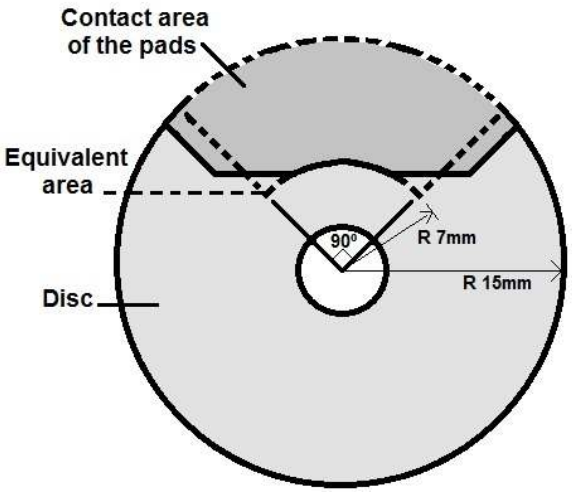

Figure 6.6: Dimensions of the disc brake.

found by

$$T = \frac{\pi}{2}\mu p_a \times \int_r^R r^2 \, \mathrm{d}r \tag{6.10}$$

$$T = \frac{\pi \mu p_a}{6} \times (R^3 - r^3)$$

where μ is the friction coefficient. Considering both materials (ferodo and steel), $\mu = 0.4$ at 150 ºC [32].

Since there will be used two pads on either side of the disc, equation (6.10) is multiplied by two (the number of pairs of mating surfaces).

For T = 3.75 Nm, $p_a = 2.95MPa = 29.5bar$.

The equation can be written to relate torque with the braking force,

$$T = \frac{4}{3}F\mu \times \frac{R^3 - r^3}{R^2 - r^2}\,, \tag{6.11}$$

Resulting for the ideal force

$$F = \frac{3T}{4\mu} \times \frac{R^2 - r^2}{R^3 - r^3} = 408N\,. \tag{6.12}$$

This force of 408 N would be capable to stop the flywheel immediately, which will not be the case. A smaller force does the work by stopping it in a few seconds, while the generated friction in the brake pads is absorbing the kinetic energy dissipated by heat through the disc. However, it is important to confirm if the electric servo is able to generate a sufficient braking force in the same range of the ideal.

From Chapter 5, it is known that the digital servo generates up to 13.6 Kg.cm of torque (T). This quantity is transmitted to the brake pads by a small arm connected to the rotating pin that actuates the brake. This force transmission is illustrated in Figure 6.7.

Knowing $1\,Kg.cm = 0.098\,N.m$, the torque generated by the servo is equal to 1.33 Nm (T_1).

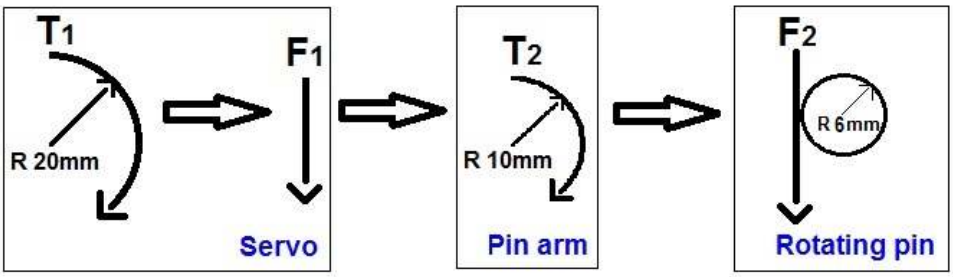

Figure 6.7: Force transmission to the rotating pin.

The servo arm has a radius (R) of 20mm, so the respective force is given by

$$F_1 = \frac{T_1}{R} = \frac{1.33}{0.02} = 66.64N\,. \tag{6.13}$$

The force F_1 actuates the pin arm (R = 10mm) transmitting a torque (T_2) to the rotating pin given by

$$T_2 = F_1 \times 0.01 = 0.6664Nm\,. \tag{6.14}$$

The rotating pin actuates the braking pads at a 45º angle with $F_2 = \frac{0.6664}{0.006} = 111.1N$.

The torque T_2 causes a moment in the 6mm ledge of the pin that actuates the brake pad. Projecting F_2 to a normal force experienced by the ledge, it is possible to obtain the braking force (F_{brake}). Figure 6.8 illustrates the schematic of (F_{brake}), applied to the disc.

$$F_{brake} = \frac{F_2}{cos(45º)} = 157.1N \tag{6.15}$$

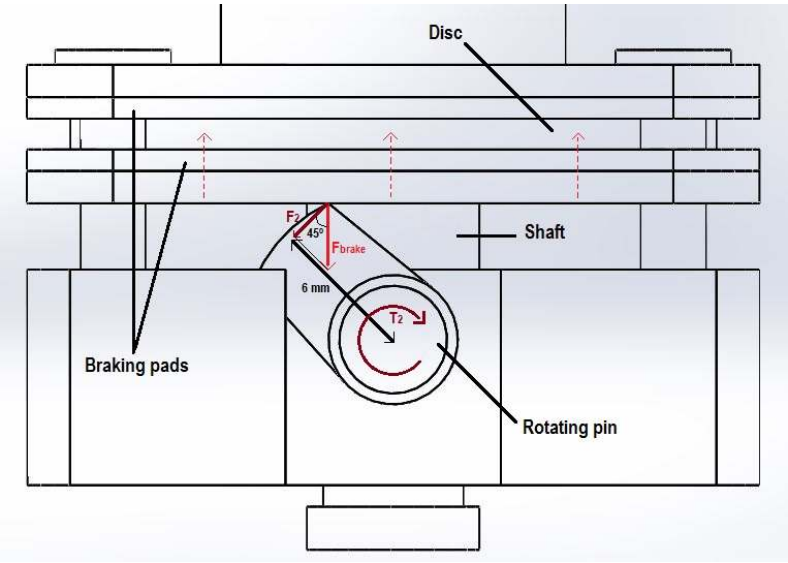

Figure 6.8: Force transmitted to the brake pads.

This is 38.5% of the ideal 408 N. It is sufficient to stop it in a few seconds, so it is viable to use the braking system of model vehicles on the test bench. Note that the braking must be continuous to prevent an abrupt stopping of the flywheel, which could cause the test stand to flip over.

6.2.4 Gear Train

The gear train comprehends two cogwheels with a gear ratio of 5. The pinion from XRay manufacturer has 14 teeth ($\phi 14mm$) and the driven cogwheel, to be implemented on the drive shaft, has 70 teeth ($\phi 70mm$). These are both made of a light and strong composite of plastic material.

In Figure 6.9 it is possible to see the spur gear to be implemented in the test bench. The driven cogwheel is assembled on a one-way bearing. It will allow the drive shaft to overrun the engine crankshaft after a run.

Figure 6.9: Composite spur gear.

6.2.5 Engine Support

The engine support blocks will be set on the table through two parallel slots as it was stated in Chapter 4. The slots must have a close tolerance regarding its length to fill the less room possible. There are components like the muffler or the servo that also need room around the engine.

The design takes into account the technical requirements for the engine dimensions. In Figure 6.10 it is possible to see the solution for locating the support blocks to lock the engine with a 5mm freedom on both *x* and *y* directions, in case different gear meshes are used or larger engines are tested.

The support blocks are locked on an aluminium block by two M4 screws each. They have specific pairs of M3 screw holes on the top to lock engines from 2.1cc to 4.5cc. These blocks can move along the slots in the *y* direction up to 42mm apart (the usual gap for a 3.5cc engine is 37mm). The aluminium block is free to move within a 10mm gap on the *x* direction.

The schematic for engine support can be seen in Figure 6.10:

6.2.6 Fuel Tank Support

The fuel tank is locked on the aluminium frame by appropriate pins used in model vehicles. In Figure 6.11 is possible to see the fuel tank from XRay XB8 (part no. 358605) and its locking pins [7]. It has a capacity of 123 mL.

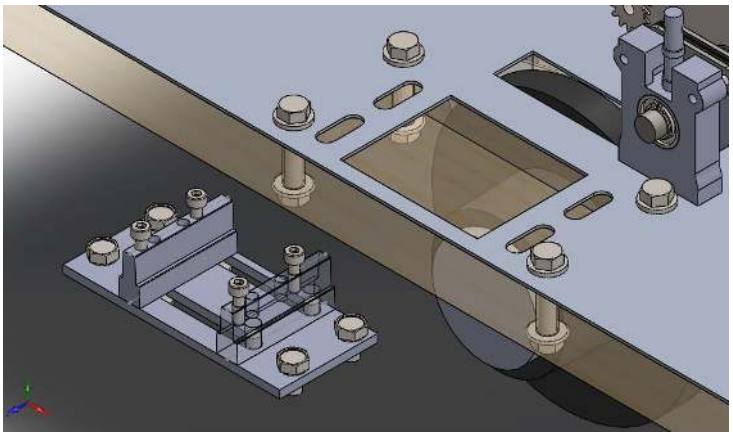

Figure 6.10: Layout of the engine support.

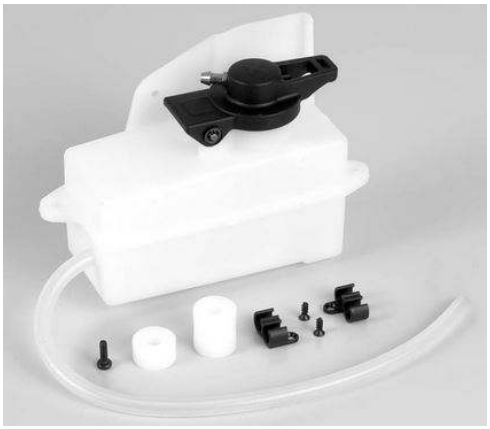

Figure 6.11: Fuel tank and its locking pins.

6.2.7 Starting System

For setting the electric starter, a pedal is designed as stated in Chapter 4, sized accordingly to the electric motor dimensions.

It is set below the test stand, secured by an hinge locked on the wooden table. The operator actuates it by pulling an handle set on the opposite side of the micro engine. The rubber adapter of the electric starter must be perfectly aligned with the crankshaft wheel to make contact and start the engine. Afterwards it rotates back to its original position. The entire system can be seen in Figure 6.12.

To heat the glow plug, it will be used a portable ”glow starter” set at 1.5V, as shown in Section 2.2.3.

6.2.8 Throttle and Brake Servo

The electric servo for control is from *Futaba*, model S9302 (Figure 5.6). It will actuate the carburetor and the disc brake as stated in Chapter 4.

The servo will be wired to a data acquisition board and controlled by a *LabView* program.

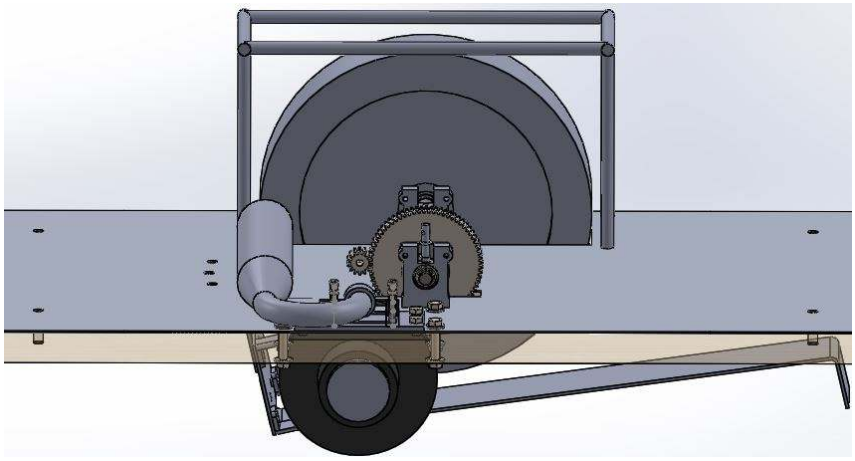

Figure 6.12: Starting system.

6.2.9 Cooling Fan

The cooling fan is a *Corsair 120mm* (Figure 5.7 b))that achieves 1500 rpm. It will be set on the side of the engine as close as possible for an efficient cooling, right next to the servo. It could not be set neither on the back nor on the muffler side due to the oils expelled by this component.

6.2.10 Flywheel Safe

A structure was designed to secure the flywheel in case this tends tu jump off the test stand. In Figure 6.12 it is possible to see that cubic structure comprising 8mm rods surrounding the flywheel. A safety net is then located around them. The four supports pass through the main frame and are locked under the test stand.

6.3 Deflection Analysis

The shaft needs to be balanced to prevent vibrations. Before doing the static balancing, deflection must be analysed to ensure it is not very high, otherwise the rotation will be unbalanced causing unexpected stress concentrations and possible failure, since the shaft can reach up to 9 000 RPM. The shaft is designed to withstand the weight of the flywheel with a conservative safety factor, so the displacement should be low because the material is stiff. To conduct the analysis, a simulation on *SolidWorks Simulation* was made by a finite element method [33]. This static analysis intends to assess the maximum displacement experienced by the shaft, due to the weight of the flywheel.

To represent the real operating conditions, the shaft was subjected to two distinct fixtures. Two supports with constraints in both *X* and *Y* direction, one at each end, and one simple support constrained only in the *Y* direction (fixed hinge). The mesh was defined with quadratic tetrahedron elements with maximum length of 2 mm. 2^{nd} degree elements such as this allow more precise results. A force of 96.1 N is applied at the flywheel section (y direction), 40 mm apart from each support.

In Figure 6.13 it is possible to see the deflection experienced by the drive shaft. Note that graphical representation has a magnifying factor of 200 for visualization purposes.

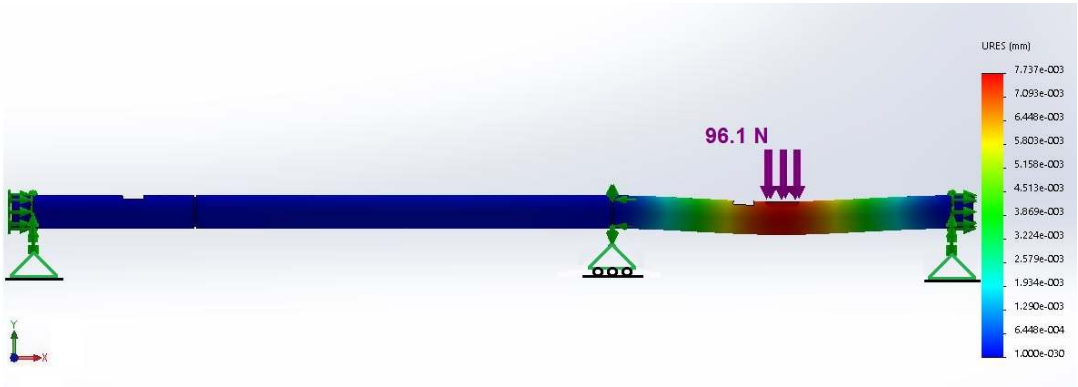

Figure 6.13: Displacement on the drive shaft.

The maximum displacement occurs, naturally, in the flywheel section. This value is equal to 0.008 mm, as it can be seen in the chart of Figure 6.13. It is a rather low value of deflection due to the close proximity of the supports and the conservative diameter of the shaft, as expected. It is known from Section 6.2.1 that the bending moment has a low influence on the overall load experienced by the drive shaft.

Chapter 7

Assembly and Wiring Layout

This chapter refers to the structural and electrical assembly of the best bench. It will be given a review of the production of some mechanical parts and their assembly with the specific parts chosen from model vehicles to build this inertia dynamometer for micro engines.

The calibration and assembly of sensors is also taking place. The actuators will be set and, finally, the wiring layout of the test bench is presented.

7.1 Production

Most of the parts for the test bench were implemented from *XRay* model cars. Despite that, the flywheel, the shaft, the main frame and some auxiliary components had to be designed and manufactured. Most of them were fabricated in *LTO* (Laboratório de Técnicas Oficinais) in *IST* (Instituto Superior Técnico). Only the main frame, the metal sheet of stainless steel which sustains the test bench components, had to be cut by laser to ensure maximum precision.

7.1.1 Flywheel

The flywheel was manufactured using a turning machine (Figure 7.1 b)). At first, the rough material acquired in *Ramada Aços* was subjected to external turning to obtain a balanced disc with 210mm of diameter and 45mm of thickness. Also, internal turning took place to remove the over-thickness of the inner disc and, at this point, the required shape for the flywheel is obtained.

The engaging for the shaft clamp required an internal turning tool to reach its final form illustrated in Figure 7.1 a).

7.1.2 Shaft

A stainless steel rod was ordered with the required 8mm of diameter as stated in chapter 6. It was cut to an effective length of 230mm by a power hack saw machine and then turned and milled to cut

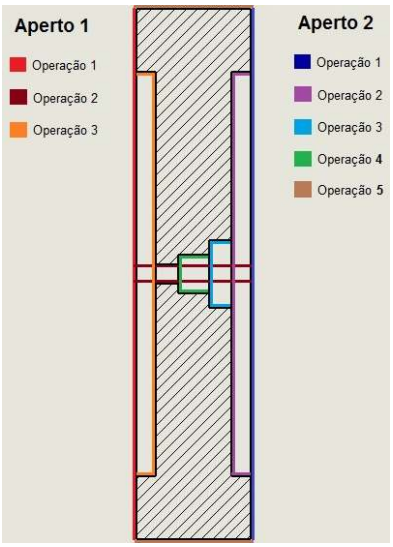

(a) Turning process.

(b) Turning in LTO.

Figure 7.1: Turning process to produce the flywheel in LTO.

the required gaps for the retaining rings of the ball bearings and the grooves for locking the hubs. An illustration of the shaft can be seen in Figure 7.2.

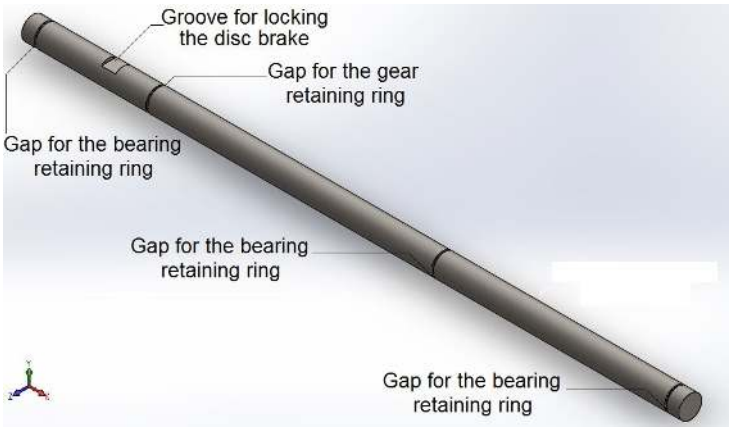

Figure 7.2: Shaft to be implemented in the test bench.

Although theoretically there is no thrust load, the retaining rings are used to ensure the correct location of the shaft components. The gear is attached on the drive shaft through a one-way bearing, which means there is no possibility of press-fitting, so a retaining ring is necessary. Note that the respective gaps are cut with minimal depth to prevent stress concentration.

7.1.3 Main Frame

It is known from Chapter 6 that the main frame is a stainless steel sheet to support all the ground components. This material is very hard to machine due to its hardness. So the process chosen to produce the main frame was laser cut. This is a very ”clean” process able to reproduce the design perfectly with great finishing results when applied to thin sheets such as this. In Figure 7.3 is possible to see the main frame.

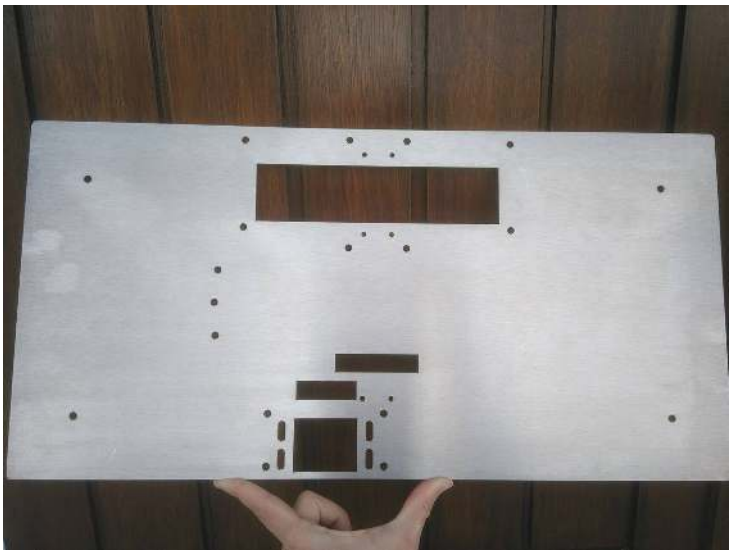

Figure 7.3: Main frame of the test bench cut by laser.

The stainless steel sheet was later attached to a wooden table completing the frame. The top stand of the table was also subjected to a series of cuts to allow the components to pass by. The electric starter will be assembled below the table and the 12V battery remains on top.

7.1.4 Flywheel Safe

To produce the cubic structure surrounding the flywheel, 8mm rods were carefully welded by MIG process. After that, the component was subjected to zinc plating in *Electrofer IV* [34] to prevent oxidation by forming a barrier of zinc oxide acting as a sacrificial anode if this barrier is damaged. It also gave the structure a shinning aspect. In Figure 7.4 it is possible to see the flywheel safe after the surface coating.

Figure 7.4: Flywheel safe after zinc plating in Electrofer IV.

7.2 Cost breakdown

One of the objectives of the test bench is to have an acceptable price for the manufacturers or customers to invest. A cost breakdown was made to assess the monetary value of the equipment. The program behind the data acquisition system should also be considered.

In Table 7.1 it is possible to see the cost of the whole equipment including mechanical components and data acquisition system components.

	Component	**Cost** $[e]$
Mechanical components	Flywheel	45
	Drive shaft and supports	25
	Electric starter and accessories	60
	Hinge	5
	Hubs, gear and one-way bearing, bearings	55
	Fuel tank	20
	Main frame sheet	40
	Bolts, nuts, rings	15
Data acquisition system	DAQ board, shielded cable, connectors block	1240
	Servo	50
	Cooling fan	15
	12V DC battery	10
	5V Relay	5
	Flow sensor	185
	Rotation sensors	5
	Temperature sensors	5
	Pressure sensor	10
	Breadboard and cables	10
	TOTAL	**1800**

Table 7.1: Cost breakdown of the test bench.

Considering an additional value of 200 euros per unit, regarding the data acquisition program, this test bench can cost around 2 000 euros, which can be acceptable for most of the customers since a model vehicle and engine cost around 800 euros [7]. For two and a half times this value, the driver has the opportunity to test any engine he might acquire.

7.3 Structural Assembly

The supports for the drive shaft are the first components to lock on the main frame. They are divided in two parts, allowing fast assembling and disassembling of the shaft. Next the hub for the braking system and the one-way bearing for the gear. There are two very important aspects to consider when locating these components. The screws that support the braking pads must be at a certain distance to give just enough gap for the disc of the brake to rotate freely, preventing friction, and at the same time the braking pads must be close enough from each other for an efficient braking. The disc can also move freely on the axis direction through the hub pins. In Figure 7.5 a) it is possible to see the assembled braking system.

Also, it must be ensured that the one-way bearing for the gear is leaning against the hub of the

(a) Assembled braking system.

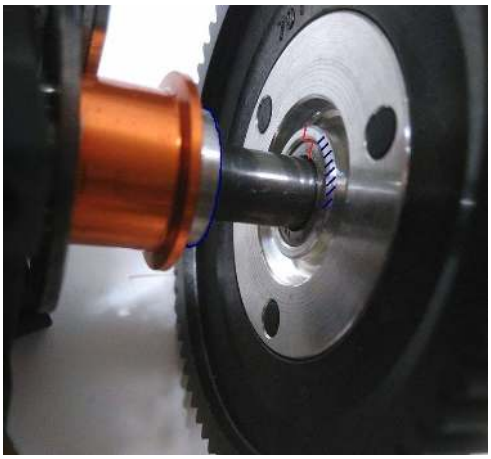

(b) Assembled one-way bearing.

Figure 7.5: Assembling of the disc brake and gear.

disc brake for a correct location. The outer-ring of the one-way bearing has exactly the same diameter than the hub tip (Figure 7.5 b)) and is salient in reference to the inner-ring, preventing friction when the overrunning occurs. On the other end there is a retaining ring to locate the gear.

Next, the flywheel is assembled (Figure 7.6). It is important not to forget that it weights almost 10 Kg. After it is in position, the shaft clamp must be tighted ensuring the flywheel does not slip. The shaft is now assembled in the supports with three ball-bearings. The top parts of the supports are locked with two bolts each to locate the drive shaft.

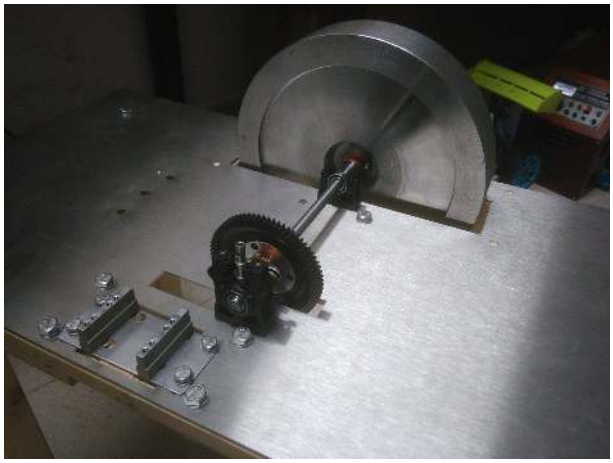

Figure 7.6: Assembled flywheel.

The engine support is mounted on the main frame by four M5 bolts, which is locked by 30mm M6 bolts and respective washers, comprising the full thickness of the table and steel sheet. Some components require nuts for the bolts, others have screw holes.

The test bench is ready to receive the micro engine. Its two support blocks are locked on the engine support by four M4 screws as it can be seen in Figure 7.7 a). It is important to check if the pinion of the engine crankshaft is perfectly aligned with the drive shaft cogwheel. The muffler is locked by a wire, previously set on the main frame very close to the flywheel but without interference.

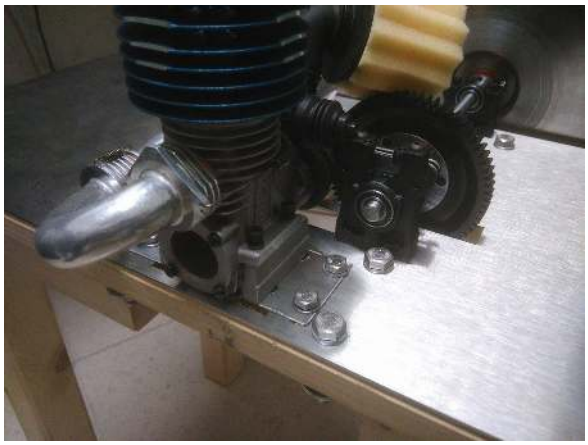

(a) Engine support.

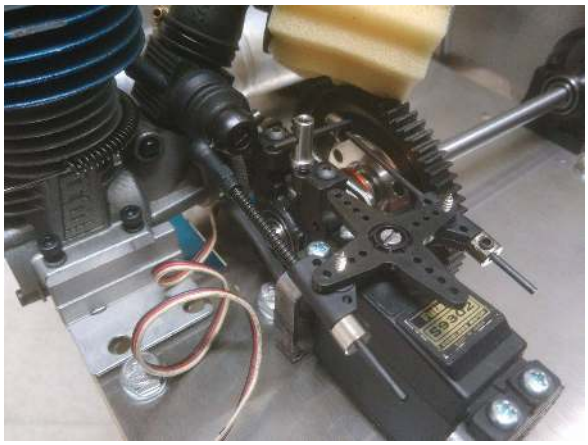

(b) Servo for throttle and brake control.

Figure 7.7: Assembling of the engine and electric servo.

The electric servo for throttle/brake control is set on the side of the engine as illustrated in Figure 7.7 b). The fuel nipple angle, connected to the throttle arm, can be adjusted ensuring both arms are at the same height. It is important to check for interferences between the throttle and the shaft support, and between the brake arm and the cogwheel. Different engines may require different settings for the servo arms.

The fuel tank is locked on the main frame in the opposite side of the muffler, next to the flywheel. The fuel lines are set, one fuel line for fuel admission linked between the tank and the carburetor, and one exhaust pressure line, linked between the top of the tank and the muffler, to pressurize the fuel tank and feed fuel in the carburetor through the fuel line.

The fan for engine cooling is locked next to the servo by two M4 screws. It is wired to a 5V relay connected to the NI Data Acquisition Board, set next to the fan.

The electric starter is set below the test stand as stated in chapter 6. The hinge is locked on the table by three M6 bolts. The metal sheet, already attached to the hinge, receives the electric motor securing it by four M4 bolts. In Figure 7.8 b) it is possible to see the assembled starter.

(a) Structural assembly completed.

(b) Assembled electric starter.

Figure 7.8: Test bench fully assembled.

In Figure 7.8 a) it is possible to see the test bench fully assembled. In the next section, the wiring of all the sensors and actuators is also explained.

7.3.1 Static Balancing

Before testing the engine, the flywheel must be subjected to a static balancing. This will allow to correct the radial distribution of mass and ensure a stable rotation.

Fortunately, the flywheel was well balanced due to a careful turning when produced. Also, the self-centering ability of the conical shaft clamp allows a precise radial balance.

If a dynamic balancing was to be made, the result had to meet the G6.3 quality grade accordingly to the ISO1940 standard for rigid rotors (Table 3.2).

7.4 Set Up of the Sensors and Actuators

7.4.1 Wiring Layout

In this section, it will be given a layout of all the necessary electric connections made during the set up of the sensors and actuators. Also the calibration of the sensors to obtain accurate results is explained.

All the sensors used in the test bench have at least three pins: the ground (GND), the power supply (+5 V) and the analog output (AO). They are wired to a connectors block (Figure 7.9 b)) which communicate directly to the data acquisition board already installed on the PC.

The (AO) signal of each sensor was connected to the respective Analog Input (AI) on the NI DAQ board. The GND were connected to the respective ground of the AI. The $+5V$ were connected to the respective $+5V$ terminal for supply. In Figure 7.9 a) it is possible to see the wiring of the sensors and actuators. The fuel consumption sensor is supplied externally by a 12V DC battery.

Table 7.2 shows the processing of each AO signal from the sensors and relative position for an accurate measurement.

Sensor	Signal processing	Relative position
$Rotation_{engine}$ RPM	$< Frequency > \times 60$	Emitter face parallel to the crankshaft wheel (distance 5mm).
$Rotation_{flywheel}$ RPM	$< Frequency > \times 60$	Emitter face parallel to the flywheel (distance 5mm).
$Volumetric\,Flow$ mL/min	$< Frequency > \times K\,factor$	Coupled with the fuel line.
$Temperature_{engine}$ °C	$< Voltage > \times m + b$	2mm from the cylinder outer-head.
$Temperature_{room}$ °C	$< Voltage > \times m + b$	Open space away from the engine.
$Pressure$ mbar	$< Voltage > \times m + b$	Open space away from the engine.

Table 7.2: Signal processing of the sensors.

The relay and throttle servo for control were connected to the AOs on the NI DAQ board. The AO 0 sends a signal that activates the relay to switch the fan ON when the engine reaches 110 °C. The AO 1

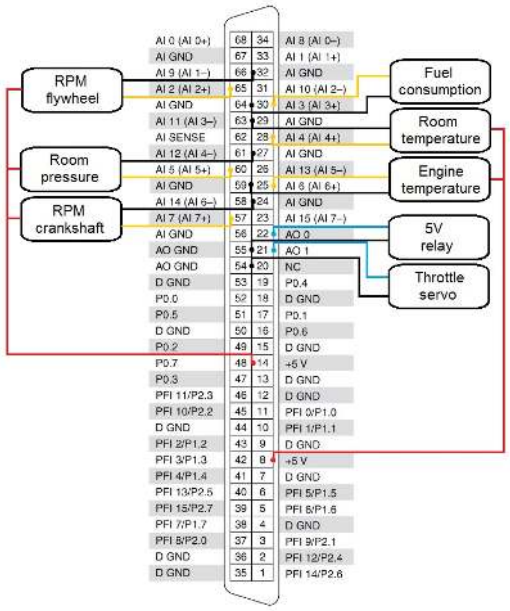

(a) Wiring of the sensors and actuators in the connectors block.

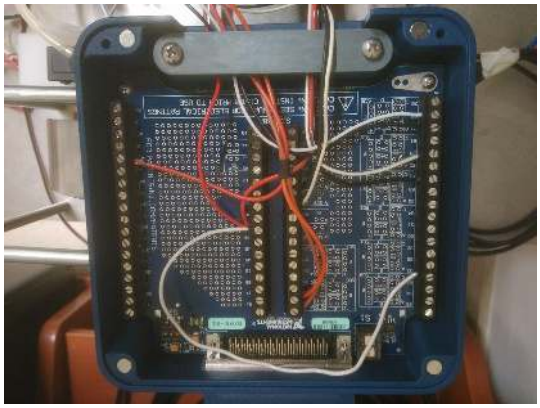

(b) Connectors block for communication with the DAQ board.

Figure 7.9: Pinout shematic of the DAQ board and power supply.

sends a signal that controls the throttle position. Both the relay and the throttle servo are too connected to a 12V DC battery.

This battery does not supply the components directly. Two switches were implemented to control the power supply. Also a bread board was used to define the wiring and implement a 5V converter for the throttle servo, as this requires an operating current that exceeds the maximum of the DAQ board. The electric scheme for external power supply can be seen in Figure 7.10.

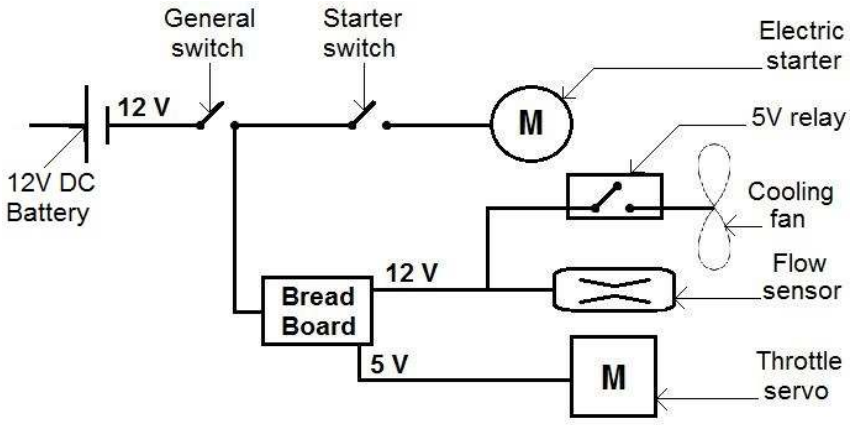

Figure 7.10: External power supply.

The detailed wiring layout of all the sensors and actuators, implemented in the test bench, can be seen in Figure 7.11.

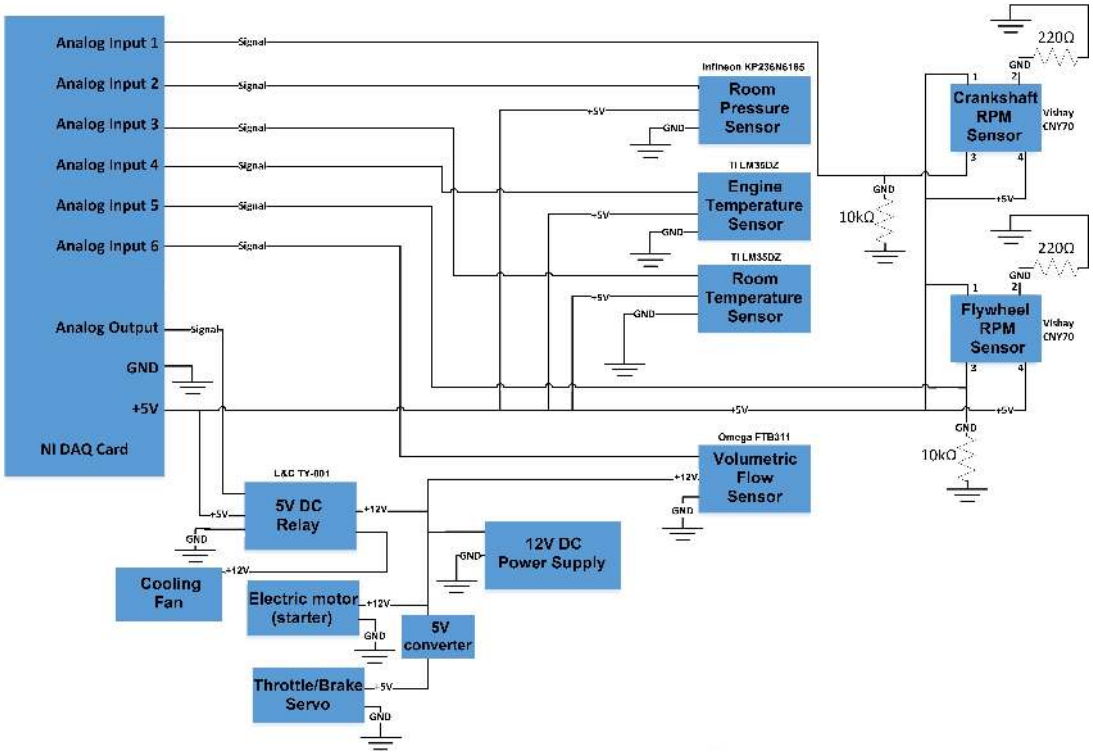

Figure 7.11: Electrical layout of the test bench.

7.4.2 Calibration

The fuel consumption sensor requires calibration in the search for the *K* factor as it can be seen in Table 7.2. The volumetric flow is given by

$$Q[mL/min] = k \times f[Hz] \tag{7.1}$$

The sensor outputs a signal of frequency (*f*) which gives the number of pulses per second. Using a DC pump, the flow sensor was put to test by draining a known quantity of water into a recipient passing by the sensor, where

$m_{water} = 395.6g$

$\rho_{(20^oC)} = 998.2Kg/m^3$, so $V_{water} = \frac{m}{\rho} = 396.3mL$

The draining took $t = 107s = 1.783min$, so $Q_{constant} = \frac{V}{t} = 222.3mL/min$

Using an interface in *LabView*, it was possible to assess the output frequency of the signal for this volumetric flow (Q), $f = 168Hz$.

So, $K = \frac{222.3}{168} = 1.323$

The data sheet of the flow sensor FTB-311 sugests a *k* factor of 1.252. There is an error of 5 % accordingly to the calibration, due to different environment conditions or calibration process, which is acceptable. This test ensured that the flow sensor is working properly ready to assess fuel consumption.

The temperature and pressure sensors were calibrated accordingly to the transfer functions present in their data sheets (Appendix B).

7.5 User Interface

The operator of the inertia dynamometer has to be capable of working with the test bench in a way that allows him to see the output data acquired from the sensors. So a graphical interface on the software *LabView* [35] was created to show the power and torque diagrams, the fuel consumption rate and other sensored quantities for the acceleration run at hand. This interface can be seen in Figure 7.12.

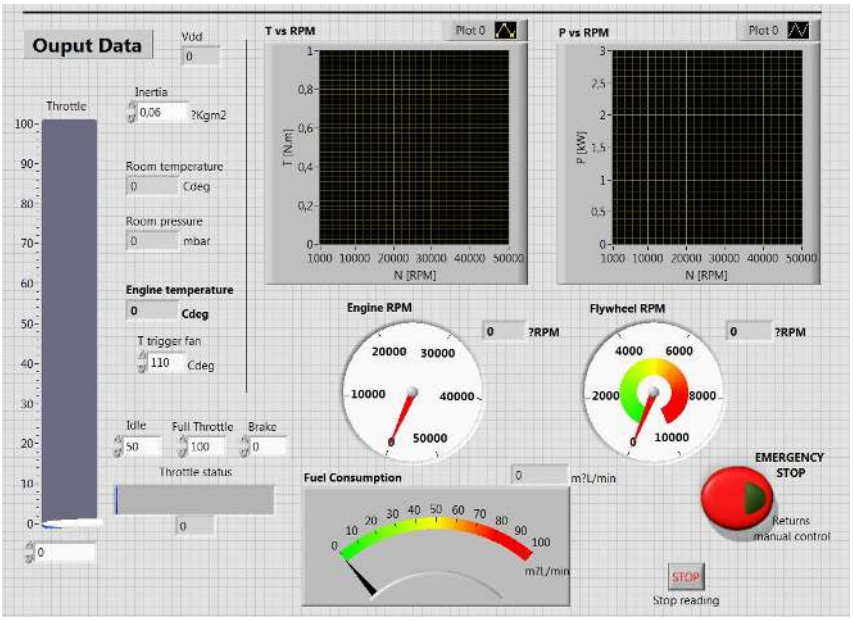

Figure 7.12: LabView interface for the dyno operator.

The *LabView* interface is designed for the operator to be aware of the data being collected from the test bench. Room temperature and pressure appear on the left for the operator to know the environment conditions at which the test is made. Engine temperature is also visible in the respective indicator. This engines should warm up to 110ºC before initiating full throttle regimes. When they reach this value, the cooling fan turns on. In fact, the fan must be always on since 110-130ºC is the ideal working temperature for most of the engines. If the indicator starts showing engine temperatures higher than 140ºC, the operator must stop doing runs for a while, until the engine temperature decreases to around 110ºC, or the fan turns off.

The engine temperature indicator is also very useful to acknowledge how long the engine takes to warm up before the first run.

There is also a series of graphic indicators to show the torque and power plots, the fuel consumption, engine RPM and flywheel RPM. At the end of a run, the operator must select the “Stop” button for *LabView* to cease data collection. The run must end when the engine rpm indicator starts to float around the same value.

One of the most important indicators is the flywheel rpm. This must never reach 10 000 RPM for safety issues. In that case, the operator must press the ”emergency stop” button immediately, which will actuate the brake and return manual control for the operator to cease braking when he sees fit.

7.5.1 Programming

The *LabView* program consists in block diagrams. In this section a quick review of the steps to program all the sensors and actuators is made.

To acquire the data from the sensors, simple tools were used to process the signal. For absolute values, the signal was subjected to ”Amplitude and Level Measurement” to obtain a mean DC of the same. Such were the case of the engine temperature, room temperature and room pressure. For frequency values, the signal was subjected to ”Tone Measurement” to obtain the frequency (Hz) of the same. Such were the case of the engine and flywheel rotation speed and the fuel consumption rate.

Afterwards, simple post processing is done including a derivative of the rotation speed to obtain the Torque values.

To control the actuators, auxiliary DAQ assistants were created to simulate both the electric servo for throttle control and the relay for fan actuation. In Figure 7.13 is possible to see the respective block diagrams.

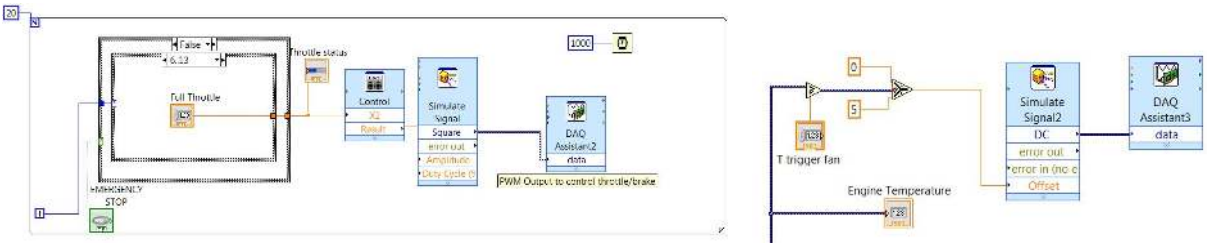

(a) Throttle control. (b) Fan control.

Figure 7.13: Throttle servo and fan relay programming.

For throttle control a *case structure* was created inside a *for loop* (Figure 7.13 a)) for full automation of the test run. The operator can decide the duration of the run, meaning when to start full throttle, when to end it and even the duration of braking. The throttle position alternates between 0 (break), 50 (idle) and 100 (full throttle) as it shows in the throttle slide of the interface (Figure 7.12).

To control the relay that actuates the fan, a simple True/False condition was implemented. As it shows in Figure 7.13 b), if the engine temperature is equal or higher than the ”T trigger fan” (110^{o}C), the program sends out a signal of 5V that actuates the relay and turns the fan on. If not, the relay stays open and the fan off.

The full layout of the *LabView* program can be seen in Figure 7.14.

7.5.2 Data Collection

LabView records the data in a *Microsoft Excel* file where each column contains the recorded value at each millisecond. The collected data is then post processed in *MatLab* [36] to generate the **torque and power diagrams**, and the **fuel consumption rate** to save the results already illustrated in the *LabView* interface.

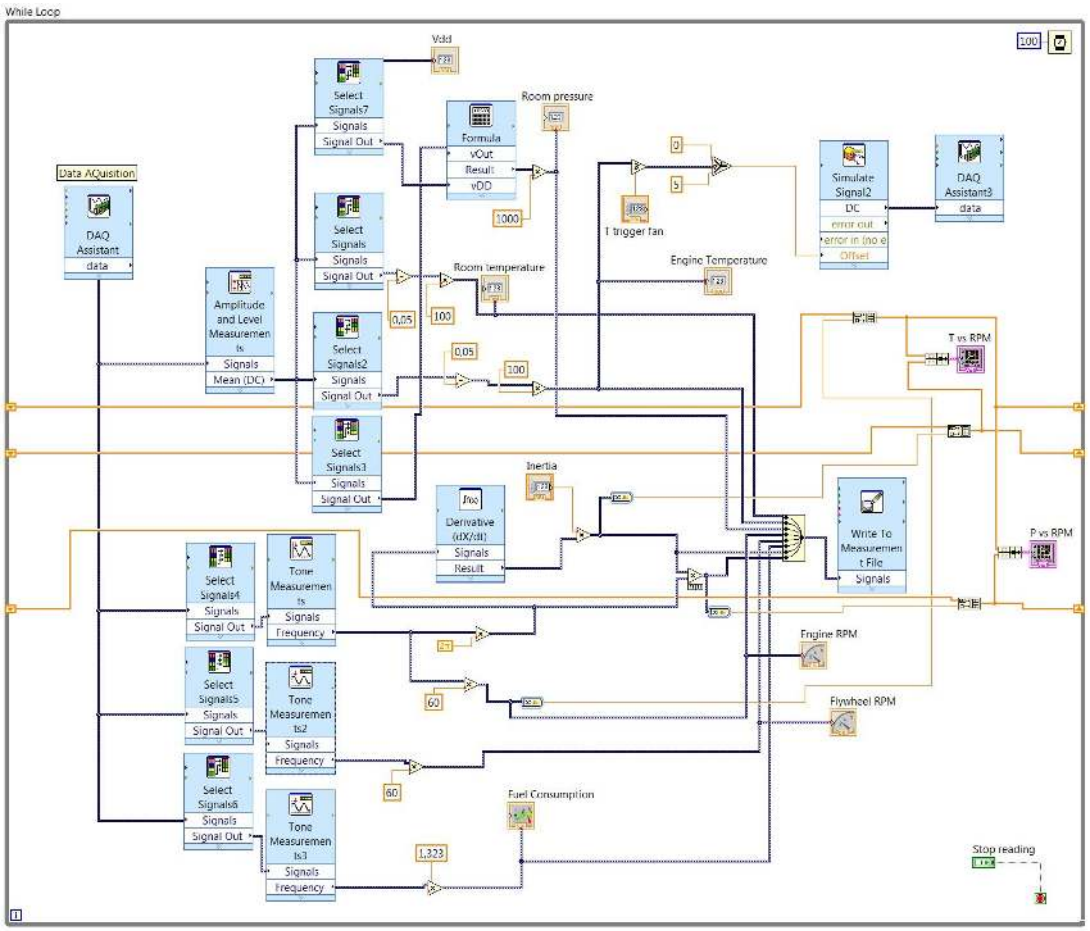

Figure 7.14: Layout of the *LabView* program.

After a few runs, the dyno operator may assess several important performance specifications of the engine by analysing the results. They are summarized in Table 7.3.

Physical quantity	**Unit**
Max Power	kW
Max Torque	Nm
Max Rotation Speed	RPM
Clutch losses	RPM
Fuel Consumption at idle speed	mL/min
Fuel Consumption at full throttle	mL/min
Time to warm up the engine	min

Table 7.3: Performance specifications obtained with the engine test bench.

All the performance specifications are given directly in the *LabView* interface, except the clutch losses. To assess this property, the column with the flywheel RPM data is multiplied by 5 (gear ratio) to give the effective engine RPM. A plot is generated for both engine RPM and effective engine RPM with time to compare the discrepancy.

Chapter 8

Demonstration Test Runs

8.1 Testing of the Instrumentation

Before running the engine on the test bench, a previous test was made for the electric motor of a gyroscope. The engine rotation speed sensor was set on the flywheel (Figure 8.1 a)) and tests were made using the *LabView* program to confirm the required data is being collected. In Figure 8.1 b) it is possible to see the acquired data of angular speed (ω) and angular acceleration (α).

(a) Assembly of the rotation speed sensor.

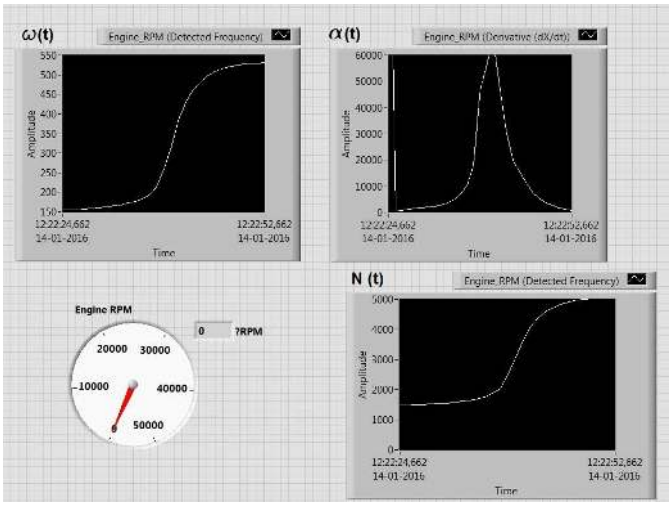

(b) Collected data.

Figure 8.1: Rotation speed test of the gyroscope electric motor.

It is known from Chapter 3 that to conduct an acceleration run, the engine is accelerated at full throttle from idle to maximum speed. So once the electric motor driving the flywheel reached a stable rotation at around 1500 RPM, the speed command was turned to its maximum and the power curves were recorded up to a maximum speed of 5 000 RPM.

As it can be seen, the program is viable. It presents the expected charts of $\omega(t)$ and $\alpha(t)$. Knowing the Inertia of the gyroscope flywheel is $0.004\,Kg.m^2$, post processing was made in *MatLab* to assess the power and torque diagrams of the electric motor. In Figure 8.2 it is possible to see the results.

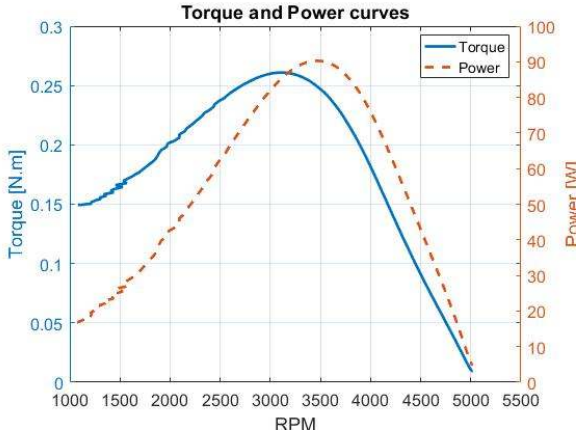

Figure 8.2: Torque and power curves of the electric motor driving the gyroscope.

These results validate the instrumentation of the test bench. In this case, the gyroscope motor was characterised with a maximum power of 90 W and a maximum torque of 0.26 N.m.

8.2 User Guide

In this section a detailed procedure for engine testing is given including the engine assembly (A), testing procedure (B) and post-processing (C).

A) Engine assembly

1. Lock the engine on its support bars.
2. Fasten the assembly on the engine support ensuring an ideal position for the gear mesh.
3. Lock the engine support on the main frame ensuring the pinion of the crankshaft and the gear are perfectly aligned.
4. Engage the fuel nipple of the carburetor with the throttle arm of the servo.
5. Connect both the fuel line and back pressure line to the carburetor and muffler, respectively.
6. Lock the muffler on its support by the respective wire.

B) Testing procedure

1. Verify that the fuel tank is full.
2. Start the engine by having the electric motor drive the crankshaft wheel (under the test bench), at the same time the glow plug is heated by a glow starter in the engine outer-head.
3. Locate the temperature sensor near the engine block.
4. Power on the *Labview* interface and start the program for reading and control.

5. Warm up the engine until it reaches about 100 °C (displayed in the engine temperature indicator) by operating the manual control slide (0 - 100). Note that *0* stands for maximum brake, *50* for idle speed and *100* for full throttle.

6. Simulate a test run by running the engine at full throttle (100) from idle to maximum rotation speed to study the ideal acceleration period.

7. Stop the reading and define the test parameters on the *Labview* interface: seconds to stand by before initiating the run, acceleration period (about 10s), brake intensity (0 - 50), temperature to trigger the cooling fan (90 - 110 °C).

8. Start the program, observe the torque and power diagrams being drawn and wait till the end of the run to stop the reading.

9. After performing all the tests, you must stop the engine by cutting its air admission. For that you must tap the carburetor reducer on top of it.

10. The collected data is automatically saved in a folder of your choosing for post-processing.

C) Post-processing

1. *LabView* generates an *Excel* file with all the data. Copy it to a *text* file and leave only two columns: time and rotation speed.

2. Import the customised file to the *MatLab* program designed to obtain the Torque and Power Diagrams.

3. Click ”Run”.

4. Save the generated diagrams of Rotation Speed [RPM], Angluar Velocity, Angular Acceleration, Engine Torque and Engine Power.

5. Import a new *text* file for every run you wish to process.

8.3 Testing the 3.5cc Glow Plug Engine

Some tests were made for a 3.5cc glow plug engine, the *Novarossi Rex P5*, to validate the design. Besides demonstrating the results, these runs ensure the structural integrity of the test bench. The results of the power curves for test 1, 2 and 3 are shown in Figure 8.3, 8.4 and 8.5, respectively.

These runs were accomplished by measuring the rotation speed at the flywheel. The engine rotation speed was obtained by multiplying those values by the gear ratio of $i = \frac{70}{13}$. Maximum speed, torque and power obtained for the *Novarossi Rex 3.5cc* engine are summarized in Table 8.1.

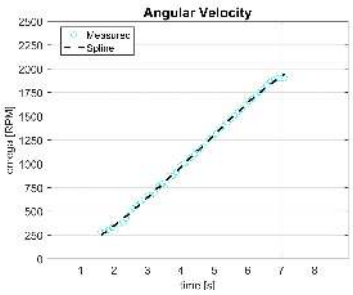

(a) Flywheel RPM of run 1.

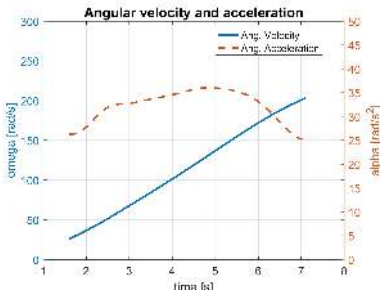

(b) Flywheel angular velocity (*rad/s*) and acceleration (rad/s^2) of run 1.

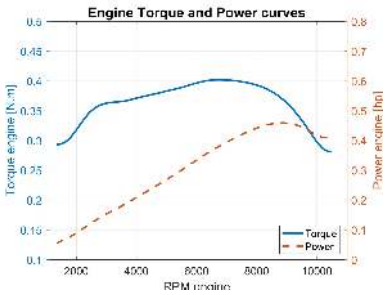

(c) Engine torque and power curves of run 1.

Figure 8.3: Results of the first test for the glow plug engine.

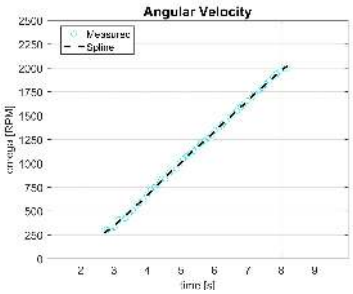

(a) Flywheel RPM of run 2.

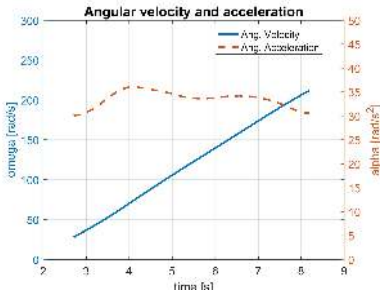

(b) Flywheel angular velocity (*rad/s*) and acceleration (rad/s^2) of run 2.

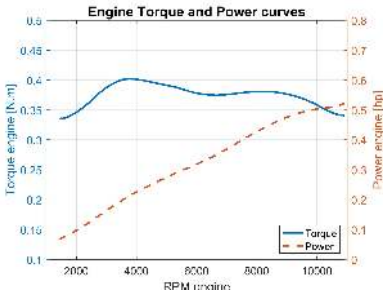

(c) Engine torque and power curves of run 2.

Figure 8.4: Results of the second test for the glow plug engine.

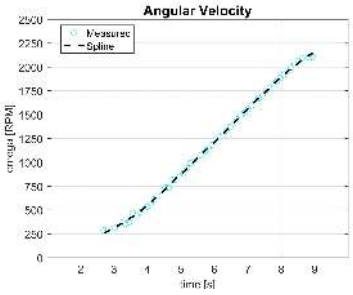

(a) Flywheel RPM of run 3.

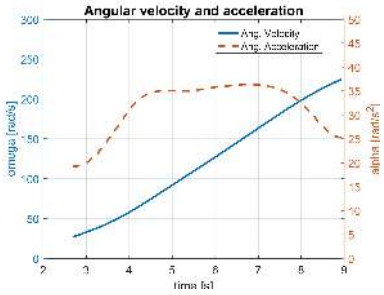

(b) Flywheel angular velocity (*rad/s*) and acceleration (rad/s^2) of run 3.

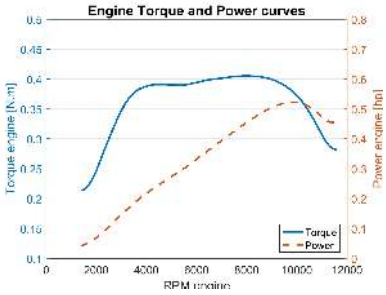

(c) Engine torque and power curves of run 3.

Figure 8.5: Results of the third test for the glow plug engine.

Test	**Max RPM**	**Max Torque [N.m]**	**Max Power [hp]**
Run 1	10 230	0.40	0.46
Run 2	10 770	0.40	0.52
Run 3	11 310	0.41	0.53

Table 8.1: Performance of the *Novarossi* 3.5cc glow plug engine on the test bench.

The runs that best represent the typical behaviour of these engines are the first and third tests where the maximum power is achieved before maximum speed and not at the same time (Test 2). Analysing both 1 and 3, it can be seen that in run 1 the engine is still warming up. It reaches a lower maximum speed one second sooner than in run 3, which suggests an incomplete burn bellow the engine full capabilities.

In Figure 8.6 is possible to see the engine assembled on the test bench after testing. Some oil splashes are visible at the muffler exit, which is common to the two-stroke micro engines. The engine must not be disassembled right after testing because it remains very hot for a certain period.

Figure 8.6: Engine after testing.

Accordingly to the results of test 3, the engine reaches a maximum rotation of N = 11 310 RPM and it achieves a maximum power of 0.53 hp at 10 000 RPM. The expected value for maximum rotation speed of 3.5cc glow plug engines was around 35 000 RPM and they are expected to achieve a maximum power between 1.5 hp and 2.5 hp. Possibly, some slipping occurred at the engine centrifugal clutch. Further tests must be performed measuring the rotation speed directly at the engine crankshaft. In Table 8.2 is possible to see the performance specifications of the *Novarossi Rex 3.5cc* accordingly to the *RCTen* internet forum.

Max RPM	**Max Torque [N.m]**	**Max Power [hp] (N)**
34 000	0.42	1.46 (25 250)

Table 8.2: Theoretical performance specifications of the *Novarossi* 3.5cc glow plug engine by *RCTen*.

This data may not be accurate, since there is no scientific proof supporting it, there is no information about the method and conditions of testing. However, comparing both values of maximum power there is an error of 64%. These reinforces the idea of slipping occurred at the engine centrifugal clutch.

Chapter 9

Conclusions

9.1 Achievements

The objective of the dissertation was to design, construct and instrument a test bench for micro combustion engines to characterise them in terms of torque, power and fuel consumption. It was built an engine inertia dynamometer because it was the best solution to obtain a dynamic test close to the real conditions as on the road. The program running the acceleration tests is fully automatic, allowing the test bench to have good repeatability which is essential to get realistic data. The cost breakdown shows a possible price of 2000 euros for an equipment like this. It is an acceptable value considering a model vehicle can cost up to 800 euros. One of the greatest challenges was the structural assembly of the test bench in IST, because the required materials were not always available, like special end mills to cut through stainless steel or a specific turning tool to cut the gaps for the retaining rings. Also, some electronic components like the flow sensor were difficult to acquire. This had to be imported from United Kingdom because there were no economic solutions in Portugal.

The main achievements of the dissertation were:

- Answer the growing need for a standard testing of micro combustion engines. With an equipment like this, drivers have a chance of knowing the real performance specifications of their engines.
- The test bench is able to test several types of micro engines. It was designed with adjustable supports and a conservative safety factor.
- The assembly of the engine and auxiliary systems in the dynamometer was designed to be easy. A user guide was developed explaining the testing procedure.
- Several sensors and actuators were set up to allow a fully automatic engine testing, ensuring a good repeatability of the acceleration runs.
- A *LabView* program was created with a graphical interface for the dynamometer operator to read the collected data live. The data is recorded in a separate file.
- An electric motor of a gyroscope was tested to validate the instrumentation.

- A 3.5cc glow plug engine was tested to demonstrate the results and validate the whole design of the test bench.
- This prototype is a new testing equipment to use in IST laboratories for academic purposes.

9.2 Future Work

There are some things than can be further improved. Safety has a lot of issues to be resolved, for example, a heavier brake can be designed to stop the flywheel faster (never too fast) and a mechanical brake system should be implemented for backup in case of emergency like power failure. The test bench can be used remotely, so further considerations about safety areas isolating the equipment from the operator can be made.

Although the design was validated, the test bench was just assembled with a car engine. Other engines for boats or aircraft should be tested as well, and even larger engines closer to 20.0 cc, to confirm if the adjustable supports are suitable. Other properties can be assessed, such as fuel emissions, and further studies can be made to reduce the cost of the test bench.

Also, an assembly/disassembly guide of the test bench should be made to help students and future customers to assemble the equipment on their own.

The engine dynamometer built is a prototype that can always be improved. Further contact to drivers and constructors is essential to validate the test bench for real application in engine testing and for further investment in this technology.

Bibliography

[1] O. Engines. Car and buggy engines. *O.S. Engines*, 2015.

[2] J. M. Lopes. *Motores de Combustão Interna - uma abordagem termodinâmica*. Técnico Lisboa, 2003.

[3] A. M. Aeronautics. Biography of ray arden. *National Model Aviation Museum*, 2004.

[4] J. B. Heywood. *Internal Combustion Engine Fundamentals*. McGraw-Hill Book Comp., 2011.

[5] B. Gardiner and C. C. M. A. C. Inc. All about glow plugs. *Fubar Hill*, 2014.

[6] G. Schnurle and O. Elwert. Two-stroke cycle internal-combustion engine. *IFI CLAIMS Patent Services*, (US2609802 A), 1952.

[7] T. XRay. Xray rx8 and xb8. *Team XRay*, 2014.

[8] T. C. Company. Methanol. *The Chemical Company*, 2014.

[9] R. Warren. Make your own e85 fuel. *Running on Alcohol*, 2004.

[10] Horiba. Engine test systems. *service.uk@horiba.com*, 2015.

[11] Horiba. Vehicle test systems. *service.uk@horiba.com*, 2015.

[12] D. B. Johnson, N. M. Newberger, and I. C. Anselmo. Vehicle drivetrain test stand and method of controlling same. *IFI CLAIMS Patent Services*, (US 8590369 B2), 2013.

[13] H. Nakanishi, S. Noguchi, and Y. Ogawa. Engine testing apparatus. *IFI CLAIMS Patent Services*, (US 6634218 B1), 2003.

[14] H. Bettes and B. Hancock. *Dyno Testing and Tuning*. CarTech Inc., 2008.

[15] L. L. Schumacher. Controllable inertia flywheel. *IFI CLAIMS Patent Services*, (US4995282 A), 1991.

[16] P. D. F. E. B. Nigro. Balanceamento de rotores. *Escola Politécnica da Universidade de São Paulo*, 2010.

[17] L. L. de Vibrações. Dinâmica de rotores. *Universidade Tecnológica Federal do Paraná*, 2004.

[18] M. A. Canto. Decoupler with free wheel system and vibration damping and one-way clutch. *IFI CLAIMS Patent Services*, (CA2884682 A1), 2014.

[19] S. Pond and C. D. Gierke. O.s. 18tz a weapon of mass combustion. *RC Nitro*, 2005.

[20] R. G. Budynas and J. K. Nisbett. *Shigley's Mechanical Engineering Design*. McGraw-Hill, 2008.

[21] F. Beer, E. R. J. Jr., and P. Cornwell. *Vector Mechanics for Engineers: Dynamics*. McGraw-Hill Book Comp., 10th edition, 2013.

[22] N. Instruments. Ni pcie-6321. *NI X Series Multifunction Data Acquisition*, 2015.

[23] Vishay. Cny70. *Leds and Chips*, 2015.

[24] Omega. Ftb-311. *OMEGA UK*, 2015.

[25] T. Instruments. Lm35dz. *Leds and Chips*, 2015.

[26] Infineon. Kp236n6165. *Lenave*, 2015.

[27] Futaba. S9302. *HP Modelismo*, 2015.

[28] Corsair. Af120. *GlobalData*, 2015.

[29] P. Lanema. H9 tolerance steels. *polylanema@lanema.pt*, 2016.

[30] RLK. 1100. *Rolisa*, 2015.

[31] R. Aços. Construction steels. *acos.lisboa@ramada.pt*, 2016.

[32] F. Racing. Racing brake pads. *Ferodo Racing*, 2014.

[33] D. Systems. Solidworks simulation 2015. *SolidWorks*, 2015.

[34] ElectroferIV. Zinc plating. *sandracoelho@electrofer.pt*, 2016.

[35] N. Instruments. Labview 2013. *LabView*, 2013.

[36] MathWorks. Matlab 2016. *MatLab*, 2016.

Appendix A

Data Acquisition Board Technical Datasheet

Technical Sales

(866) 531-6285
orders@ni.com

Requirements and Compatibility | Ordering Information | Detailed Specifications | Pinouts/Front Panel Connections
For user manuals and dimensional drawings, visit the product page resources tab on ni.com.

Last Revised: 2015-04-09 07:52:22.0

NI X Series Multifunction Data Acquisition

Overview

NI X Series devices for USB, PCI Express and PXI Express are the most advanced data acquisition devices ever designed by National Instruments. They feature significant improvements in onboard timing and triggering and optimizations for use with multicore PCs. X Series devices integrate high-performance analog, digital, and counter/timer functionality onto a single device, making them well-suited for a broad range of applications, from basic data logging to control and test automation.

Back to Top

Requirements and Compatibility

OS Information

- PharLap
- Real-Time OS
- Windows 7
- Windows 7 64-bit
- Windows Vista x64/x86
- Windows XP

Driver Information

- NI-DAQmx

Software Compatibility

- ANSI C/C++
- LabVIEW
- LabVIEW Real-Time Module
- LabWindows/CVI
- Measurement Studio
- SignalExpress
- Visual Basic
- Visual Studio .NET

Back to Top

Comparison Tables

Bus	Model Number	Analog Inputs (AI)	Max AI Sampling Rate (1-channel)	Max Total AI Throughput	Analog Outputs (AO)	Max AO Update Rate	Digital I/O Lines	Max Digital I/O Rate	Triggering
PCI Express	6320	16	250 kS/s	250 kS/s	0	-	24	1 MHz	Digital
PCI Express	6321	16	250 kS/s	250 kS/s	2	900 kS/s	24	1 MHz	Digital
PCI Express	6323	32	250 kS/s	250 kS/s	4	900 kS/s	48	1 MHz	Digital
USB, PCI Express, PXI Express	6341	16	500 kS/s	500 kS/s	2	900 kS/s	24	1 MHz	Digital
USB, PCI Express	6343	32	500 kS/s	500 kS/s	4	900 kS/s	48	1 MHz	Digital
USB, PCI Express	6351	16	1.25 MS/s	1.25 MS/s	2	2.86 MS/s	24	10 MHz	Analog, Digital
USB, PCI Express	6353	32	1.25 MS/s	1.25 MS/s	4	2.86 MS/s	48	10 MHz	Analog, Digital

Bus	Model Number	Analog Inputs (AI)	Max AI Sampling Rate (1-channel)	Max Total AI Throughput	Analog Outputs (AO)	Max AO Update Rate	Digital I/O Lines	Max Digital I/O Rate	Triggering
USB, PCI Express, PXI Express	6361	16	2 MS/s	2 MS/s	2	2.86 MS/s	24	10 MHz	Analog, Digital
USB, PCI Express, PXI Express	6363	32	2 MS/s	2 MS/s	4	2.86 MS/s	48	10 MHz	Analog, Digital
USB, PXI Express	6356	8 simultaneous	1.25 MS/s/channel	10 MS/s	2	3.33 MS/s	24	10 MHz	Analog, Digital
PXI Express	6358	16 simultaneous	1.25 MS/s/channel	20 MS/s	4	3.33 MS/s	48	10 MHz	Analog, Digital
USB, PXI Express	6366	8 simultaneous	2 MS/s/channel	16 MS/s	2	3.33 MS/s	24	10 MHz	Analog, Digital
PXI Express	6368	16 simultaneous	2 MS/s/channel	32 MS/s	4	3.33 MS/s	48	10 MHz	Analog, Digital

Back to Top

Application and Technology

NI-STC3 Timing and Synchronization Technology

NI X Series multifunction data acquisition (DAQ) devices include the NI-STC3, an ASIC designed by NI for advanced timing, triggering, and synchronization. This technology includes the following:

- Four counter/timers with more functionality than ever before, such as the ability to create a finite pulse train with a single counter
- A 100 MHz timebase for faster triggering response and more precise generation of analog and digital sample clocks
- Independent analog and digital timing engines
- Retriggerable measurement tasks for analog I/O, digital I/O, and counter/timers

Native PCI Express Interface

In contrast to a PCI-to-PCI Express bridge chip, which limits the bandwidth of the device to that of the PCI bus and introduces latency, PCI Express and PXI Express X Series devices use a native x1 PCI Express interface that provides up to 250 MB/s in each direction. National Instruments has also optimized this interface for low latency in single-point control applications. You can use X Series PCI Express boards in any PCI Express slot from x1 up to x16.

NI Signal Streaming

USB X Series devices include patented NI Signal Streaming, a technology that uses message-based instructions and device-side intelligence to ensure high-speed, bidirectional data transfer over USB. With USB X Series, you can concurrently transfer analog, digital, and counter data in both directions. The total device throughput over USB is PC-dependent; on some systems, up to 32 MB/s sustained transfers are possible.

Improved Mechanical Enclosure

USB X Series devices introduce a redesigned, extruded aluminum enclosure with an easy-access magnetic lid. This lid keeps signal wiring secured and shielded and can be opened easily when needed. The underside of the lid has a device-specific pinout label so that you can quickly determine the corresponding screw terminals for a given channel. The enclosure also includes a lockable USB port to prevent accidental removal during operation and a security slot that can be used with ordinary laptop locks to secure the device to a desk or workstation.

Software Enhancements

PCI Express and PXI Express X Series devices are compatible with NI-DAQmx Version 9.0 or later driver software. USB X Series devices require NI-DAQmx Version 9.2 or later. More than a basic driver, NI-DAQmx includes the NI Measurement & Automation Explorer (MAX) configuration utility, the DAQ Assistant for rapid development of basic applications, and hundreds of example programs for NI LabVIEW and text-based languages. NI-DAQmx also includes LabVIEW SignalExpress LE basic data-logging software.

NI-DAQmx 9.0 introduces the ability to synchronize multiple PCI Express or PXI Express X Series devices with a single NI-DAQmx task, which previously took several tasks and manual routing of clocks and triggers. This version also introduces the fastest, easiest way to acquire measurement data to disk in the Technical Data Management Streaming (TDMS) format with the new Configure Logging VI. NI-DAQmx 9.2 introduces the ability to log acquired data to TDMS files within the DAQ Assistant Express VI.

With NI-DAQmx and intuitive LabVIEW graphical programming, you can easily develop applications that take advantage of today's multicore systems so you can perform acquisition, signal processing, and data logging on different CPU cores.

Simultaneous Sampling X Series

Some X Series devices for USB and PXI Express offer simultaneous sampling, with the same channel counts and connectivity as multiplexed devices.

Unlike multiplexed devices that reduce sampling rates as you add more channels, you can use simultaneous sampling devices to maintain sampling rates as you expand the number of channels. Simultaneous sampling X Series devices are available with up to 16 differential channels per device, and, with PXI Express, you can sample more than 200 channels simultaneously.

Simultaneous X Series devices for USB include 32 or 64 MS onboard memory to ensure the transfer of finite acquisitions, even in the presence of heavy USB traffic.

Applications

Acquisition and Visualization

X Series devices include analog, digital, and counter circuitry for the most common types of static and waveform measurements. With LabVIEW, you can easily acquire the data and view it on a variety of graphs and displays. You can use configuration-based wizards called Express VIs to take measurements and perform signal processing with minimal programming.

Data Logging

Whether you are validating a new hardware design, monitoring conditions on a factory floor, or recording temperature changes during a scientific experiment, you need to take measurements, visualize your data, and often log it to disk. With X Series multifunction DAQ, you can develop a user-defined measurement system by using intuitive graphical programming software and incorporating the exact visualization, analysis, and data-logging capabilities your application requires.

Control Systems

If you need to control the temperature of a room, the speed of a motor, or the pressure of hydraulic fluids, you can use X Series DAQ hardware to connect sensors and actuators to your computer and build the control system that meets your exact application needs. The low-latency PCI Express bus improves single-point I/O performance, and with LabVIEW software and NI-DAQmx driver software, you can easily take sensor measurements, compare values to a setpoint, and update output signals. X Series devices also have four counter/timers for performing quadrature encoder measurements, pulse-width modulation, pulse train generation, frequency measurements, and much more, making them ideal for basic motor control.

Due to the inherent higher latency of USB as compared to PCI Express, National Instruments recommends that you use PCI Express or PXI Express X Series devices for applications that require single-point control or deterministic operation.

Test Automation

X Series DAQ hardware provides analog inputs, analog outputs, hardware-timed digital I/O, and four counter/timers on a single device, making it a cost-effective option for basic device under test characterization and test automation. With NI-DAQmx software, you can easily synchronize acquisition or generation on multiple subsystems, such as an analog input and analog output channel. In addition, you can easily synchronize two or more X Series devices for further expansion by using a RTSI cable for PCI Express devices or over the PXI Express backplane for PXI Express modules. It is possible to synchronize two or more USB X Series devices by exporting sample or reference clocks from the master device to the slave device, and using external wiring.

Compatible Accessories

PCI Express and PXI Express X Series devices use either a single or dual-stack 68-pin VHDCI female connector, depending on the number of analog and digital channels on the device. National Instruments offers several options for cables, from 0.5 to 10 m and from low-cost to high-performance with shielding. Connector blocks are available with screw terminal, BNC, or custom connector types.

For measurements requiring signal conditioning, you can use X Series with SCXI signal conditioning modules.

You can purchase DIN-rail or panel mount kits for USB X Series devices as well as replacement power supplies and latching USB cables. See the model page for ordering information.

Upgrading

Because X Series DAQ devices use the same NI-DAQmx driver software as NI M Series DAQ devices, upgrading is easy. In addition, PCI Express and PXI Express X Series devices use the same VHDCI connector as PCI and PXI M Series. You can reuse your code and preserve your investment in accessories. The pinouts for X Series devices are backward-compatible with M Series devices.

Back to Top

Ordering Information

For a complete list of accessories, visit the product page on ni.com.

Products	Part Number	Recommended Accessories	Part Number
NI PCIe-6320			
NI PCIe-6320 Requires: 1 Cables , 1 Connector Blocks ;	781043-01	**Cables:** Shielded - SHC68-68-EPM Cable (2m) ***Also Available: [Unshielded]*	192061-02
		Connector Blocks: Spring-Screw_Terminals - SCB-68A ***Also Available: [BNC_Terminals]*	782536-01
NI PCIe-6321			
NI PCIe-6321 Requires: 1 Cables , 1 Connector Blocks ;	781044-01	**Cables:** Shielded - SHC68-68-EPM Cable (2m) ***Also Available: [Unshielded]*	192061-02
		Connector Blocks: Spring-Screw_Terminals - SCB-68A ***Also Available: [BNC_Terminals]*	782536-01
NI PCIe-6323			
NI PCIe-6323 Requires: 2 Cables , 2 Connector Blocks ;	781045-01	**Connector 0:**	
		Cables: Shielded - SHC68-68-EPM Cable (2m) ***Also Available: [Unshielded]*	192061-02
		Connector Blocks: Spring-Screw_Terminals - SCB-68A ***Also Available: [BNC_Terminals]*	782536-01
		Connector 1:	
		Cables: Shielded - SHC68-68-EPM Cable (2m) ***Also Available: [Unshielded]*	192061-02
		Connector Blocks: Spring-Screw_Terminals - SCB-68A ***Also Available: [BNC_Terminals]*	782536-01

Back to Top

Software Recommendations

LabVIEW Professional Development System for Windows

- Fully integrated graphical system design software
- Support for a wide range of measurement hardware, I/O, and buses
- Custom, event-driven user interfaces for measurement and control
- Extensive signal processing, analysis, and math functionality
- Advanced compiler to ensure high-performance execution and code optimization
- Professional software development with code quality review, unit testing, and executable creation

SignalExpress for Windows

- Quickly configure projects without programming
- Control over 400 PC-based and stand-alone instruments
- Log data from more than 250 data acquisition devices
- Perform basic signal processing, analysis, and file I/O
- Scale your application with automatic LabVIEW code generation
- Create custom reports or easily export data to LabVIEW, DIAdem or Microsoft Excel

Measurement Studio Professional Edition

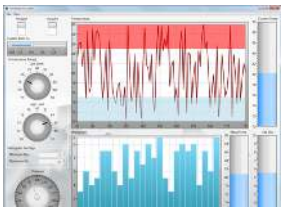

- Customizable graphs and charts for WPF, Windows Forms, and ASP.NET Web Forms UI design
- Analysis libraries for array operations, signal generation, windowing, filters, signal processing
- Hardware integration support with native .NET data acquisition and instrument control libraries
- Automatic code generation for all NI-DAQmx data acquisition hardware
- Intelligent and efficient data-logging libraries for streaming measurement data to disk
- Support for Microsoft Visual Studio .NET 2012/2010/2008

Back to Top

Support and Services

System Assurance Programs

NI system assurance programs are designed to make it even easier for you to own an NI system. These programs include configuration and deployment services for your NI PXI, CompactRIO, or Compact FieldPoint system. The NI Basic System Assurance Program provides a simple integration test and ensures that your system is delivered completely assembled in one box. When you configure your system with the NI Standard System Assurance Program, you can select from available NI system driver sets and application development environments to create customized, reorderable software configurations. Your system arrives fully assembled and tested in one box with your software preinstalled. When you order your system with the standard program, you also receive system-specific documentation including a bill of materials, an integration test report, a recommended maintenance plan, and frequently asked question documents. Finally, the standard program reduces the total cost of owning an NI system by providing three years of warranty coverage and calibration service. Use the online product advisors at ni.com/advisor to find a system assurance program to meet your needs.

Calibration

NI measurement hardware is calibrated to ensure measurement accuracy and verify that the device meets its published specifications. To ensure the ongoing accuracy of your measurement hardware, NI offers basic or detailed recalibration service that provides ongoing ISO 9001 audit compliance and confidence in your measurements. To learn more about NI calibration services or to locate a qualified service center near you, contact your local sales office or visit ni.com/calibration.

Technical Support

Get answers to your technical questions using the following National Instruments resources.

- **Support** - Visit ni.com/support to access the NI KnowledgeBase, example programs, and tutorials or to contact our applications engineers who are located in NI sales offices around the world and speak the local language.
- **Discussion Forums** - Visit forums.ni.com for a diverse set of discussion boards on topics you care about.
- **Online Community** - Visit community.ni.com to find, contribute, or collaborate on customer-contributed technical content with users like you.

Repair

While you may never need your hardware repaired, NI understands that unexpected events may lead to necessary repairs. NI offers repair services performed by highly trained technicians who quickly return your device with the guarantee that it will perform to factory specifications. For more information, visit ni.com/repair.

Training and Certifications

The NI training and certification program delivers the fastest, most certain route to increased proficiency and productivity using NI software and hardware. Training builds the skills to more efficiently develop robust, maintainable applications, while certification validates your knowledge and ability.

- **Classroom training in cities worldwide** - the most comprehensive hands-on training taught by engineers.
- **On-site training at your facility** - an excellent option to train multiple employees at the same time.
- **Online instructor-led training** - lower-cost, remote training if classroom or on-site courses are not possible.
- **Course kits** - lowest-cost, self-paced training that you can use as reference guides.
- **Training memberships** and training credits - to buy now and schedule training later.

Visit ni.com/training for more information.

Extended Warranty

NI offers options for extending the standard product warranty to meet the life-cycle requirements of your project. In addition, because NI understands that your requirements may change, the extended warranty is flexible in length and easily renewed. For more information, visit ni.com/warranty.

OEM

NI offers design-in consulting and product integration assistance if you need NI products for OEM applications. For information about special pricing and services for OEM customers, visit ni.com/oem.

Alliance

Our Professional Services Team is comprised of NI applications engineers, NI Consulting Services, and a worldwide National Instruments Alliance Partner program of more than 700 independent consultants and integrators. Services range from start-up assistance to turnkey system integration. Visit ni.com/alliance.

Back to Top

Detailed Specifications

Specifications listed below are typical at 25 °C unless otherwise noted. Refer to the *X Series User Manual* for more information about NI PCIe-6320/6321/6323 devices.

Analog Input	
Number of channels	
NI 6320/6321	8 differential or 16 single ended
NI 6323	16 differential or 32 single ended
ADC resolution	16 bits
DNL	No missing codes guaranteed
INL	Refer to the *AI Absolute Accuracy Table*
Sampling rate	
Maximum	250 kS/s single channel, 250 kS/s multi-channel (aggregate)
Minimum	No minimum
Timing accuracy	50 ppm of sample rate
Timing resolution	10 ns
Input coupling	DC
Input range	±10 V, ±5 V, ±1 V, ±0.2 V
Maximum working voltage for analog inputs (signal + common mode)	±11 V of AI GND
CMRR (DC to 60 Hz)	100 dB
Input impedance	
Device on	
AI+ to AI GND	>10 GΩ in parallel with 100 pF
AI– to AI GND	>10 GΩ in parallel with 100 pF
Device off	
AI+ to AI GND	1200 Ω
AI– to AI GND	1200 Ω
Input bias current	±100 pA
Crosstalk (at 100 kHz)	
Adjacent channels	–75 dB
Non-adjacent channels	–90 dB
Small signal bandwidth (–3 dB)	700 kHz

Input FIFO size	4,095 samples
Scan list memory	4,095 entries
Data transfers	DMA (scatter-gather), programmed I/O
Overvoltage protection (AI <0..31>, AI SENSE, AI SENSE 2)	
Device on	±25 V for up to two AI pins
Device off	±15 V for up to two AI pins
Input current during overvoltage condition	±20 mA max/AI pin
Settling Time for Multichannel Measurements	
Accuracy, full scale step, all ranges	
±90 ppm of step (±6 LSB)	4 µs convert interval
±30 ppm of step (±2 LSB)	5 µs convert interval
±15 ppm of step (±1 LSB)	7 µs convert interval
Analog triggers	None
Typical Performance Graphs	

Settling Error Versus Time for Different Source Impedances

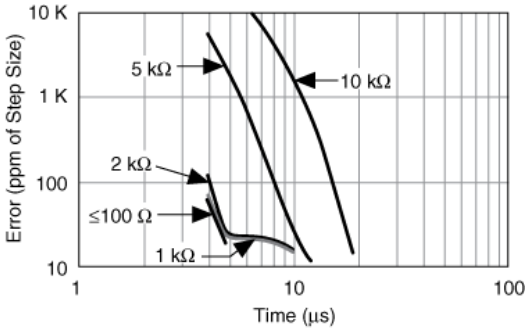

Analog Output	
Number of channels	
NI 6320	0
NI 6321	2
NI 6323	4
DAC resolution	16 bits
DNL	±1 LSB
Monotonicity	16 bit guaranteed
Maximum update rate	
1 channel	900 kS/s
2 channels	840 kS/s per channel
3 channels	775 kS/s per channel
4 channels	719 kS/s per channel
Timing accuracy	50 ppm of sample rate
Timing resolution	10 ns
Output range	±10 V
Output coupling	DC
Output impedance	0.2 Ω
Output current drive	±5 mA

Overdrive protection	±15 V
Overdrive current	15 mA
Power-on state	±20 mV
Power-on/off glitch	2 V for 500 ms
Output FIFO size	8,191 samples shared among channels used
Data transfers	DMA (scatter-gather), programmed I/O
AO waveform modes: ▪ Non-periodic waveform ▪ Periodic waveform regeneration mode from onboard FIFO ▪ Periodic waveform regeneration from host buffer including dynamic update	
Settling time, full scale step 15 ppm (1 LSB)	6 µs
Slew rate	15 V/µs
Glitch energy	
Magnitude	100 mV
Duration	2.6 µs

Calibration (AI and AO)

Recommended warm-up time	15 minutes
Calibration interval	1 year

AI Absolute Accuracy Table

Nominal Range		Residual Gain Error (ppm of Reading)	Gain Tempco (ppm/°C)	Reference Tempco (ppm/°C)	Residual Offset Error (ppm of Range)	Offset Tempco (ppm of Range/°C)	INL Error (ppm of Range)	Random Noise, σ (μV_{rms})	Absolute Accuracy at Full Scale[1] (µV)
Positive Full Scale	Negative Full Scale								
10	–10	65	7.3	5	13	24	60	229	2200
5	–5	72	7.3	5	13	25	60	118	1140
1	–1	78	7.3	5	17	37	60	26	257
0.2	– 0.2	105	7.3	5	27	93	60	12	69

AI Absolute Accuracy Formulas

AbsoluteAccuracy = Reading · (GainError) + Range · (OffsetError) + NoiseUncertainty
GainError = ResidualGainError + GainTempco · (TempChangeFromLastInternalCal) + ReferenceTempco · (TempChangeFromLastExternalCal)
OffsetError = ResidualOffsetError + OffsetTempco · (TempChangeFromLastInternalCal) + INL_Error
NoiseUncertainty = (RandomNoise · 3) / √ 10,000, for a coverage factor of 3 σ and averaging 10,000 points.

[1]Absolute accuracy at full scale on the analog input channels is determined using the following assumptions:

TempChangeFromLastExternalCal = 10 °C
TempChangeFromLastInternalCal = 1 °C
number_of_readings = 10,000
CoverageFactor = 3 σ

For example, on the 10 V range, the absolute accuracy at full scale is as follows:

GainError = 65 ppm + 7.3 ppm · 1 + 5 ppm · 10
GainError = 122 ppm

OffsetError = 13 ppm + 24 ppm · 1 + 60 ppm
OffsetError = 97 ppm

NoiseUncertainty = (229 µV · 3) / √ 10,000
NoiseUncertainty = 6.9 µV

AbsoluteAccuracy = 10 V · (GainError) + 10 V · (OffsetError) + NoiseUncertainty
AbsoluteAccuracy = 2,200 µV

Accuracies listed are valid for up to one year from the device external calibration.

AO Absolute Accuracy Table

Appendix B

Sensors Technical Datasheets

B.1 RPM sensor datasheet

Reflective Optical Sensor with Transistor Output

21835

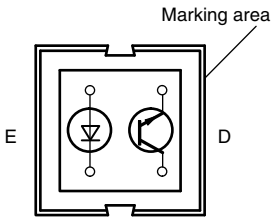

19158_1

FEATURES

- Package type: leaded
- Detector type: phototransistor
- Dimensions (L x W x H in mm): 7 x 7 x 6
- Peak operating distance: < 0.5 mm
- Operating range within > 20 % relative collector current: 0 mm to 5 mm
- Typical output current under test: I_C = 1 mA
- Emitter wavelength: 950 nm
- Daylight blocking filter
- Lead (Pb)-free soldering released
- Material categorization: For definitions of compliance please see www.vishay.com/doc?99912

Pb-free

e4

RoHS COMPLIANT

DESCRIPTION

The CNY70 is a reflective sensor that includes an infrared emitter and phototransistor in a leaded package which blocks visible light.

APPLICATIONS

- Optoelectronic scanning and switching devices i.e., index sensing, coded disk scanning etc. (optoelectronic encoder assemblies).

PRODUCT SUMMARY				
PART NUMBER	DISTANCE FOR MAXIMUM CTR_{rel} (1) (mm)	DISTANCE RANGE FOR RELATIVE I_{out} > 20 % (mm)	TYPICAL OUTPUT CURRENT UNDER TEST (2) (mA)	DAYLIGHT BLOCKING FILTER INTEGRATED
CNY70	0	0 to 5	1	Yes

Notes

(1) CTR: current transfere ratio, I_{out}/I_{in}

(2) Conditions like in table basic charactristics/sensors

ORDERING INFORMATION			
ORDERING CODE	PACKAGING	VOLUME (1)	REMARKS
CNY70	Tube	MOQ: 4000 pcs, 80 pcs/tube	-

Note

(1) MOQ: minimum order quantity

ABSOLUTE MAXIMUM RATINGS (T_{amb} = 25 °C, unless otherwise specified)				
PARAMETER	TEST CONDITION	SYMBOL	VALUE	UNIT
COUPLER				
Total power dissipation	$T_{amb} \leq 25$ °C	P_{tot}	200	mW
Ambient temperature range		T_{amb}	- 40 to + 85	°C
Storage temperature range		T_{stg}	- 40 to + 100	°C
Soldering temperature	Distance to case 2 mm, t £ 5 s	T_{sd}	260	°C
INPUT (EMITTER)				
Reverse voltage		V_R	5	V
Forward current		I_F	50	mA
Forward surge current	$t_p \leq 10$ µs	I_{FSM}	3	A
Power dissipation	$T_{amb} \leq 25$ °C	P_V	100	mW
Junction temperature		T_j	100	°C

ABSOLUTE MAXIMUM RATINGS (T_{amb} = 25 °C, unless otherwise specified)				
PARAMETER	**TEST CONDITION**	**SYMBOL**	**VALUE**	**UNIT**
OUTPUT (DETECTOR)				
Collector emitter voltage		V_{CEO}	32	V
Emitter collector voltage		V_{ECO}	7	V
Collector current		I_C	50	mA
Power dissipation	$T_{amb} \leq 25$ °C	P_V	100	mW
Junction temperature		T_j	100	°C

ABSOLUTE MAXIMUM RATINGS

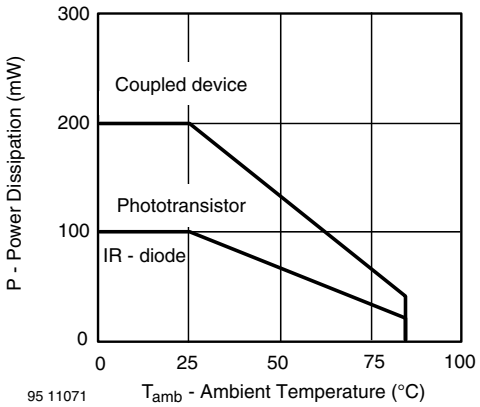

Fig. 1 - Power Dissipation vs. Ambient Temperature

BASIC CHARACTERISTICS (T_{amb} = 25 °C, unless otherwise specified)						
PARAMETER	**TEST CONDITION**	**SYMBOL**	**MIN.**	**TYP.**	**MAX.**	**UNIT**
COUPLER						
Collector current	V_{CE} = 5 V, I_F = 20 mA, d = 0.3 mm (figure 1)	I_C (2)	0.3	1.0		mA
Cross talk current	V_{CE} = 5 V, I_F = 20 mA, (figure 2)	I_{CX} (3)			600	nA
Collector emitter saturation voltage	I_F = 20 mA, I_C = 0.1 mA, d = 0.3 mm (figure 1)	V_{CEsat} (2)			0.3	V
INPUT (EMITTER)						
Forward voltage	I_F = 50 mA	V_F		1.25	1.6	V
Radiant intensity	I_F = 50 mA, t_p = 20 ms	I_e			7.5	mW/sr
Peak wavelength	I_F = 100 mA	λ_P	940			nm
Virtual source diameter	Method: 63 % encircled energy	d		1.2		mm
OUTPUT (DETECTOR)						
Collector emitter voltage	I_C = 1 mA	V_{CEO}	32			V
Emitter collector voltage	I_E = 100 µA	V_{ECO}	5			V
Collector dark current	V_{CE} = 20 V, I_F = 0 A, E = 0 lx	I_{CEO}			200	nA

Notes

(1) Measured with the “Kodak neutral test card”, white side with 90 % diffuse reflectance

(2) Measured without reflecting medium

B.2 Flow sensor datasheet

3.0 Specifications

Max. Working Pressure:	
PVC lens,	130 psig (9 bar) @ 70° F (21° C)
PVDF lens,	150 psig (10 bar) @ 70° F (21° C)
Max. Fluid Temperature:	
PVC lens, F/NPT connectors	130° F (54° C) @ 0 PSI
PVDF lens, tubing connectors	200° F (93° C) @ 0 PSI
Full scale accuracy	+/- 6%
Input Power requirement:	9 - 28 VDC
Sensor only output cable:	3-wire shielded cable, 6ft
Pulse output signal:	Digital square wave (2-wire) 25ft max. Voltage high = 5Vdc, Voltage low < .25Vdc 50% duty cycle
Output frequency range:	4 to 500Hz
Alarm output signal:	Open collector. Active low above programmable rate set point. 30Vdc maximum, 50mA max load. Active low < .25Vdc
Enclosure:	NEMA type 4X, (IP56)
Approximate shipping wt:	1 lb. (.45 kg)

3.1 Temperature and Pressure limits

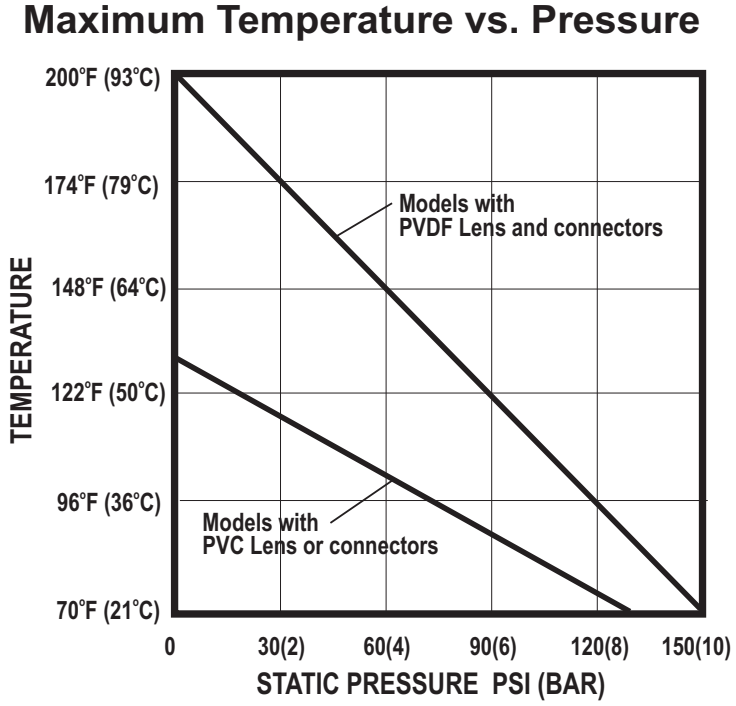

3.2 Dimensions

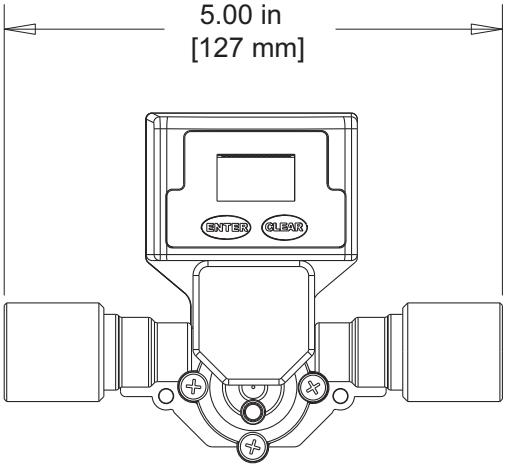

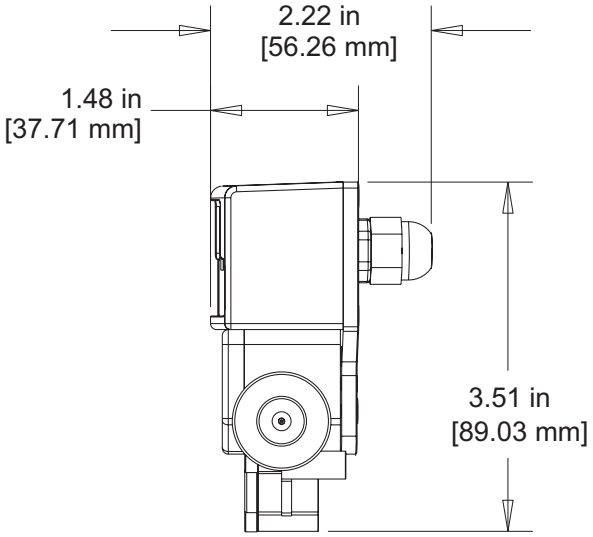

3.3 Replacement Parts

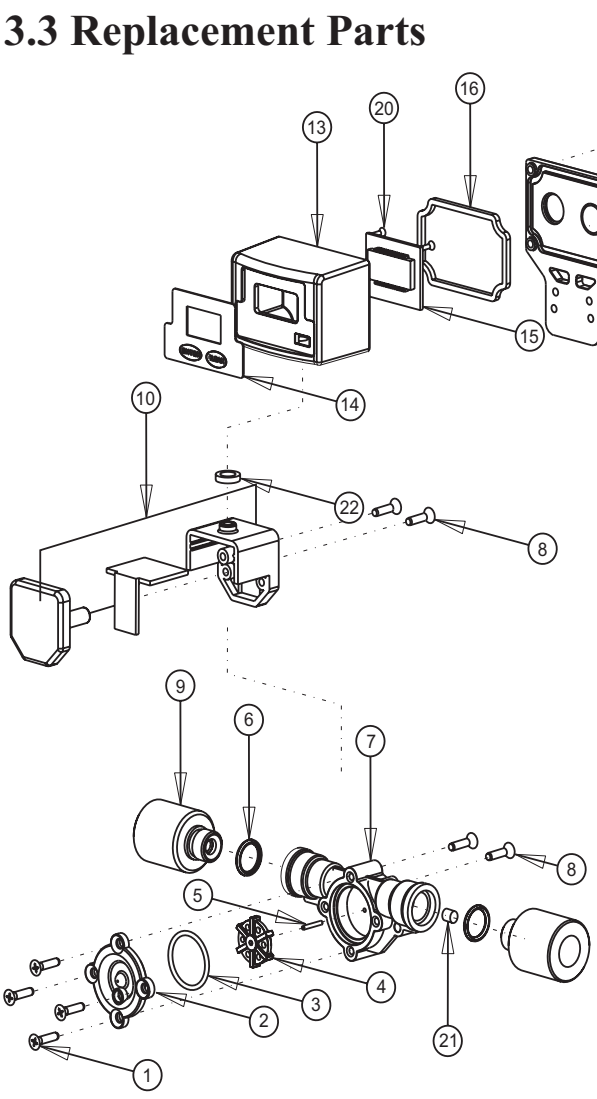

PARTS LIST

Key	Part No.	Description	Qty.
1	90011-081	Screw 6-32x.50 Phil Flt SS	4
2	90002-227	Lens Cap Clear PVC	1
	90002-228	Lens Cap Opaque PVDF	3
	90003-143	O-Ring Viton	1
	90003-146	O-Ring EP	
4	90002-230	Paddle PVDF	1
5	90007-592	Axle PVDF	1
6	90003-012	O-Ring Viton	2
	90003-011	O-Ring EP	
7	76001-300	Body S1 PVDF (30-300ml/min)	1
	76001-301	Body S2 PVDF(100-1000ml/min)	
	76001-302	Body S2 PVDF (200-2000ml/min)	
	76001-303	Body S2 PVDF (300-3000ml/min)	
	76001-304	Body S2 PVDF (500-5000ml/min)	
	76001-305	Body S2 PVDF (700-7000ml/min)	
8	90011-113	Screw #4x.50 Phil Blk	4
9	76000-137	Adapter .250 F/NPT PVC	2
	76000-456	Adapter .125 F/NPT PVC	
	90002-038	Adapter .37OD x .25ID Tube PVDF	
10	90012-252	Sensor	1
13	90002-242	Enclosure, Valox	1
14	90012-254	LCD display	1
15	90010-260	Circuit board	1
16	90006-604	Gasket, rear enclosure	1
17	90002-243	Cover, enclosure rear	1
18	90008-199	Liquid Tight Connector Set	1
19	90011-178	Screw #4x.62 Phil SS Blk	4
20	90011-177	Screw #2x.25 L Phil St	2
21	76001-299	Tubing connector seal	1
22	90006-605	Gasket, sensor mount seal	1

4.0 Installation

4.1 Wiring Connections

On sensor mounted units, the output signal wires must be installed through the back panel using a second liquid-tite connector (included). To install the connector, remove the circular knock-out. Trim the edge if required. Install the extra liquid-tite connector.

On panel or wall mounted units, wiring may be installed through the enclosure bottom or through the back panel. See below.

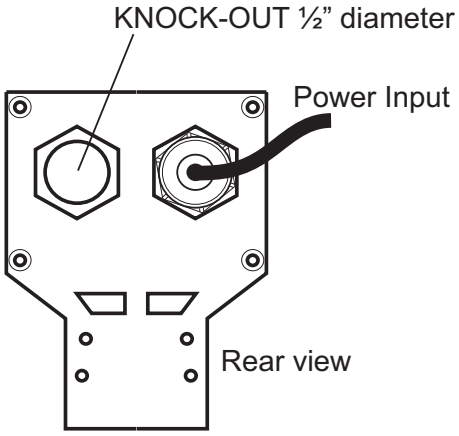

4.2 Circuit Board Connections

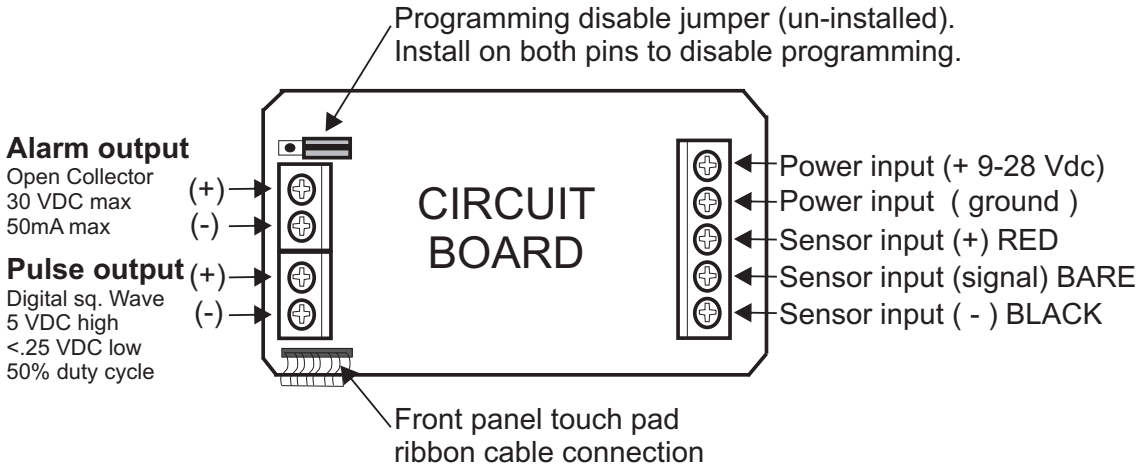

B.3 Temperature sensor datasheet

5 Pin Configuration and Functions

NDV Package
3-Pin TO-CAN
(Top View)

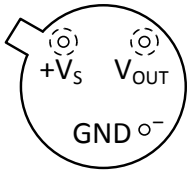

Case is connected to negative pin (GND)

D Package
8-PIN SOIC
(Top View)

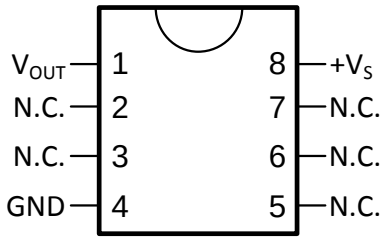

N.C. = No connection

LP Package
3-Pin TO-92
(Bottom View)

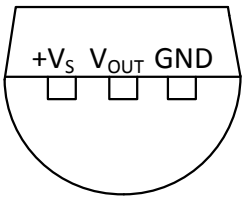

NEB Package
3-Pin TO-220
(Top View)

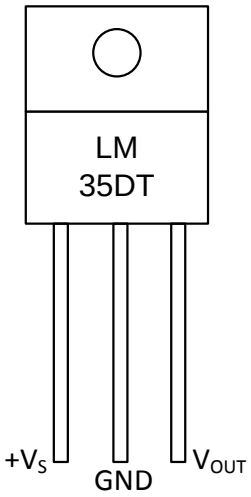

Tab is connected to the negative pin (GND).

NOTE: The LM35DT pinout is different than the discontinued LM35DP

Pin Functions

PIN					TYPE	DESCRIPTION
NAME	TO46	TO92	TO220	SO8		
V_{OUT}	—	—	—	1	O	Temperature Sensor Analog Output
N.C.	—	—	—	2	—	No Connection
	—	—	—	3		
GND	—	—	—	4	GROUND	Device ground pin, connect to power supply negative terminal
N.C.	—	—	—	5	—	No Connection
	—	—	—	6		
	—	—	—	7		
$+V_S$	—	—	—	8	POWER	Positive power supply pin

6 Specifications

6.1 Absolute Maximum Ratings

over operating free-air temperature range (unless otherwise noted)(1)(2)

		MIN	MAX	UNIT
Supply voltage		–0.2	35	V
Output voltage		–1	6	V
Output current			10	mA
Maximum Junction Temperature, $T_J$max			150	℃
Storage Temperature, T_{stg}	TO-CAN, TO-92 Package	–60	150	℃
	TO-220, SOIC Package	–65	150	

(1) If Military/Aerospace specified devices are required, please contact the Texas Instruments Sales Office/ Distributors for availability and specifications.
(2) Absolute Maximum Ratings indicate limits beyond which damage to the device may occur. DC and AC electrical specifications do not apply when operating the device beyond its rated operating conditions.

6.2 ESD Ratings

			VALUE	UNIT
$V_{(ESD)}$	Electrostatic discharge	Human-body model (HBM), per ANSI/ESDA/JEDEC JS-001(1)	±2500	V

(1) JEDEC document JEP155 states that 500-V HBM allows safe manufacturing with a standard ESD control process.

6.3 Recommended Operating Conditions

over operating free-air temperature range (unless otherwise noted)

		MIN	MAX	UNIT
Specified operating temperature: T_{MIN} to T_{MAX}	LM35, LM35A	–55	150	℃
	LM35C, LM35CA	–40	110	
	LM35D	0	100	
Supply Voltage (+V_S)		4	30	V

6.4 Thermal Information

THERMAL METRIC(1)(2)		LM35				UNIT
		NDV	LP	D	NEB	
		3 PINS		8 PINS	3 PINS	
$R_{\theta JA}$	Junction-to-ambient thermal resistance	400	180	220	90	℃/W
$R_{\theta JC(top)}$	Junction-to-case (top) thermal resistance	24	—	—	—	

(1) For more information about traditional and new thermal metrics, see the *IC Package Thermal Metrics* application report, SPRA953.
(2) For additional thermal resistance information, see *Typical Application*.

B.4 Pressure sensor datasheet

2.1 Pin Configuration

Figure 1 shows the pin configuration.

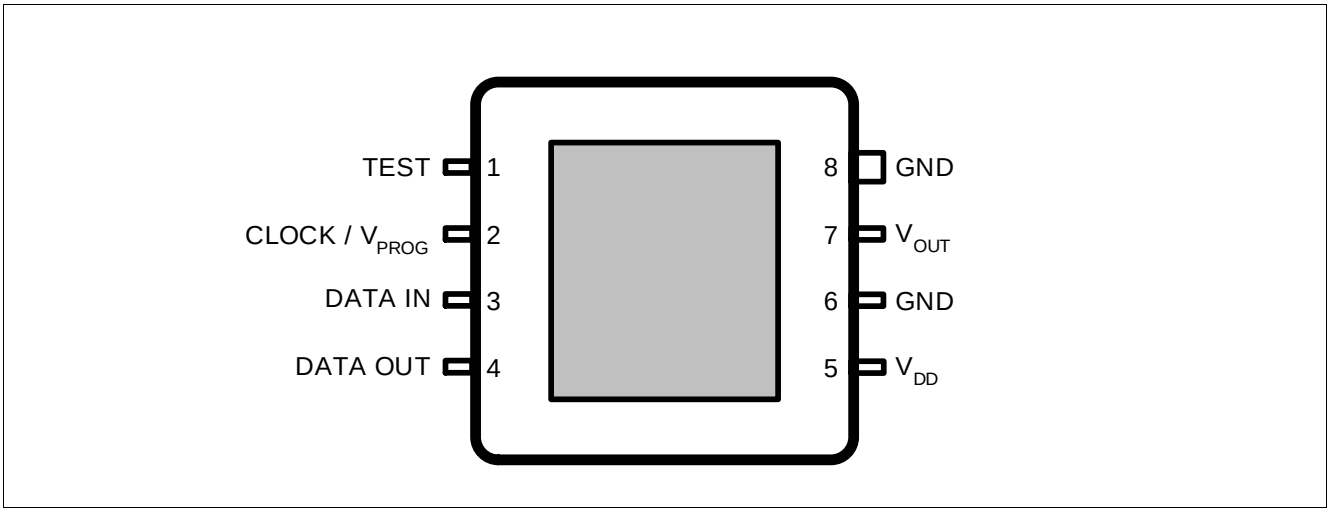

Figure 1 Pin configuration (top view, figure not to scale)

2.2 Pin Description

Table 1 shows the pin description.

Table 1 Pin Description

Pin No.	Name	Function
1	TEST	Test pin[1)]
2	CLOCK / V_{PROG}	External clock for communication / programming voltage[1)]
3	DATA IN	Serial data input pin[1)]
4	DATA OUT	Serial data output pin[1)]
5	V_{DD}	Supply voltage
6	GND	Circuit ground potential[2)]
7	V_{OUT}	Analog pressure signal output
8	GND	Circuit ground potential[2)]

1) Digital pins are used only during calibration and test. It is recommended to leave these pins floating (in case of an open GND connection, the floating pins prevent from a cross grounding through the corresponding ESD diodes).

2) It is recommended to connect both GND pins.

2.3 Block Diagram

Figure 2 shows the functional block diagram.

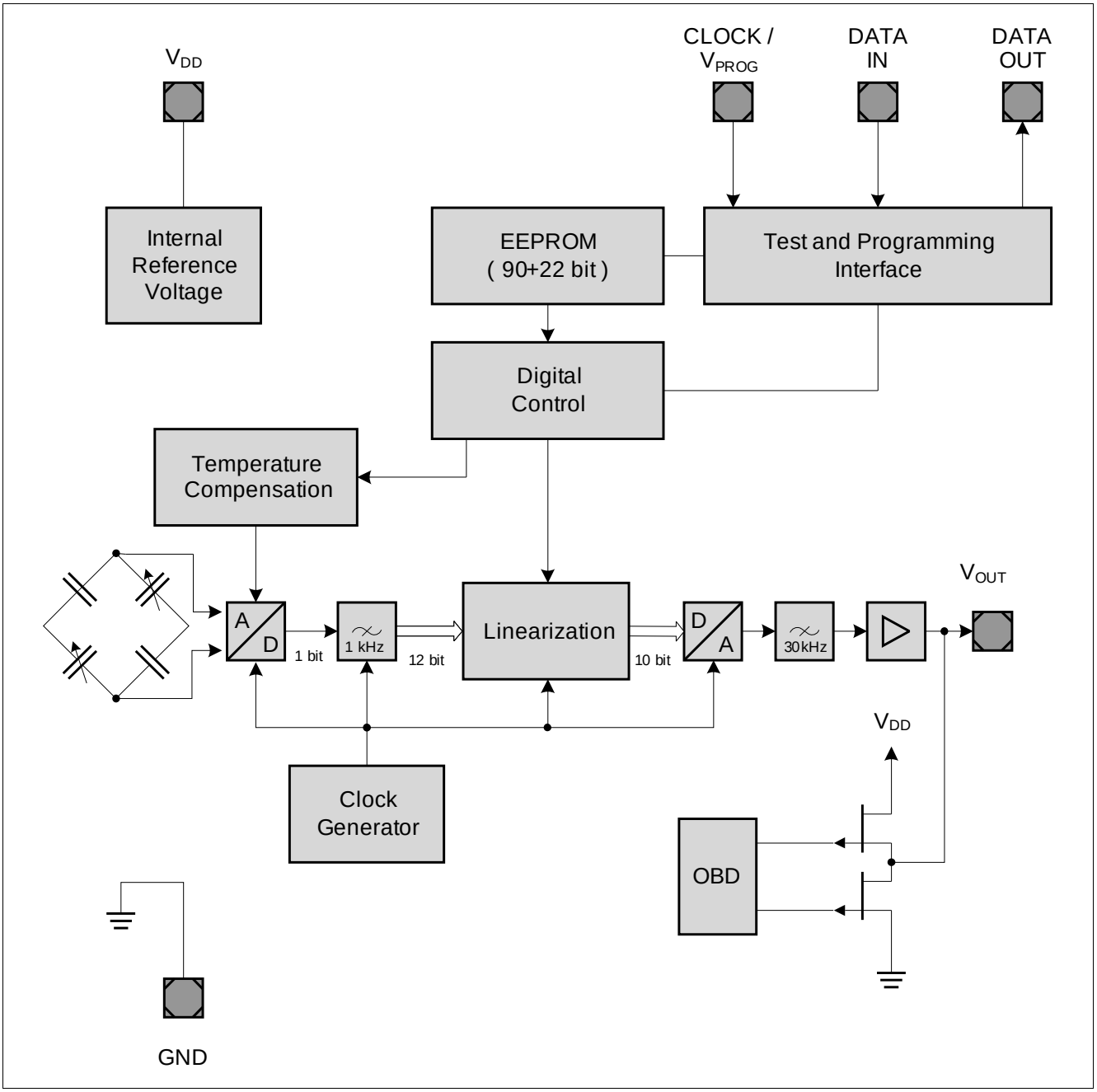

Figure 2 Functional block diagram

2.4 Transfer Function

The KP236N6165 device is fully calibrated on delivery. The sensor has a linear transfer function between the applied pressure and the output signal:

$$V_{OUT} = V_{DD} \times (a \times P + b)$$

The output signal is ratiometric. Gain **a** and offset **b** are determined during calibration in order to generate the required transfer function.

Calibrated Transfer Function

The following calibration is adjusted with the parameters **a** and **b:**

Table 2 Transfer function

Pressure			Output Voltage @ $V_{DD} = V_{DD,Typ}$				Gain and Offset		
Symbol	**Values**	**Unit**	**Symbol**	**Values**	**Unit**		**Symbol**	**Value**	**Unit**
$p_{IN,1}$	60	kPa	$V_{OUT,1}$	0.2	V		*a*	0.00876	1/kPa
$p_{IN,2}$	165	kPa	$V_{OUT,2}$	4.8	V		*b*	-0.48571	–

Note: The points $p_{IN,1}/V_{OUT,1}$ and $p_{IN,2}/V_{OUT,2}$ define the calibrated transfer function and not the operating range. The operating pressure range is defined by the parameter 2.4 ***"Ambient operating pressure range" on Page 19***

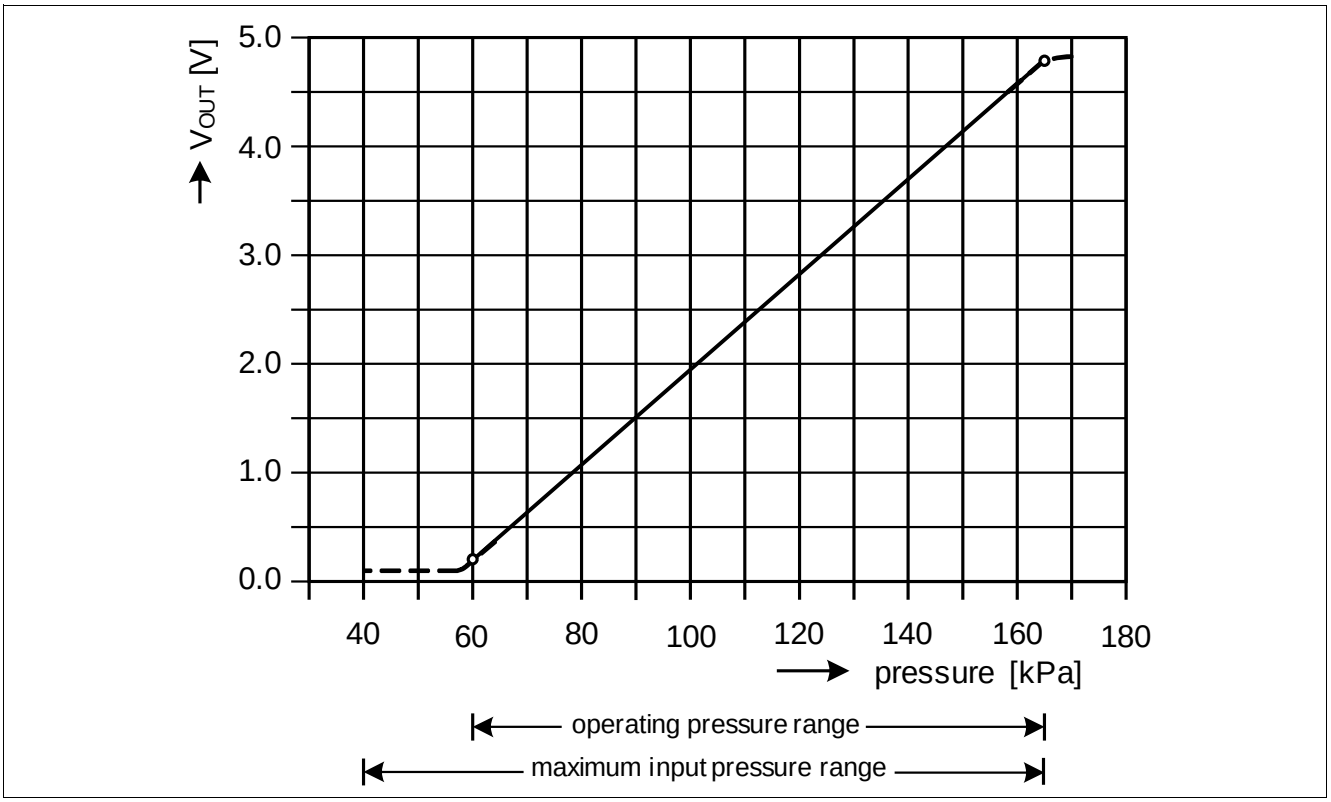

Figure 3 Transfer function

Note: The application circuitry determines the current driven by the device and thus may have an impact on the output voltage delivered by the sensor.